

**IDENTIFICATION AND CHARACTERIZATION OF A NOVEL  
CA<sup>2+</sup>-BINDING PROTEIN IN AVIAN ERYTHROCYTES**

Thesis by

**Jian Zhu**

In Partial Fulfillment of the Requirements

for the Degree of

Doctor of Philosophy

California Institute of Technology

Pasadena, California

1994

(Submitted November 22, 1993)

IIa

© 1994

Jian Zhu

All Rights Reserved

ii<sub>b</sub>

To my family

## Acknowledgements

The influence, support and encouragement of many special people lies behind the thesis, but its greatest impulse has been from Elias Lazarides. Being my research advisor over the past five years, he has enthusiastically supported me to finish the whole project, encouraged me to overcome many difficulties encountered, given me great freedom to pursue whatever I felt was necessary, guided me to develop systemic approaches to scientific problems and helped me understand the world beyond science. He has always been generous with his knowledge, insights and encouragement. To him, I owe a very special debt of gratitude.

I am deeply grateful to Catherine Woods for her meticulous, industrious and valuable work in the entire research and the preparation of the thesis. This thesis would not have been possible without her invaluable advice, immeasurable encouragement and altruistic support.

I would like to thank William Dunphy, Howard Lipshitz, Elliot Meyerowitz and Barbara Wold for serving as members of my thesis committee and providing invaluable suggestions for the research.

The thesis owes its origin to Steven Bloom whose enthusiasm initiated the whole project. Douglas Murphy and William Brinkley generously provided antibodies to allow me to continue the research. My thanks to all.

It has been a great pleasure to work in both the laboratories at Caltech and Merck Research Laboratories. I thank all the members of both laboratories. I am particularly grateful to Ping Ye and Debbie Carlyle for their dedicated technical help, Thomas Coleman for his enthusiastic collaboration in the early phases of the research and Daniel Bollag for making microtubule analysis possible.

I am indebted to all the members of the Caltech protein sequencing facility and monoclonal antibody facility. I am also grateful to secretaries and administrators of the Biology Division and the Graduate Student Office, in particular to Nancy Gill and Janet Davis.

I thankfully acknowledge the financial support of the California Institute of Technology, the Merck Research Laboratories and the American Cancer Society.

I also owe a special debt to my family: my mother, my wife and my daughter. The thesis might not have been finished without their wholehearted love and encouragement.

## Abstract

A novel  $\text{Ca}^{2+}$ -binding protein with Mr of 23 K (designated p23) has been identified in avian erythrocytes and thrombocytes. p23 localizes to the marginal bands (MBs), centrosomes and discrete sites around the nuclear membrane in mature avian erythrocytes. p23 appears to bind  $\text{Ca}^{2+}$  directly and its interaction with subcellular organelles seems to be modulated by intracellular  $[\text{Ca}^{2+}]$ . However, its unique protein sequence lacks any known  $\text{Ca}^{2+}$ -binding motif. Developmental analysis reveals that p23 association to its target structures occurs only at very late stages of bone marrow definitive erythropoiesis. In primitive erythroid cells, p23 distributes diffusely in the cytoplasm and lacks any distinct localization. It is postulated that p23 association to subcellular structures may be induced in part by decreased intracellular  $[\text{Ca}^{2+}]$ . In vitro and in vivo experiments indicate that p23 does not appear to act as a classical microtubule-associated protein (MAP) but p23 homologues appear to be expressed in MB-containing cells of a variety of species from different vertebrate classes. It has been hypothesized that p23 may play a regulatory role in MB stabilization in a  $\text{Ca}^{2+}$ -dependent manner.

Binucleated (bnbn) turkey erythrocytes were found to express a truncated p23 variant (designated p21) with identical subcellular localization as p23 except immunostaining reveals the presence of multi-centrosomes in bnbn cells. The p21 sequence has a 62 amino acid deletion at the C-terminus and must therefore have an additional ~40 amino acids at the N-terminus. In addition, p21 seems to have lost the ability to bind  $\text{Ca}^{2+}$  and its supramolecular interactions are not modulated by intracellular  $[\text{Ca}^{2+}]$ . These apparent differences between p23 and p21 raised the possibility that the

p23/p21 allelism could be the Bn/bn genotype. However, genetic analysis suggested that p23/p21 allelism had no absolute correlation with the Bn/bn genotype.

**Table of Contents**

	<u>Page</u>
<b>Chapter 1</b>	
Introduction.	1
Microtubules: dynamic instability and stability.	2
The dual role of centrosomes: microtubule organizing center and cell cycle pacemaker	13
The role of Ca <sup>2+</sup> and Ca <sup>2+</sup> -binding proteins in microtubule and centrosome structure and function	22
Scope of this thesis	25
<b>Chapter 2</b>	
Existence of a normal and truncated form of a low molecular weight Ca <sup>2+</sup> -binding protein in turkey erythrocytes	28
<b>Chapter 3</b>	
Identification of a novel calcium-binding protein that specifically associates with the marginal bands and centrosome of mature chicken erythrocytes and thrombocytes.	59
<b>Chapter 4</b>	
P23 fails to interact directly with microtubules	113
<b>Chapter 5</b>	
Search for p23 homologues in other species	125
<b>Chapter 6</b>	
Conclusions	133
References	136

## Chapter One

### Introduction

Erythropoiesis is a sequential event of functional and morphological differentiation steps whereby a pluripotent stem cell becomes committed to the erythroid lineage. During this process, the cell cytoarchitecture is reorganized from a fluid, dynamic state of the round, proliferative precursor cells, into highly ordered, specialized arrays that confer the unique morphology of the terminally differentiated cells, required for a functional erythrocyte. In addition to the expression of erythroid-specific genes (Lazarides, 1987; Woods & Lazarides, 1988), some of the differentiation program of erythroid progenitor cells involves dramatic transitions in the properties of subcellular structures. For example, a dense erythroid membrane skeleton is elaborated during later erythroblast stages; dynamic microtubules emanating from centrosomes in progenitor cells are observed to become highly stabilized microtubule bundles (named the marginal band, Behnke, 1970; Barret and Dawson, 1974) which encircle the peripheral rim of differentiated erythrocytes; in early progenitor cells, centrosomes serve as microtubule organizing centers (MTOC, Pickett-Heaps 1969) and govern microtubule arrays and cell morphology, but they become inactive as MTOC in late polychromatophilic stages when they are no longer associated with microtubules. The studies of these transitions during the erythropoiesis can provide insight into the mechanisms underlying the changes from progenitor cells into the highly specialized form of terminal differentiated erythrocytes.

## Microtubules: Dynamic Instability and Stability

Microtubules (MTs) are composed of heterodimers of two closely related proteins,  $\alpha$  and  $\beta$  tubulin, assembled into a tubular structure with a diameter about 24 nm (Dustin, 1984). The modulation of the physical properties of this tubular structure (for example, length, number, stability, bundling, interactions with other components), enables MTs to play a key role in a wide range of cellular processes including cell morphogenesis, cell motility, cell polarity, intracellular transport and organization of organelles, chromosome segregation and cell division (Dustin, 1984). All these functions can be attributed to two fundamental properties of MTs: dynamic instability and stability (see review, Kirschner & Mitchison, 1986; Kirschner, 1989; Gelfand & Bershadsky, 1991). An understanding of MT function requires a knowledge of the molecular basis for the apparently antagonistic properties of MT instability and stability *in vivo*.

Dynamic instability is a model that has been proposed to explain the co-existence of growing and shrinking MTs observed both in *in vitro* MT polymerization from purified tubulin and *in vivo* in proliferating cultured cells. Before this model was proposed, several models of MT assembly dynamics were hypothesized, including single equilibrium subunit exchange at MT ends (Oosawa & Kasai, 1962) and the treadmilling model (Margolis & Wilson, 1978). The first model predicted MT polymerization would reach steady state after a certain period of time; thereafter no further net growth or depolymerization would occur at MT ends. The treadmilling model suggested that the growth of the plus end [(+) end, MT end distal from the basal body] can be compensated by the depolymerization of the minus end [(-) end, MT end proximal to basal body]. This mechanism predicted that MT number and length should remain unchanged at steady

state. However, both models were challenged by the observations that during tubulin polymerization at steady state *in vitro*, the number of MTs in solution gradually decreased over time but the length increased (Mitchison & Kirschner, 1984a;b). Furthermore, both ends of MTs were shown to incorporate biotin-labelled tubulin subunits (Kristofferson et al., 1986). These results indicated that both MT ends can either grow or shrink and are in constant flux (Mitchison & Kirschner, 1984b; Hill & Chen, 1984; Chen & Hill, 1983). Horio & Hotani (1986) visualized MT behavior directly by video-enhanced darkfield microscopy. They demonstrated that at steady state, MTs underwent random growth and shrinkage with the shrinkage rate being more rapid than the growth rate. This behaviour of MTs was named dynamic instability (Mitchison & Kirschner, 1984a, b; Horio & Hotani, 1986; Cassimeris et al., 1988; Walker et al., 1988; Sammak & Borisy, 1988a,b). These authors defined the following phases of MT instability: no growth at nucleation centers, slow growth, and rapid shrinkage. Rapid transitions occurred between the three phases: a) nucleation, a transition from no polymerization to growth; b) catastrophe, an abrupt transition from slow growth to rapid shrinkage and c) rescue, a switch from rapid shrinkage to regrowth. More detailed analysis by video-enhanced DIC microscopy was used to calculate the growth rate, shrinkage rate, catastrophe and rescue frequency for both ends of MTs *in vitro* (Walker et al., 1988). Reduction of tubulin concentration increased the catastrophe frequency and decreased the rescue frequency, or *vice versa*. Most significantly, observation of net growth of MTs at (-) ends and net shrinkage at (+) ends provided evidence that contradicted the treadmilling hypothesis.

MT dynamics have also been studied *in vivo* by employing different approaches: photobleaching zones of individual MTs (Salmon et al., 1984; Saxton et al., 1984);

injection of hapten-modified tubulin followed by visualization of the hapten-tubulin in MTs by anti-hapten antibodies (Soltys & Borisy, 1985; Schulze & Kirschner, 1986) and injection of FITC-labelled tubulins followed by photobleaching and antibody localization of the FITC (Sammak et al., 1987). Visualization by low light fluorescence (Sammak & Borisy, 1988b; Schulze & Kirschner, 1988) or video-enhanced DIC (Cassimeris et al., 1988) microscopy of living cells revealed a dynamic behavior of MTs in living cells which was similar to that observed with MTs *in vitro*. Thus, individual MTs in cells grow, rapidly shrink back (catastrophe) and grow again (rescue) with catastrophe and rescue being random events. However, the dynamic behaviour *in vivo* is more complex than that observed *in vitro*. For example, not all catastrophe and rescue events are stochastic. Rather MTs may repeatedly shrink back and grow at a given site (Schulze & Kirschner, 1988); these sites may possibly be mitochondria (Gupta, 1990). Furthermore, a significant fraction of MTs may be highly stable (e.g., 10-20% of the MT population in BSC-1 cells) and cannot be labelled by using injected FITC-tubulin (Schulze & Kirschner, 1986, 1987). Thus, additional factors appear to modulate the inherent dynamic instability properties of MTs. This is particularly evident in highly differentiated cells, which exhibit very stable, highly defined MT arrays. For example, stable MT arrays are observed in neurons (Baas & Black, 1990; Reinsch et al., 1991; Tanaka & Kirschner, 1991), myocytes (Tassin et al., 1985a, b), nucleated erythrocytes (Behnke, 1970; Murphy, et al., 1986; Birgbauer & Solomon, 1989), platelets (Kenney & Linck, 1985; Kowit et al., 1988) and axonemes (Chretien & Wade, 1991). A variety of mechanisms may be involved in establishing these stable MT populations, including divergence of tubulin isoforms, tubulin posttranslational modification, and MT interactions with microtubule-associated proteins (MAPs, Olmsted, 1986).

Several different isoforms of  $\alpha$  and  $\beta$  tubulin subunits, generated by both alternate splicing or from different genes, have been identified in various species (see reviews, Raff, 1984; Cleveland & Sullivan, 1985; Sullivan, 1988). Genetic analysis and molecular characterization of different  $\beta$  tubulin genes suggest that, despite the fact that  $\beta$ -tubulins share high degree of homology among intra- and inter- species, they have a viable region between amino acid 30 and 100, and a hypervariable C-terminal region downstream from amino acid 430 (Sullivan, 1988). The expression of these different  $\beta$ -tubulin isoforms is variable: a few exhibit tissue-specific expression (for example, chicken erythrocyte  $\beta$ -tubulin, Murphy 1983a), but many exhibit a widespread pattern of expression. Although many  $\beta$ -tubulins appear to be used interchangeably in cells, not all tubulins are functionally equivalent. For example, when the *Drosophila*  $\beta$ -2 tubulin gene, which despite widespread tissue distribution is not expressed in germ cells, was expressed in  $\beta$ -3 minus germ cells ( $\beta$ -3 is a *Drosophila* germ-cell specific  $\beta$ -tubulin), only a few cytoplasmic MTs were formed. When  $\beta$ 2- $\beta$ 3 were co-expressed, low levels of  $\beta$ 2-tubulin expression relative to the endogenous  $\beta$ 3 levels of expressions had little affect on cell morphology; but when  $\beta$ 2-tubulin expression was increased to more than 20% of total tubulin, the cytoplasmic and mitotic MTs were normal but the flagellar tail disappeared (Hoyle & Raff, 1990). These data implied that the  $\beta$ 2 and  $\beta$ 3 isotypes of tubulin were not functionally equivalent. Chicken erythrocyte  $\beta$ -tubulin (c $\beta$ 6, Murphy et al., 1983a, 1986) provides another example of functional non-equivalence in the  $\beta$ -tubulin family. Compared to chicken brain  $\beta$ -tubulin, *in vitro* formation of c $\beta$ 6-containing MTs

requires a lower tubulin critical concentration, and fewer but longer MTs are formed (Murphy & Wallis, 1983b) that are non-dynamic in nature (Trinczek et al., 1993).

Several posttranslational modifications, particularly of  $\alpha$ -tubulin, have been noted to correlate with stable MT populations. These include phosphorylation (Edde et al., 1981; Gard & Kirschner, 1985); acetylation/deacetylation (L'Hernault & Rosenbaum, 1985; Ledizet & Piperno, 1987); tyrosination / detyrosination (Barra, 1973; Schulze et al., 1987; Bulinski & Gundersen, 1991); glutamylation (Edde et al., 1992; Wolff et al., 1992) and ADP-ribosylation (Scaife et al., 1992). Tubulin tyrosination/detyrosination has been studied in the most detail. Barra (1973) originally discovered that tubulins can be tyrosinated (Tyr-tubulin) by a tubulin-tyrosine ligase (TTL) and can be detyrosinated (leaving a Glu at the terminus, named Glu-tubulin) by a tubulin carboxypeptidase (TCP). TTL acts preferentially on unassembled tubulin dimers (Arce et al., 1978; Wehland & Webev, 1987) while TCP acts exclusively on assembled MT polymers (Kumar & Flavin, 1981; Arce & Barra, 1983). By following tubulin modification in successive rounds of de- and repolymerization, newly polymerized MTs were found to be composed of Tyr-MT assembled from Tyr-tubulin; however, Glu-MTs appeared some time after MT assembly, only being observed in relatively stable MTs (Gundersen et al., 1987). However, injection of antibodies against TTL into cells produced Glu-MTs but these MTs exhibited the same dynamics as their Tyr-counterpart in uninjected cells (Webster et al., 1990). Indeed, stable marginal band MTs from toad and chicken erythrocytes contain no Glu-tubulin (Gundersen & Bulinski, 1986; Beltramo et al., 1989). Overall, the data suggest detyrosination is the result of stabilization, rather than the cause of stable MTs (Bulinski & Gundersen, 1991). Nevertheless, Glu-MTs do seem to be a reasonable

'marker' for the stabilized MTs. Similarly, the acetylation of Lys40 for  $\alpha$ -tubulin from *Chlamydomonas reinhardtii* (L'Hernault & Rosenbaum, 1985; Ledizet & Piperno, 1987) and the phosphorylation of Ser444 for class III  $\beta$ -tubulin (Gard & Kirschner, 1985) appear to occur as a consequence of stabilized MTs. In contrast, ADP-ribosylation of both  $\alpha$  and  $\beta$  tubulins results in the inhibition of MT assembly and rapid depolymerization (Scaife et al., 1992). But in general, the post-translation modification of tubulin seems to be a consequence of MT stability rather than a causal factor. Thus the functional significance of these modifications remains unknown.

Microtubule-associated proteins (MAPs, see reviews Olmsted, 1986; Matus, 1988; Tucker, 1990; Goedert et al., 1991) actively modulate MT structure and function. MAPs can be classified into two groups: motor and structural MAPs. The motor MAPs consist of the mechanoenzymes, kinesin, dynein and dynamin (see reviews McIntosh & Pfarr, 1991; Vale & Goldstein, 1990), that interact with MTs to generate MT movement and sliding. Structural MAPs, which include MAP1 (380 kDa), MAP2 (280 kDa), MAP4 (200 kDa), and tau proteins (50-70 kDa), are directly involved in MT nucleation, growth, bundling, and even dynamic instability both *in vivo* and *in vitro* (Olmsted, 1986; MacRae, 1992). Synthesis of structural MAPs is developmentally and spatially regulated. For example, MAP2C is abundant in embryonic and newborn brain but disappears after birth, while MAP2B remains constant throughout development (Riederer & Matus, 1985). In addition, MAPs may become differentially localized at different sites within the same cell. For instance, following synthesis in the neuronal cell body, MAP2 localizes predominantly in the cell body and dendritic sites whereas tau localization is restricted to the axon (Berhardt & Matus, 1984; Binder et al., 1985). MAPs are

associated with MTs *in vivo* and *in vitro* (Olmsted, 1986; Drechsel et al., 1992; Brandt & Lee, 1993), stimulating the growth and stability of MT by decreasing catastrophe frequency and increasing the elongation rate of MTs. Heterologous expression of tau and MAP2 in transfected cells results in MT bundling (Kanai et al., 1989; Baas et al., 1991; Chen et al., 1992). Furthermore, MAP activity *in vivo* can be regulated by phosphorylation (Johnson, 1992; Scott et al., 1993), which appears to dampen the effects MAPs usually have on MT polymerization. The dramatic changes in MT arrays and dynamics during the interphase/mitotic transition are preceded by a wave of MAP and centrosomal phosphorylation events (Karsenti et al., 1987; Verde et al., 1990; Ohta et al., 1993).

In addition to classical MAPs, some basic proteins of diverse functions can also modulate MT stability. Erickson & Voter (1976) found that basic proteins, such as histones and RNase as well as the polycation, DEAE-dextran, could all substitute for MAPs in inducing MT polymerization. Centonze & Sloboda (1986) reported that a low MW basic protein fraction from extracts of *Bufo marinus* erythrocytes could cause MT bundling but not cross-linking. These authors suggested that this was due to the nonspecific ionic interaction between basic proteins and acidic tubulin that induced such an effect which might not be relevant to MT stability *in vivo* but rather an artifact of cell lysis. Recently, however, Multigner et al. (1992) found histone H1 localizes to sea urchin sperm flagella *in vivo*, and causes axonemal MT stabilization. Interestingly, a 20 kDa protein, defined as a stable-tubulin-only protein (STOP, Pirollet et al., 1989), was characterized as a Ca<sup>2+</sup>/calmodulin binding and regulated protein and found associated specifically with stable MTs that are resistant to the MT-destabilizing effects of Ca<sup>2+</sup>, drugs and low temperature, was subsequently defined as bovine myelin basic protein

(Pirollet et al., 1992). Therefore, the definition of specific as opposed to "opportunistic" MAPs needs to be clarified by more detailed *in vivo* studies.

Dynamic MTs are usually individual MTs, which are susceptible to MT depolymerizing drugs and are observed mostly in interphase and mitotic cells. These MTs associate with microtubule-organizing centers (MTOC, Pickett-Heaps 1969) and stochastically shrink and grow. In contrast, stabilized MTs exhibit quite different behavior: they are resistant to these drugs, some are even resistant to cold temperature; they are usually found in differentiated cells; they are not necessarily associated with MTOCs and they are invariably bundled into higher order arrays (Gelfand & Bershadsky, 1991; MacRae, 1992). Understanding the issues underlying the transition from dynamic MT arrays emanating from MTOCs in proliferating cells to the highly ordered and stable arrays in certain terminally differentiated cell types is an important step towards understanding the mechanisms by which the acquisition of specific cellular form and function are achieved during terminal differentiation. The marginal band (MB) MTs in nucleated erythrocytes, thrombocytes and mammalian platelets (Behnke, 1970; Barrett and Dawson, 1974; Cohen, 1978; Nemhauser et al., 1980) offers many advantages as an experimental system to study this issue. In the case of erythrocytes, the mature backbone structure has been defined biochemically and the successive cellular stages from early progenitors through mature erythrocytes are well characterized (Lazarides, 1987; Woods & Lazarides, 1988); erythrocyte uniform populations can be readily obtained at the different stages of commitment and differentiation. A detailed understanding of the mechanisms underlying the formation of this unique structure may provide a paradigm for understanding the elaboration of other stable MT arrays in more complex cells, e.g., neurons.

The MB is a highly stable coil of MTs encircling the equatorial plane under the cell membrane which serves to maintain cell shape and preserve integrity against deformation during circulation (Barrett and Dawson, 1974; Joseph-Silverstein & Cohen, 1984). Avian erythrocytes contain a unique erythroid  $\beta$ -tubulin isoform (c $\beta$ 6) that constitutes 90-95% of the total  $\beta$ -tubulin pool of these cells (Murphy & Wallis, 1983a, b). This c $\beta$ 6 tubulin is the most divergent (17% divergence) of the  $\beta$ -tubulin family (Murphy et al., 1987). The assembly of c $\beta$ 6 tubulin *in vitro* is characterized by lower critical concentration, longer lag time, fewer nucleation sites and longer individual MTs compared to brain tubulin (Murphy & Wallis, 1983b). Detailed measurement of c $\beta$ 6 assembly by X-ray scattering and video-enhanced dark field microscopy has verified these characteristics as well as revealed that catastrophe events are rare, rescue events are frequent and shrinking rates are slow (Trinczek et al., 1993). These data confirm the non-dynamic nature of c $\beta$ 6-containing MTs. Thus c $\beta$ 6 tubulin expression seems to be pivotal to the inherent structure and stable nature of MBs. However, c $\beta$ 6 tubulin alone is not sufficient for MB formation. Following MB depolymerization, the MB structure can be reformed from calf brain tubulin in detergent-treated chicken erythrocytes (Swan & Solomon, 1984). Interestingly, unlike other stable MTs marked by "Glu-tubulin", the MB MTs consist mostly of Tyr-tubulin (Gundersen & Bulinski, 1986). Tyr-tubulin in MB can not be detyrosinated by tubulin carboxypeptidase (TCP), even though an active form of this enzyme exists in mature erythrocytes (Beltramo et al., 1989). The rate of exchange between MB MTs and soluble tubulin is extremely low.

MB-associated MAPs have been proposed to play a role in MB formation, especially in bundling and stabilization. Protein extracts from *Bufo marinus* erythrocytes

were fractionated into high MW (>120 kDa), intermediate MW (70 kDa < IMW < 120 kDa), and low MW (<70 kDa) fractions. A 280 kDa protein in the HMW fraction which reacted with MAP2 antibodies was identified as a MT cross-linker while the LMW fraction could induce MT bundling but not cross linking (Centoze & Slobada, 1986). Recently, a 280 kDa protein (syncolin, Feick et al., 1991), which reacted with anti-MAP2 antibodies, was isolated from chicken erythrocytes, was found to associate with the MB in a MT- dependent manner and was proposed to be involved in MB bundling. A MAP2-related 280 kDa protein has also been found in bovine platelets (Tablin & Castro, 1991). In addition, platelet MBs are associated with a 210 kDa protein that appears to be similar to MAP4 (Tablin et al., 1988). In contrast, in other studies the only MAP that has been identified in chicken and frog erythrocyte MBs is tau (Murphy & Wallis, 1983b; Sanchez et al., 1990).

Another important feature of MB MTs is their lateral interaction with the cytoplasmic face of plasma membrane, a phenomenon also exhibited by MT arrays in some protozoa (Peck et al., 1991; Adoutte et al., 1991). It has been observed that both endogenous and exogenous tubulin (calf brain tubulin) can reassemble onto the original MB site following what appears to be complete depolymerization of MBs (Swan & Solomon, 1984; Miller & Solomon, 1984). These authors suggested that lateral factors (or determinants) specified the MB position in these erythrocytes. Subsequently an ezrin-like protein was found to be co-localized at the MB in a MT dependent manner (Birgauer & Solomon, 1989). This protein has both MT- and microfilament associated properties, raising the possibility that it could serve to link MB MTs to the erythroid spectrin-actin based membrane skeleton. Recently, it has been shown that ezrin contains a cytoskeletal and membrane-binding domain and so could potentially serve as a

membrane-cytoskeleton linking protein (Algrain et al., 1993). However, given that the ezrin-like protein appears to localize to MBs only after rather than preceding the formation of the MBs, it remains questionable whether it is the lateral factor determining the MB position. Two other proteins, 78 kDa and 48kDa, have also been found to associate both with the membrane skeleton and tubulin (Stetzkowski-Marden et al., 1991) and localize with MB. Clearly, there is much still to be learned about the mechanisms underlying the elaboration of this stable MT bundle and its linkage to the plasma membrane specifically at the equatorial plane of the cell.

MB formation is highly regulated during development as revealed by the following observations. Upregulation of c $\beta$ 6 expression occurs specifically in later erythroblastic stages (Murphy et al., 1986). This is reflected by the fact that MT tyrosination and detyrosination are still active in erythroblasts but little such activity occurs in mature erythroid cells (Beltramo et al., 1989). Although syncoilin and ezrin-like proteins are synthesized in early erythroblasts, these proteins remain soluble, localizing to the MB only after the MB has formed (Feick et al., 1991; Birgauer & Solomon, 1989). Also, whereas MTs in erythroblast cells are sensitive to MT destabilizing drugs, MBs in mature cells are drug-resistant. Following MB depolymerization, the reformation of MTs in mature cells occurs with high fidelity, but not in developing erythroblasts (Kim et al., 1987). Centrosomes are actively involved as MTOCs in erythroblasts but not in mature cells (Murphy et al., 1986; Miller & Solomon, 1984); MTs and assembled actin becomes colocalized only during later stages of erythropoiesis (Kim et al., 1987). Taken together, it is evident that MB formation requires sequential changes involving assembly of components that contribute the transformation from dynamic MT arrays in precursor erythroblasts into this ultra stable

MT structure in mature cells. Despite attempts to elucidate the developmental process of MB formation, many questions still remain unanswered. For instance, is the MB composed of a single MT coiling around the periphery of the cell or of many individual MTs bundled together? Where is the nucleation site (or MTOC) directing the formation of the MB? How do MTs interact with each other within the MB bundle? How do MBs maintain their high degree of stability? How is the MB anchored to the cytoplasmic face of the plasma membrane? Is it via a spectrin-actin bridge? What other components are involved in these events? Resolving these issues in the simplified avian erythrocyte system can provide a paradigm for understanding MT stability in more complex cell types, e.g., neurons.

### **The dual role of centrosomes: microtubule organizing center and cell cycle pacemaker**

In animal cells, centrosomes usually consist of a pair of centrioles surrounded by an electron-dense, amorphous pericentriolar material (PCM, Gould & Boisy, 1977). As the dynamic center of the cell," the true division center of the cell where division creates the center of the daughter cells" (from Mazia, 1984) and the general microtubule organizing center (MTOC, Pickett-Heaps, 1969), centrosomes serve as master determinants for the assembly of MT cellular arrays and for preserving the fidelity of cell division (see reviews, Brinkley, 1985; Mazia, 1984, 1987; Kimble & Kuriyama, 1992). Thus by organizing MT structures in interphase and mitotic cells, this organelle governs cell shape, motility, polarity, and division.

It has been well established both *in vitro* and *in vivo* with proliferating cells that centrosomes not only are the preferred sites for MT initiation and assembly but also provide the determinants for the properties of MTs emanating out from them, such as the number, length, orientation and lattice structure (Brinkley, 1985). Following drug or cold-temperature-induced depolymerization, regrowth of cellular MTs is usually initiated from the centrosomes in ordered arrays (Brenner & Brinkley, 1982) while regrowth in acentrosomal cytoplasts, is limited to a few MTs forming in random directions (Karsenti et al., 1984). The effect of adding centrosomes to purified tubulin *in vitro* indicates that centrosomes are the preferred site for MT nucleation rather than spontaneous assembly. In the presence of centrosomes, MT polymerization occurs at normal physiological tubulin concentrations, which are much lower than the critical concentration required for assembly of purified tubulin alone into MTs (Mitchison & Kirschner, 1984a). These observations clearly reveal the MT nucleation activity of centrosomes. Brenner & Brinkley (1982) demonstrated that besides nucleating MT assembly, the centrosomes of lysed 3T3 cells retain the capacity to assemble purified tubulins into discrete MT arrays of a finite length, number and orientation. The authors therefore suggested that centrosomes contained a finite number of MT nucleation sites. The dynamic instability model favored this hypothesis. Kirschner & Mitchison (1986) suggested that nucleation sites could determine the number and length of MTs. Increase in the number of nucleation sites could result in the increasing number of shorter but more dynamic MTs. Indeed, the increasing number of MT nucleating sites in centrosomes from cell-free extracts of *Xenopus* eggs is partly due to the accumulation of pericentriolar material (Ohta et al., 1993). It should be noted that centrosomes also control the lattice structure of assembled MTs. MTs assembled *in vitro* from purified tubulins (Evans et al., 1985) or *in vivo* from non-centrosomal MTOCs (Tucker, 1993) consist of 14 or 15 protofilaments

in their lattice structure. However, MTs assembled from centrosomes *in vivo* or *in vitro* are composed of 13-protofilaments (Evans et al., 1985). Moreover, centrosomes dictate MT orientation with the minus ends towards centrosomes (McIntosh & Euteneuer, 1984).

The nucleation function of centrosomes is localized in the PCM and is independent of the centrioles.(Gould & Borisy, 1977). Indeed, some cells, such as plant cells (Vandré et al.,1986) and an acentrosomal cell line in *Drosophila* (Debec et al., 1982), lack centrioles but contain components antigenically-related to the PCM. Mazia (1984) has suggested the centriole provides the morphological "address" and "valence" of centrosomes. Recent studies have shown the existence and duplication of centrioles may play a role in the cell cycle in those cell types that normally contain centrioles (Maniotis & Schliwa, 1991). It has been demonstrated by EM analysis that the PCM may exist as a cluster of electron-dense granules dispersed around the centrioles (Brinkley & Stubblefield, 1970; Wolfe, 1972) or a dense cloud a short distance away from the centrioles (Kuriyama et al., 1984). When cells blocked in mitosis by colcemid are allowed to recover, the PCM is associated with the multipolar spindle pole (Sellitto & Kuriyama, 1988; Maekawa et al., 1991) which eventually results in multipolar mitosis. Recently, Vidair et al. (1993) reported that heat shock could induce an alteration in the PCM of CHO, cells resulting in the formation of multipolar mitotic spindles and multi-nucleated cells. These observations support the concept that the PCM may contain a cluster of microtubule nucleating elements (MTNE, Gould & Borisy, 1977) which can be dispersed into numerous foci under various conditions (e.g., drug and heat- shock treatment). In turn, the multi-foci PCM alters the normal function of the centrosomes, eventually leading to cell death.

Until very recently, very little was known about PCM biochemistry.  $\gamma$ -tubulin was the first component to be identified as a centrosomal MT nucleating factor.  $\gamma$ -tubulin was first identified as the product of the *mipA* gene (Weil et al., 1986), an extragenic suppressor of *benA 33* (a heat-sensitive B-tubulin mutation, Oakley & Morris, 1981) in *Aspergillus nidulans*. Sequence analysis revealed that the *mip A* product is closely related to  $\alpha$ - and  $\beta$ - tubulin (29-30%, 33-35% identity, respectively) and hence it was named  $\gamma$ -tubulin (Oakley & Oakley, 1989). The disruption of the *mipA* gene resulted in a block of MT nucleation (Oakley et al., 1990). Immunofluorescence and EM analysis showed  $\gamma$ -tubulin localized to the spindle pole (yeast) or PCM (animal cells) (Sterns et al., 1991; Horio et al, 1991; Zheng et al, 1991). The  $\gamma$ -tubulin genes from *Homo sapiens*, *Drosophila*, *S. pombe* and *Xenopus* have since been cloned (Horio et al., 1991; Sterns et al., 1991; Zheng et al., 1991) and all share a high homology. Recently, it was reported that  $\gamma$ -tubulin also localizes in the vicinity of basal bodies of retinal photoreceptors and ciliated epithelia (Muresan et al., 1993) and a  $\gamma$ -tubulin related protein has been found associate with MT arrays of higher plants (Liu et al.. 1993). To assay  $\gamma$ -tubulin function, Joshi et al. (1992) microinjected antibodies raised against  $\gamma$ -tubulin peptides into lysed 3T3 cells. This blocked MT regrowth, following prior disassembly by nocodazole or cold, and inhibited mitotic spindle assembly. Taken together the evidence suggests that  $\gamma$ -tubulin is a conserved PCM protein in all eukaryotic species and appears to be involved in MT nucleation. However, the biochemical mechanisms by which  $\gamma$ -tubulin nucleates MT formation remain unclear. Very recent studies (Raff et al., 1993) have demonstrated that only 10-15% of  $\gamma$ -tubulin in *Drosophila* embryo extracts is competent to bind to MTs, with the majority binding with high affinity to two centrosomal MAPs (DMAP60 and DMAP190, Kellog & Alberts, 1992). In

contrast, Marchesi & Ngol (1993) reported that, in the presence of ATP or GTP, an assembly complex containing  $\alpha$ -,  $\beta$ -,  $\gamma$ - tubulins, heat shock protein 70 (hsp 70) and an elongation factor 1 (EF-1) could be formed *in vivo*. The authors suggested the complex may be the precursor for MT nucleation in centrosomes. Interestingly, hsp 70 and EF-1 like proteins have been found to localize in centrosomes (Rattner, 1991; Toriyama et al., 1988). Additional centrosomal components other than  $\gamma$ -tubulin have also been linked to PCM MT nucleation activity, including a 51 kDa EF 1-like protein of sea urchin spindle (Toriyama et al., 1988; Ohta et al., 1990); a 59 kDa SPA1-like protein (Snyder & Davis, 1988) in mammalian species; a 62-64 kDa calcium binding protein from HeLa & KE 37 cells (Moudjou et al., 1991); a 165 kDa centrin-related protein in PtK2 cells (Baron et al., 1991); the phosphorylated epitope recognized by MPM-2 Mab in CHO cells (Centonze & Borisy, 1990); centrophilin detected by 2D3 Mab in HeLa cell (Tousson et al., 1991); and a CHO2 antigen from CHO cells (Sellitto et al., 1992). All these proteins share in common the fact that they localize to the centrosome and that introduction of antibodies against them (added either by injecting into intact cells or by adding directly to lysed cells) prevents MT regrowth from centrosomes. However, little is known about the mechanisms underlying their molecular interactions within the centrosome or how such interactions might generate MT nucleation sites.

Even less is known about how centrosome become blocked in their MTOC activity, It has become increasingly evident that many differentiated cell types elaborate their unique MT arrays from dispersed non-centrosomal MTOCs (Tucker, 1992). Tassin (1985a, b) reported the disappearance of centrosomes when myoblasts fused into myotubes. The subsequent nucleation of MTs occurred at the periphery of nuclei, colocalizing with PCM components and Golgi structures. MTs in *Drosophila* wing

epidermal cells appear to be generated from the apical surface of these cells rather than any centrosomal structure (Tucker et al., 1986; Morgesen & Tucker, 1987). Many other examples have been found of cells containing centrosomes which are devoid of associated MTs, where the MT arrays appear quite independent of centrosomes. These include stable MTs in MDCK cells (Bré et al., 1990; Wacker et al., 1992), axonal MT bundles in neurons (Baas & Black, 1990; Reinsch et al., 1991; Tanaka & Kirschner, 1991), marginal band MTs in erythrocytes (Behnke, 1970; Murphy, et al., 1986; Birgbauer & Solomon, 1989) and MTs of mouse cochlea pillar cells (Tucker et al, 1992). This loss of centrosomal MTOC activity is not just restricted to highly differentiated cells containing highly stable MT arrays, it can also be found in undifferentiated cells. Absence of MTOC-functioning centrosomes has been reported in early mouse eggs and embryos (Calarca-Gillam et al., 1983). In several cases the lack of centrosomal activity is cell cycle related with the PCM becoming active in establishing spindle apparatus, reverting to an inactive state during interphase. Whether this is caused by inhibition of MT nucleating sites or the relocation of the PCM to some other organelle separate from the centrioles (e.g., the nuclear membrane) is unknown. What is the fate of disappearing centrosomes? Are there additional cellular sites equivalent to centrosomes? How can one centrosome be inactivated while another remains functional within the same cell? The answers to these questions should provide considerable insight into the nature of these fascinating organelles.

In addition to its MTOC function the centrosome appears to be intimately involved in cell cycle regulation, although there are many many controversies surrounding this issue. Centrosomes undergo their own cycle, usually duplicating in the G1-S phase. While some have suggested that this duplication requires the nucleus

(Kuriyama & Borisy, 1981) and protein synthesis (Phillips & Rattner, 1976), recent studies have indicated that centrosomes could continue their duplication in the presence of DNA or protein synthesis inhibitors (Raff & Golve, 1988; Gard et al., 1990; Sluder et al., 1990). Centrosomal duplication was considered to rely on pre-existing centrosomes (Mazia, 1984; 1987), but there is conflicting evidence that centrosomes may be generated *de novo* (Fulton & Dingle, 1971; Kallenbach, 1982; Schatten et al., 1986). To resolve these issues, Maniotis & Schliwa (1991) successfully removed centrosomes from BSC-1 cells and followed the behavior of acentriolar and centrosomal karyoplasts. They observed that centrosome-containing karyoplasts could continue to progress through the cell cycle after a slight delay but centrosome-free karyoplasts could only complete S-phase, enlarging beyond normal size. They elaborated an MTOC-like structure but failed to undergo further cell division. These results supported the concept that duplication required the presence of pre-existing centrosomes. However, these studies could not explain some exceptional cases such as the existence of acentriolar *Drosophila* cell lines (Debec, 1982). In support of the hypothesis that centrosomes and their duplication cycle might serve as check points in the cell cycle it has been shown that centrosomes closely interact with M-phase promoting factor (MPF, Nurse, 1990; Norbury & Nurse, 1992), a key factor inducing the entry of cell into mitosis. One major component of MPF, p34<sup>cdc2</sup> protein kinase, localizes in centrosomes and has been postulated to play a role in mitotic spindle formation (Bailly et al, 1989; Alfa et al., 1990, Rattner et al., 1990). Addition of p34<sup>cdc2</sup> and cyclin, the other major MPF component, to cell-free extracts from *Xenopus* eggs greatly increases MT instability and nucleation from centrosomes (Verde et al., 1990; Ohta et al., 1993). In turn centrosomes and mitotic spindle formation may be required for *cdc2* activation. It has been reported that MT depolymerization can prevent cyclin degradation and inhibit the tyrosine-dephosphorylation of p34<sup>cdc2</sup> which is the

key event for the activation of MPF (Alfa et al., 1990; Dessev et al., 1991). Recently, cyclin B was found associated with centrosomes in mitotic *Drosophila* cells (Debec & Montmory, 1992), as was the regulatory subunit (RII) of cAMP-dependant protein kinase (Decamilli et al., 1986; Keryer et al., 1993). Interestingly, a novel protein serine/threonine phosphatase has also been localized to centrosomes (Brewis, 1993). In summary although a multiplicity of phosphorylation events and compositional changes have been reported to occur in centrosomes during the cell cycle, the nature of the mechanisms underlying the centrosomal cycle requires further investigation.

Molecular genetic analysis in yeast, fungi, and *Drosophila* has provided considerable information on the role of centrosomes in the cell cycle, especially the coordination of centrosome duplication with the cell cycle. It is conceivable that if centrosomes fail to duplicate or duplicate more than once the following mitosis/meiosis will inevitably be abnormal. Indeed, many examples have illustrated that aberrant centrosomes/SPB produce anomalous or mutilpolar spindle structures, non-disjunction of chromosomes, chromosome loss and/or mutilpolar nuclei. These examples can be categorized into four groups. The first group, including genes of *kar1* (Rose & Fink, 1987; Vallen et al., 1992), *msh1* (Winey et al., 1991), *cdc31* (Baum et al., 1986), *ndc1* (Thomas & Botstein, 1986), *kem1* (Kim et al., 1990) from *S. cerevisiae*, *mes1* (Shimoda et al., 1985) from *S. pombe*, and *asp* (Gonzalez et al., 1990) and *mgr* (Gonzalez et al., 1988) from *Drosophila*, are defective in centrosome duplication. The cells carrying these mutant genes always display monopolar spindles, arrest of cell cycle or block of chromosome segregation. The molecular nature of these genes are mostly unknown except for *kar1* (Rose & Fink, 1987) and *cdc 31* (Baum et al., 1986). *CDC31* shares a high homologue with calmodulin which interacts with the mitotic spindle and

caltractin/centrin, a 20 kDa calcium binding centrosomal protein identified in *Chlamydomonas* (Huang et al., 1988 a; b). The second group, consisting of *spo15* (Yeh et al., 1986), *kip1*, *kip2* (Roof et al., 1992), *cin8* (Hoyt et al., 1992; Saunders & Hoyt, 1992) and *kar3* (Meluh & Rose, 1990) of *S.cerevisiae*; *cut7* (Hagan & Yanagida, 1990; 1992) of *S. pombe*; *bimC* (Enos & Morris, 1990) of *Aspergillus nidulans*; and *dal* (Sullivan et al., 1990), *ncd* (Kimble & Church, 1983; Endow et al., 1990; McDonald & Goldstein, 1990; Chandra et al., 1993), *nod* (Zhang & Hawley, 1990; Knowles & Hawley, 1991) of *Drosophila*, contains duplicated but unseparated centrosomes/SPBs which eventually result in a high rate of chromosome nondisjunction, nuclear fusion and a disorganized spindle structure. The gene product of *spo 15* shares a homology with the MT binding protein dynamin (Yeh et al., 1991). Sequence analysis reveals that *cut7*, *bimC*, *ncd*, *kar3*, *kip1*, *kip2* and *cin8* all contain a common domain that is similar to the motor domain of kinesin (Roof et al., 1992; Hoyt et al., 1992), indicating that the separation of duplicated centrosomes/SPBs involves a MT motor protein. However, these kinesin-like proteins act as minus end driven motors whilst kinesin is a plus end driven motor (McDonald et al., 1990; Walker et al., 1990). The third group, exemplified by the *eps1* gene in *S. cerevisiae* (Baum et al., 1988; McGrew et al., 1992), *cut1* in *S. pombe* (Uzawa et al., 1990) and *bimB3* in *Aspergillus nidulans* (May et al., 1992), uncouples the centrosome/SPB duplication from cell cycle, resulting in multiple centrosomes/SPBs and a failure to enter mitosis. The three gene products are highly similar and are probably the negative regulator of centrosome/SPB duplication. The final group are the components of centrosome/SPB which are involved in MT nucleation and spindle structure formation. Mutations in the *polo* (Sunkel & Glover, 1988) gene of *Drosophila*, the *dv* gene (Staiger & Cande, 1990) of maize, and disruption of the *spa1* (Snyder & Davis, 1988) gene of *S.cerevisiae* result in abnormal and multipolar spindles,

missegregated chromosomes and severe defects in mitosis/meiosis.

Considerable insight into the role of centrosomes in the cell cycle has been obtained from genetic studies in yeast, fungi and *Drosophila* and biochemical research in *Xenopus* oocytes/embryos and mammalian cultured cells. However, the role of the centrosome in cell-cycle control of terminally differentiating/differentiated cells expressing distinct stable MT arrays is much less well defined. A rare recessive mutation (bnbn) in turkey erythrocytes has been described that affects the final cell division step of bone marrow erythropoiesis, resulting in a binucleated phenotype of mature circulating erythrocytes (Bloom et al., 1970). Electron microscopy has revealed that the binucleation in turkey erythrocytes results from non-disjunction of chromosomes which is caused by malpositioning and aberrant function of the centrosomes occurring at the final mitotic step in definitive erythropoiesis (Searle & Bloom, 1979). It seems that the bnbn genotype results in a malfunction in the coordination of centrosomes specifically in the final division steps of definitive erythroid cells. The molecular nature of the bn gene and how it affects the centrosome function however are completely unknown.

### **The role of $\text{Ca}^{2+}$ and $\text{Ca}^{2+}$ binding proteins in microtubule and centrosome structure and function**

It is well known that high  $[\text{Ca}^{2+}]$  can inhibit MT polymerization in vitro (Weisenberg, 1972). Increase of cytosolic  $[\text{Ca}^{2+}]$  can also cause MT "intercalary destabilization and breakdown" in *Actinocoryne contractilis*, inducing an increased disassembly rate of  $3 \times 10^7$  subunits /s, which is  $10^4$  times faster than the regular MT

shrinkage rate (Febvre-Chevalier & Febvre, 1992). Purified *Xenopus* MBs by themselves can not be disassembled by  $\text{Ca}^{2+}$  but can be induced to disassemble by an unknown  $\text{Ca}^{2+}$ -activated factor (Gambino et al., 1985). Calmodulin has been found to associate with the mitotic spindle (Welsh, 1978;1979) and bind to MAP2 (Lee & Wolff, 1984; Kotani et al., 1985), tau (Sobue et al., 1981) and STOP (Pirrollet, 1989; 1992). Calmodulin enhances  $\text{Ca}^{2+}$ -dependent MT depolymerization in the presence of calcium. Another major  $\text{Ca}^{2+}$  binding protein, S-100, also regulates MT assembly-disassembly in an analogous manner to calmodulin (Dontio, 1991). However, how  $\text{Ca}^{2+}$ /  $\text{Ca}^{2+}$  binding proteins interact with MT or MAPs to effect MT assembly and disassembly remains unknown.

Many  $\text{Ca}^{2+}$ -binding proteins are also actively involved in centrosomal function which is reflected by the gross changes in centrosomal morphology induced by  $\text{Ca}^{2+}$ . Moudjou (1991) identified a 62-64 kDa  $\text{Ca}^{2+}$ -binding protein in Hela and KE3T centrosomes using antibodies against a 230-kDa contractile protein from Polyplastron cytoskeleton. This protein proved to be involved in centrosomal MT nucleation. Caltractin/centrin (McFadden et al., 1987; Huang et al., 1988a,b), a 20 kDa  $\text{Ca}^{2+}$  binding contractile protein localizing in *Chlamydomonas* basal bodies, was shown to be involved in basal body reorientation (Coling & Salisbury, 1992). Molecular analysis of caltractin/centrin (Huang et al., 1988a,b) indicated that the protein shared high homology with calmodulin and the CDC31 gene product of *S. cerevisiae* (Baum et al., 1986). Mutation of the CDC31 gene results non-duplication of spindle pole bodies in yeast (Baum et al., 1986).

Molecular analysis of  $\text{Ca}^{2+}$  binding proteins has revealed that most  $\text{Ca}^{2+}$  binding

proteins can be categorized into two major groups: the "EF-hand" family typified by calmodulin (Kretsinger, 1980) and the annexin family (Burgoyne & Geisow, 1989; Romisch & Paques, 1991). The members of the first family exhibit conserved structural features including multiple common repeated domains that consist of a loop of 10-12 amino acids flanked by two helices, the "E" helix and "F" helix (Kretsinger, 1980). This group includes calmodulin, troponin-C, parvalbumin, S-100 protein, calpain and calbindin to name a few (Nakayama et al., 1992). These proteins are usually involved in activation of enzymes, protein phosphorylation/dephosphorylation, assembly / disassembly of the cytoskeleton, and the buffering and transporting of intracellular  $\text{Ca}^{2+}$  (Persechini et al., 1989; Heizmann & Schafer, 1990). Members of the second family, which include calpactin, lipocortin, calelectrin, annexin I-X, exhibit 4 or 8 homologous repeats about 70 amino acids each. These proteins play a regulatory role in phospholipase A2 inhibition, membrane-membrane fusion, membrane-cytoskeleton linkage, and signal transduction (Burgoyne & Geisow, 1989). Although the majority of  $\text{Ca}^{2+}$  binding proteins fall into one of the two groups, there are many exceptions. For example, cadherins, a  $\text{Ca}^{2+}$  binding protein involved in  $\text{Ca}^{2+}$ -dependent intercellular interactions, does not exhibit any consensus sequence for any known  $\text{Ca}^{2+}$  binding motif (Geiger & Ayalon, 1992). Synaptic vesicle proteins (Kelly, 1993; Kelly & Grote, 1993), such as synaptophysin (Buckley et al., 1987; Wiedenmann et al., 1987) and synaptotagmin (Brose et al., 1992; DeBello et al., 1993), also lack any known  $\text{Ca}^{2+}$  binding motif sequence. Thus  $\text{Ca}^{2+}$  binding activity can be accommodated by multiple structural binding site motifs and is not limited to the EF-hand or annexin type  $\text{Ca}^{2+}$  cage. Much remains to be learned about the exact 3D nature of these  $\text{Ca}^{2+}$  binding sites and the mechanisms by which  $\text{Ca}^{2+}$  binding is transduced to specific effector pathways.

## The Scope of the Thesis

The initial focus of the thesis was to molecularly characterize the binucleated mutation (bnbn) in turkey erythrocytes and attempt to understand how this leads to the malfunction of the centrosomes that occur specifically at the final mitotic step during definitive erythropoiesis. By comparing the protein constituents of turkey erythrocytes isolated from normal (BnBn or Bnbn) and mutant (bnbn)birds, this laboratory observed that a band of  $M_r \approx 23$  K (p23) present in normal phenotype birds was missing in mutant birds. Once anti-p23 antibodies had been developed, it became apparent that mutant birds did not lack this protein but they expressed a lower  $M_r$  variant ( $M_r \sim 21$  K, p21). While genetic analysis was initiated in cooperation with Dr. Steve Bloom at Cornell University to ascertain whether indeed the p23/p21 allelism corresponded to the Bn/bn genotype, molecular characterization continued in our laboratory and provides the basis of this thesis. A battery of high-titer MAbs were raised and used to help purify the proteins for amino acid and sequence analysis. The antibodies were used to isolate cDNA clones whose identity was verified by protein compositional and sequence analysis. It has been found that p23 but not p21 may bind to  $Ca^{2+}$  directly despite the lack of any known  $Ca^{2+}$ -binding motifs. Immunofluorescence analysis has revealed that both p21 and p23 localize to the centrosomes, marginal bands (MBs) and nuclear membrane of erythrocytes. The genetic analysis suggested that the p23/p21 allelism was not equivalent to the Bn/bn genotype. Any further studies on the mutant p21 were blocked because of closure of the Cornell turkey farm due to lack of funding (Chapter two).

Consequently, detailed analysis has been carried out in chicken erythrocytes

which also express an immunologically related polypeptide of Mr  $\approx$ 23 K but are much easier to obtain in staged embryonic development. Molecular cloning revealed this protein to be highly homologous (90% identity) to turkey p23. Similarly to turkey p23, chicken p23 also acts like a  $\text{Ca}^{2+}$ -binding protein and localizes to MB and centrosomes. Developmental analysis showed that p23 only localizes to the MB after MB formation in bone marrow derived erythrocytes of the definitive lineage. Furthermore, p23 association to the MB is dependent on MB integrity and is modulated by intracellular  $[\text{Ca}^{2+}]$ . It is suggested that p23 is unlikely to be involved in MB formation but could be involved in MB stabilization after its formation and the interaction to MB and centrosomes may be induced in part by a decrease in intracellular  $[\text{Ca}^{2+}]$  during the terminal stages of definitive erythropoiesis (Chapter three).

The fact that p23 is a highly basic protein and localizes to avian erythrocyte MBs raised the possibility that this protein might be a specific microtubule-associated protein (MAP). However, the protein failed to co-purify with MTs during sequential cycles of MT assembly and disassembly. It does not appear to modulate MT assembly as measured by turbidity changes or to induce MT bundling as determined by electron microscopy. Thus p23 does not appear to interact directly with MTs or play a role in MT assembly or bundling at least in a simple binary fashion (Chapter four).

p23 was also found to be expressed in chicken thrombocytes, the only other avian cell lineage known to express a MB structure (Chapter three). Thus the protein appears to be expressed exclusively in MB-containing cells. Therefore, the question arose whether p23 homologues were expressed in MB-containing cell lineages of other vertebrate classes. Erythrocytes, thrombocytes and platelets of various species were

examined by immunofluorescence staining. They all contained cross-reactive components to chicken p23 localizing to the MB of other species. Cross species Southern blotting also revealed several bands in genomic DNA of other species. This would suggest that p23 expression is not limited to the avian species but is also found in species of other vertebrate classes. Definitive proof would require more detailed molecular characterization (Chapter five).

The overall summary of the results and future directions that would add to an understanding of p23 are discussed in Chapter six.

## Chapter Two

### **Existence of a normal and truncated form of p23 in turkey erythrocytes**

#### **Introduction**

The centrosome is a key organelle which plays a critical role in the process of cell division and also serves as the major microtubule (MT) organizing center (MTOC) for interphase MT arrays in most animal cells (Brinkley, 1985; Mazia, 1984, 1987; Kimble & Kuriyama, 1992). The centrosome undergoes its own cycle, duplicating between S<sub>1</sub>/G<sub>2</sub> to give rise to two pairs of centrioles, each surrounded by a cloud of pericentriolar material (PCM, Gould & Boisy, 1977). The PCM contains the MT nucleating activity of the centrosome. Prior to M phase the centrosomes segregate and migrate to the future spindle pole sites. The PCM structure undergoes concomitant changes in its MT nucleating activity, heralding the switch from centrosomally-directed cytoplasmic MT arrays of interphase cells to the dense MT spindle structure (Mazia, 1987; Kimble & Kuriyama, 1992). Not only are the centrosomally-directed MT dynamics of the spindle a critical part of orderly chromosomal segregation but also the centrosome location determines the spindle orientation and hence the future plane of cell division.

Although centrosomes were discovered over 100 years ago (from Mazia, 1984), their composition, structure and exact role in regulating the cell cycle remain poorly defined. However, their importance for cell cycle progression has been underscored by two avenues of research, local ablation experiments and genetic analysis in yeast,

*Aspergillus* and *Drosophila*. Centrosome-depleted BSC-1 cells become blocked in G<sub>2</sub> and fail to elaborate centrosomes *de novo* (Maniotis and Schliwa, 1991). Interestingly, acentrosomal cells are capable of regenerating cytoplasmic MTOC activity. Mutant strains of *S. cerevisiae* that are defective in spindle pole body (the fungal equivalent of the centrosome) duplication, e.g., *cdc31* (Baum et al., 1986), *kar 1* (Rose & Fink, 1987), and *mps 2* (Winey et al., 1991), display cell cycle arrest, also at the G<sub>2</sub> stage of the cell cycle. It has been postulated that the presence of the centrosome and its duplication step could provide check points for cell cycle progression (Maniotis and Schliwa, 1991; Bailly & Bornens, 1992). A reciprocal dependence of centrosomal replication on the DNA cycle (cell cycle) does not appear to exist. Thus inhibition of DNA synthesis (Raff & Glover, 1988) or protein synthesis (Sluder et al., 1990; Gard et al., 1990) or enucleating embryos (Picard et al., 1988) all failed to block centrosomal duplication. Spindle pole duplication can proceed abnormally; this occurs without inducing G<sub>2</sub> arrest but is generally manifested by a variety of abnormalities including anomolous spindle arrays, chromosome nondisjunction, chromosome loss and multinucleate phenotypes (Baum et al., 1988; Sunkel & Glover, 1988; Gonzalez et al., 1990; May et al., 1992). Of the cell division mutants which have been molecularly defined, a few have proved to be lesions in spindle pole body components. Thus, disruption of the *mipA* gene in *Aspergillus nidulans* results in poor MT assembly from the spindle pole body (Oakley et al., 1990). The *mipA* gene product has been identified as  $\gamma$ -tubulin, a unique tubulin isoform found in centrosomes and spindle pole bodies of all animal and fungal cells, respectively, examined to date (Oakley & Oakley, 1989; Sterns et al., 1991; Horio et al., 1991; Zheng et al., 1991).  $\gamma$ -tubulin has been postulated to function in MT nucleation (Joshi et al., 1992). *cdc31* is a homologue of centrin/caltractin, a 20kDa Ca<sup>2+</sup>-binding protein which is a component of *Chlamydomonas* basal body centrosomes (Baum et al.,

1986; Huang et al., 1988). Overall the data point to the importance of the centrosome and spindle pole body in cell cycle regulation but the exact mechanisms by which this is achieved remain poorly defined.

Although much of what is known about centrosome structure and function has been derived from studies of lower organisms that are more amenable to genetic manipulation, there are examples in vertebrates of nuclear abnormalities arising from centrosomal malfunction. One such mutation has been described in turkey. Designated the bbn genotype, this mutation is manifested by a binucleated phenotype in a fraction (up to 30%) of circulating bone marrow-derived erythrocytes and results in hemolytic anaemia (Bloom et al., 1970). Closer analysis by electron microscopy revealed that anomalous centrosomal positioning and aberrant function appeared to be the likely cause of the observed nondisjunction of the chromosomes (Searle & Bloom, 1979). Here we describe a protein, designated p23, that was found to exist as a truncated form in all the bbn individuals analyzed in the first generation. The longer p23 variant found in all normal Bn containing individuals, exhibits high homology with a chicken erythrocyte homologue (see chapter 3). Like the chicken protein, p23 undergoes a  $\text{Ca}^{2+}$ -induced gel shift in SDS-PAGE whereas the truncated p21 exhibits no such shift in apparent  $M_r$ . This difference in  $\text{Ca}^{2+}$ -sensitivity is further highlighted by the difference between the two forms in  $\text{Ca}^{2+}$ -sensitivity of complex formation in erythrocyte lysates. Molecular analysis indicates that although the core of p21 is homologous (92%) to p23, it contains a 62 amino acid deletion at the 3' end and appears to have acquired an additional 40 amino acids at the 5' end. Immunohisto-chemical analysis reveals that a fraction of p23 localizes to the marginal band of MTs (MB), the centrosomes and at discrete sites around the nuclear membrane. p21 exhibits a similar pattern of localization except it reveals the

presence of multiple centrosomes around the nuclei of mutant turkeys. Despite these promising observations, highlighting a centrosomal link between the p23/p21 and the Bn/bn phenotypes, parallel studies (Thomas Coleman, Elias Lazarides, Steven Bloom, unpublished data) revealed that the exact correlation between the expression of p23 with the Bn phenotype and p21 with the bbn phenotype that held up through the F<sub>2</sub> generation failed to show an absolute correlation in the F<sub>3</sub> generation.

## **Materials & Methods**

### **Materials**

Sephacryl-200, CNBr-activated Sepharose-4B, ProRPC HR5/10, FPLC, oligo-d(T) cellulose spun columns (Pharmacia, LKB); RNA ladder standards,  $\lambda$ EH10x™ vector (Novagen); endoproteinases (Boehringer Mannheim, Promega); Zeta-Probe nylon membrane (Bio-Rad); alkaline-phosphatase, fluorescein- and rhodamine-conjugated secondary antibodies (Cappel, Boehringer Mannheim); goat-serum, VectorShield™ (Vector Lab); Decaprime random primer labelling (Ambion); Polyvinylidene Difluoride (PVDF) Membrane™ (Millepore); Diafine film developer (Acufine).

### **Methods**

#### **1. Cells**

BnBn, Bbn and bbn turkey erythrocytes were obtained from lines developed by Steven Bloom (Cornell University) as previously described (Searle & Bloom, 1979).

Adult turkey blood was collected in 155mM Choline Chloride, 10 mM HEPES (pH 7.6) buffer, cells pelleted at 1000g for 5min, washed twice, passed through a cotton plug to remove white blood cells and pelleted. The erythrocyte pellet was lysed in 8 vol of hypotonic lysis buffer ( 5mM Tris-HCl, pH7.5, 5mM MgCl<sub>2</sub>, 1mM EGTA, 1mM Na<sub>3</sub>N, 5μg/ml PMSF, 5μg/ml leupeptin) for 30 min on ice followed by 30 min centrifugation at 10,000g , 4°C. The pellet was discarded and the supernatant (SN) was stored at -80°C until used. Erythrocytes from 8d turkey embryos were collected into heparinized PBS according to the procedure of Blikstadt & Lazarides (1983).

## **2. p23/p21 purification**

Turkey lysate SN was loaded onto a Sephacryl-200 gelfiltration column (2cm X 100cm) after adjusting the salt concentration to 50mM by addition of NaCl. Low molecular weight fractions containing p23 or p23 were pooled and applied onto an affinity column made by coupling (NH<sub>4</sub>)<sub>2</sub>SO<sub>4</sub>-purified monoclonal antibodies raised against p23 to CNBr-activated Sepharose-4B. The specifically-bound protein was eluted with citrate buffer (100mM citric acid, pH 3.0). The resulting eluant was adjusted to 0.085% TFA (trifluoroacetic acid) and loaded onto a ProRPC HR5/10 reverse phase column on a FPLC system. The column was eluted with a linear gradient of 0-100% acetonitrile in 0.1%TFA . Those fractions containing p23 were lyophilized using a speed vac and stored at -80°C. Protein purity was tested by SDS-PAGE and capillary electrophoresis.

## **3. Amino acid compositional analysis and partial protein sequence**

The affinity column eluant (about 70% pure p23) was run on 20% SDS-PAGE and electroblotted onto a Polyvinylidene Difluoride (PVDF) Membrane™. The protein band was visualized by its "water-tracer" on PVDF and cut out for *in situ* hydrolyzation as described (LeGendre and Matsudaria, 1988). Amino acid analysis was carried out by the California Institute of Technology sequencing facility.

Initially partial sequence analysis of p23 was carried out using *in situ* trypsin and V-8 proteinase digestion of p23 or p21 bound to nitrocellulose according to the method of Abersold (1987). Subsequently, once the reverse phase chromatography step was shown to yield p23 or p21 of high purity, the proteins were cleaved directly by endoproteinases (Arg-C, Asp-N, Glu-C, Lys-C) using the method recommended by the manufacturer (Promega). Separation of cleaved fragments and peptide sequencing was performed by the California Institute of Technology protein sequencing facility.

#### **4. Protein gel electrophoresis**

Proteins were separated by 20% SDS-PAGE and then either visualized by Commassie blue staining or transferred to nitrocellulose by the semi-dry method (Kyhse-Andersen, 1984). For Western blot analysis, following electroblotting onto nitrocellulose, the membrane was blocked in TBST (10 mM Tri-HCl, pH 8.0, 150 mM NaCl, 0.1% Tween-20, 1mM MgCl<sub>2</sub>, 1mMEDTA, 1mM Na<sub>3</sub>N) containing 5% non-fat milk for 1 h at 37°C, then incubated with anti-p23 MAb at a dilution of 1:1000 for 1 hr at room temperature, washed 3 X 10 min in TBST, and incubated with alkaline-phosphatase conjugated goat anti-mouse antibodies (1:7000) for 1 hr before being developed in BCIP (5-bromo-4-chloroindoxyl phosphate) and NBT (nitroblue tetrazolium). The membrane

was then kept in TBST plus 10 mM EGTA in the dark at 4°C.

To study the calcium effect on protein mobility under SDS-PAGE, 1 mM Ca<sup>2+</sup> was included in the gel sample buffer, running buffer and SDS-gel mix as described (Burgess et al., 1980). The protein band was visualized by Western blot analysis.

## **5. Production of monoclonal antibodies against turkey p23/p21**

Proteins in normal (BnBn) turkey erythrocyte lysates were separated by 20% SDS-PAGE. The protein of Mr~23 K was electroeluted from SDS-gel slices, dialyzed against TBS (10mM Tris-HCl, pH 8.0, 10mM NaCl, 1mM EGTA), lyophilized in a speed vac, and injected into mice together with RIBI adjuvant. Hybridoma production and culture were carried out by the California Institute of Technology monoclonal antibody facility. Five different monoclonal antibodies (16F32E1, 16F32H5, 20E12B1, 20E12H5, 20E11B2) were found to have high titer by both Western blotting and immunofluorescence (IF) analyses.

## **6. cDNA cloning and sequencing**

Total RNA was isolated from 8d turkey embryo erythrocytes by homogenizing in guanidium isothiocyanate and pelleting through cesium chloride (Sambrook et al., 1989). Poly(A<sup>+</sup>) RNA was then isolated using two cycles of oligo-d(T) cellulose spin columns and was used to construct an expression cDNA library in the EHlox vector. Mixed cocktails of monoclonal antibodies at 1:50 dilution were used to screen the resultant 1 X 10<sup>6</sup> plaques. 17 positive clones were plaque-purified to homogeneity and auto-subcloned

into pEXlox (Palazzolo et al., 1990). The sequence was determined by dideoxy sequencing of all the clones. 5'-RACE and direct PCR on the phage library were used to obtain the 5' flanking region of p23 and the remaining 5' reading frame of p21. For 5'-RACE, first stand cDNA synthesis was primed using a turkey p23 gene-specific anti-sense oligonucleotide p23-tur-GSP1 ([323-339]: 5'-ACG CCG TGC TCC TTC AT-3') derived from the cDNA sequencing data, the tailed cDNA was then amplified by a nested p23-tur-GSP2 ([123-139]: 5'-AGC GCC GGG TTC CGA ACC- 3'). For direct PCR, 10<sup>7</sup> pooled library phages were used directly as the template for the first amplification using two primers: the T7 gene 10 primer ( 5'-TGAGGTTGTAGAAGTTCCG-3', in the vector) and tur-AV3 (5'-ACGCCGTGCTCCTTCATGGC-3', in the reading frame). The PCR product was then used as a template for a second amplification using another two primers: EX5 (5'-GTTCCGCACCTCACCGC-3', a nested primer in the vector) and VL3 (5'-AGCAGCGCCGGGTTCCGAAC-3', a nested primer within the reading frame). The fragments were gel-purified, blunt-end ligated into the pBluescript-KS vector and sequenced.

## 7. Northern blot

1 µg Poly (A<sup>+</sup>) RNA was fractionated on a 1% agarose gel containing 2.2M formaldehyde, capillary blotted onto Zeta-Probe GT nylon membrane, UV cross-linked and baked for 1hr at 80°C. A <sup>32</sup>P-probe was generated by random primer labelling of a PCR fragment generated from the p23 reading frame (two primers were used for the fragment: p23-tur-Met5 [5'-ATGGATCGCGATCGGCGCGT-3'] and p23-tur-TGA3 [5'-AGCCGTAGTGCCCGCACAC-3']). This was then hybridized with the blot for 18

hr at 65°C in 0.25M Na<sub>2</sub>HPO<sub>4</sub>, pH 7.2, 7% SDS. The blot was then washed twice in 20mM Na<sub>2</sub>HPO<sub>4</sub>, 5% SDS for 30 min and twice in 20 mM Na<sub>2</sub>HPO<sub>4</sub>, 1% SDS for 30min at 65°C before being exposed to film.

## **8. Immunofluorescence**

Mature turkey erythrocytes were allowed to adhere onto coverslips in TBS (10mM Tris-HCl, pH 7.8, 150 mM NaCl, 5mM MgCl<sub>2</sub>, 1mM EDTA, 1mM Na<sub>3</sub>N) for 10min at room temperature, fixed for 10 min with 2% formaldehyde in TBS then permeablized for 10 min with 0.5% Triton X-100 in TBS. The cells were then incubated with either anti-p23 MAbs or anti human centrosomal antiserum for 1 hr and secondary antibodies ( RITC conjugated goat anti mouse IGg or FITC conjugated goat anti human IGg) for 45 min. The coverslips were mounted in VectorShield™ and visualized with a Leica microscope using a 63X lens. Images were photographed using Kodak TX 400 film shot at an ASA setting of 1600 and developed in Diafine.

## **Results**

### **Identification of p23 and p21 in turkey erythrocytes lysates**

As a first step to determine the biochemical nature of the bnb mutation, erythrocytes from BnBn and bnb turkeys were fractionated into hypotonic insoluble "cytoskeletal" and soluble fractions which were then analyzed by low (7.5) and high (20) percent acrylamide SDS-PAGE to check whether any differences in protein profiles between normal and mutant bird erythrocytes could be detected. 20% SDS-PAGE

revealed a Coomassie-blue stained band of apparent Mr~23K present in the soluble fraction of erythrocyte lysates from normal BnBn birds that was absent from all mutant bnb n birds tested (Fig. 1A). This protein was designated p23. Polyclonal and monoclonal antibodies raised against p23 all reacted with a single polypeptide band in Western blot analysis of normal turkey erythrocytes (Fig. 1B: lane 5). Interestingly, these antibodies revealed that rather than lacking p23 altogether, lysates from the bnb n birds all expressed an immunoreactive species of Mr~21 K (Fig. 1B: lane 1, 2, 4), with erythrocytes from heterozygotes expressing both 21 and 23 K immunoreactive species (Fig. 1B: lane 3). The fact that all hybridomas found to cross-react with p23 also cross-reacted with p21 strongly suggested that these two polypeptides were indeed homologous. No MABs were identified that showed specificity for only one of the variants.

### **Protein purification and analysis**

Gel filtration of hypotonic lysates resulted in a 10 fold purification of p23, removing 60-70% of the hemoglobin. p23-containing fractions were pooled and applied to an anti-p23 affinity column. This step yielded 75% pure p23. Ion-exchange chromatography proved to be unsuccessful as a further purification step as p23 failed to bind or elute as a discrete entity, indicating that p23 exhibited heterogeneity in its pI. However, reverse phase chromatography on FPLC yielded over 99% pure p23 eluting at 34% acetonitrile (Fig. 2).

Amino acid (AA) analysis was initiated with affinity-purified proteins from either BnBn or bnb n erythrocytes by fractionating the eluant by SDS- PAGE , transferring to

PVDF followed by digesting of p23 and p21 *in situ* prior to analysis. Fig. 3 shows the amino acid compositions of p21 and p23. The estimated M. Wt of p23 and p21 calculated from the amino acid composition analysis match exactly the Mr observed by SDS-PAGE. P23 contained an additional ~16 amino acids to p21, which yielded a molecular mass difference of ~ 2 kDa; this matched the difference in mobility observed between p23 and p21 on SDS-PAGE. The AA analysis confirmed that p21 and p23 were related but nonidentical polypeptides.

More direct evidence that p23 and p21 were related homologues was obtained by direct peptide sequence analysis. Preliminary attempts to directly sequence affinity purified protein by Edman degradation were unsuccessful because the N-terminus was blocked. Therefore, electroblotted proteins were initially cleaved *in situ* by trypsin, V-8 proteinase and CNBr. Once the final reverse phase step was developed, the 99% FPLC purified protein was used directly for digestion with endoproteinase Arg-C. All the partial peptide sequences obtained from both p23 and p21 are designated by the underlines in Fig. 4. All the partial sequences obtained from p23 were identical to those obtained from p21.

### **Isolation and characterization of cDNA clones**

Poly (A+) RNA was isolated from circulating erythroid cells of 8d turkey embryos expressing both p23 and p21 and used to construct an EXlox expression cDNA library. The resultant 10<sup>6</sup> plaques of the turkey library were screened with a cocktail of anti-p23 MAbs. 17 positive clones were identified, purified and auto-subcloned into the pEXlox vector. DNA sequencing analysis of all 17 clones revealed that 12 of the 17

clones all contained the polyadenylated 3' end through to the initiation codon ATG at the 5' end (Fig. 4A). Out of the remaining 5 clones, 4 contained sequences lacking the polyadenylated 3' and ATG 5' ends (Fig. 4B). The remaining clone proved to be a false positive.

The 12 polyadenylated cDNA clones were 1534 bases in length and contained a 627bp open reading frame which encoded a polypeptide of 208 amino acids. The sequence exhibited a perfect match with that deduced by partial peptide sequence analysis (see underlines of Fig. 4A). The encoded polypeptide had the same number of amino acids as p23 protein from chicken erythrocytes (Fig. 5B, also see Chapter three). The amino acid composition deduced from the cDNA sequence corresponded well to that determined experimentally with purified turkey p23. Moreover, the calculated molecular mass of the encoded protein (~22.3 kDa) showed good agreement with that estimated by amino acid composition and SDS-PAGE analyses. Taken together, these data suggest that all the 12 polyadenylated cDNAs represent the cDNA sequence of turkey p23.

The four unpolyadenylated cDNA clones contained an open reading frame of 447 bases which encoded a polypeptide of 149 amino acids lacking an initiating methionine. The polypeptide encoded by these truncated sequences contained sufficient homologous peptide sequence to the experimentally deduced sequences determined from purified p21 (Fig. 4B, underlines). The unpolyadenylated ones contained a TAG stop codon, which corresponds to 186 bases (or 62 amino acids) upstream from the stop codon in the p23 clones. These data taken together with the fact that p21 has 16 amino acids fewer than p23 (Fig. 3) imply that if p21 lacks 62 amino acids at the 3' end, the full length sequence must contain an additional ~40 amino acids at the 5' end. Two approaches were used to

search for any 5' clones that may have been missed by antibody screening: 5' RACE of turkey erythrocyte poly (A<sup>+</sup>) RNA and direct PCR using the library phages as templates. All fragments obtained by these methods yielded an almost identical 5' position within 6 base pairs of the first base shown in Fig. 4A. This difficulty in cloning the 5' region was taken to be indicative of a strong secondary structure at the 5' terminus of p23.

A computer search of the GCG Wisconsin data base revealed that p23 and p21 exhibited no significant homology with any other protein characterized to date. Turkey p23 shows high homology with chicken p23 (90% identity, Fig. 5B). The partial p21 sequence exhibited 92% identity within the first 146 amino acid sequence of p23 with a 100% homology in a 124 amino acid fragment (from AA 13 to 136) of the p23 sequence (Fig. 5A).

### **Northern analysis**

When a <sup>32</sup>P-labelled probe derived from the p23 coding region was used to hybridize poly (A<sup>+</sup>) RNA blot of BnBn, bnbn and Bbnb erythrocyte RNA, single bands of 4.0 Kb and 3.9 Kb were revealed in p23- and p21- expressing erythrocyte RNA respectively, with both bands being present in mRNA from heterozygote cells (Fig. 6). This confirmed that p21 and p23 were encoded by different mRNAs. However, the size of the transcripts by Northern blot analysis (~4.0 Kb) was substantially larger than that deduced from p23 cDNA (~1.6 Kb). This could be either indicative of marked secondary structure retarding transcript mobility during electrophoresis or of long uncloned 5' sequences or a combination of both.

**p23 but not p21 may bind Ca<sup>2+</sup> directly**

Initially, prior to the molecular analysis, we sought to determine whether the difference in Mr exhibited by p23 and p21 represented a real shift in molecular mass or was the result of charge-difference induced by some posttranslational modification. Pretreatment of the lysate with alkaline phosphatase or hydroxylamine (to remove fatty acyl chains) prior to SDS-PAGE and Western analysis failed to modify p23 and p21 mobility, indicating differences in phosphorylation or fatty acylation were not the root cause of the differences in mobility (data not shown). However, as shown in Fig. 7, the mobility of p23, but not p21, in SDS-PAGE was sensitive to the presence or absence of Ca<sup>2+</sup>. In the presence of 1mM Ca<sup>2+</sup> in the gel and running buffer, p23 exhibited an Mr of 21 K, comigrating with p21 in the mutant lysates, whereas in regular or EGTA containing gels p23 migrated with an Mr of 23 K. This Ca<sup>2+</sup>-induced shift in Mr is a characteristic of Ca<sup>2+</sup>-binding proteins (e.g., calmodulin) which retain their ability to bind to Ca<sup>2+</sup> even in the presence of SDS (Burgess, 1980), resulting in an apparent increase in mobility. Strikingly, p21 exhibited no such shift.

To investigate how calcium might modulate p23 and p21 properties, the erythroid hypotonic lysates were adjusted to 1mM CaCl<sub>2</sub> or 1mM EGTA and analyzed by gel filtration. As shown in Fig. 7B, turkey p23 segregated into both high molecular weight (HMW) and low molecular weight (LMW) species in the presence of 1 mM EGTA but the majority of p23 ran as LMW species in the presence of 1mM Ca<sup>2+</sup> (Fig. 7B). In contrast, the majority of p21 existed as HMW species in the absence of Ca<sup>2+</sup> shifting to a mixture of HMW and LMW species in presence of calcium (Fig. 7B). The HMW fractions exhibiting Mr > 200 K could represent either self-aggregation of p23 and p21 or

p23 (p21) complexes containing other unknown constituent polypeptides whose composite Mr exceeded ~200 K. The LMW species on the other hand, migrated in a manner consistent with being monomeric species. Thus the two variants appear to respond differently to calcium. p23 exists in an equilibrium between free monomer and a HMW-complex form in the absence of  $\text{Ca}^{2+}$ , but predominantly in monomeric form in the presence of  $\text{Ca}^{2+}$ . In contrast p21 exists in a HMW complex regardless of  $\text{Ca}^{2+}$  concentration, although there is a partial shift towards the monomeric pool in the presence of 1 mM  $\text{Ca}^{2+}$ . p21 is far less sensitive to  $\text{Ca}^{2+}$  modulation of HMW complex formation.

### **Immunocytochemical localization of p23 and p21 in turkey erythrocytes**

Immunofluorescence staining of both BnBn and bnb n turkey erythrocytes with the high titer Mabs is shown in Fig. 8. The antibodies stained two dot structures at each end of the nuclear membrane, the equatorial plane of the cell equivalent to the peripheral bundle of MTs, the marginal band, and at discrete sites around the nuclear membrane of BnBn turkey erythrocytes (Fig. 8). Double labelling with human antisera against centrosomes and anti-p23 MAb confirmed that the dot structures stained by the anti-p23 antibodies were indeed the centrosomes (Fig. 9). IF staining of bnb n erythrocytes revealed similar MB, centrosome, and nuclear membrane staining as observed in BnBn normal erythrocytes but also revealed the presence of an abnormal number of centrosomes (Fig. 8).

### **Discussion**

The data presented here reveal that p23, a unique MB and centrosomal-associated, Ca<sup>2+</sup>-modulated protein, exhibits allelism in turkeys. One allele encodes a variant that is highly homologous to chick p23 and exhibits the same Ca<sup>2+</sup>-sensitive gel shift. The other encodes a truncated variant, p21. Molecular analysis indicates that p21 contains a highly homologous region to the 150 amino acid sequence encoded by the full length cDNA for p23 but bears a 62 amino acid deletion at the 3' end. Given that the amino acid analysis indicates a Mr of 21K and that full length p21 should be about 16 amino acids shorter than p23, this implies that the sequence obtained here lacks 40 amino acids from the 5' end. The fact that all the unpolyadenylated clones ended at the same site at the 5' end and all subsequent attempts to clone the remaining 5' end resulted in clones that ended within 6 bp of this site suggests the likelihood of strong secondary structure upstream from this site. The two sequences diverge markedly upstream of Ala<sup>12</sup> and downstream of Ala<sup>137</sup> for p23. Taken together the data suggest that p21 may have arisen by insertion of approximately a 130 amino acid region into another gene. An obvious way to obtain the 5' end would be by genomic cloning but unfortunately this was not feasible due to the closure of the Cornell turkey farm.

p23 exhibits several interesting properties. It undergoes a Ca<sup>2+</sup>-dependent shift in Mr, under SDS-PAGE, a classically defined characteristic of direct Ca<sup>2+</sup>-binding proteins (Burgess et al., 1980). The mutant protein, in marked contrast, exhibits no such Ca<sup>2+</sup>-dependent Mr shift. The potential for direct Ca<sup>2+</sup> modulation of p23 interaction was analyzed by incubating hypotonic lysates in the absence or presence of 1mM Ca<sup>2+</sup> followed by gel filtration and Western blot analysis. These experiments revealed that in gel filtration chromatography p23 segregated into HMW and LMW fractions in the absence of Ca<sup>2+</sup>, but in the presence of Ca<sup>2+</sup> the majority p23 appeared in the LMW

portion. In contrast, p21 was found only in the HMW fraction in the absence of  $\text{Ca}^{2+}$  shifting to an equal mixture of HMW and LMW fractions in the presence of  $\text{Ca}^{2+}$ . Further studies are required to resolve whether the high MW complexes represent p23 or p21 polymers or complexes with additional polypeptides. It is noteworthy that the conditions under which the hypotonic lysates are prepared (30 min on ice in low salt buffer and addition of  $\text{Ca}^{2+}$  in the lysate) would also promote MT disassembly, even that of the stable MB.

Immunohistochemistry revealed that a fraction of both p23 and p21 pools were associated with the MB, centrosomes and distinct sites around the nuclear membrane. The putative centrosomal localization was confirmed by double IF staining with anti-p23 and human antacentrosomal antisera. Interestingly in mutant erythrocytes, p23 IgG revealed the presence of multiple centrosomes around the nucleus instead of the usual pair found at opposing nuclear ends in nucleated erythrocytes. The centrosomal localization was interesting in light of the fact that the root cause of the binucleated phenotype has been reported to cause anomalous centrosomal function, with mutant cells accumulating multiple chromosomes (Searle & Bloom, 1979). It has now been well demonstrated in *Drosophila*, yeast and *Aspergillus* that mutations in centrosomal or spindle pole body constituents can result in abnormalities in centriolar function and replication, leading to a variety of cell division abnormalities, including multipolar spindles, non-disjunction of chromosomes and multinucleated phenotypes. For example, the *esp1* mutant in *S.cerevisiae* (Baum et al., 1990; McGrew et al., 1992), *cut1* in *S.pombe* (Uzawa et al., 1990) and *bimB3* of *A.nidulans* (May et al., 1992) cause spindle pole body replication to be uncoupled from the cell cycle, resulting in multipolar spindle pole bodies. This in turn results in aberrant cell division from non-disjunction of

chromosomes. Heat shock or colcemid treatment of CHO cells induce the development of multiple spindle poles which in return results in multinucleated cells (Sellitto & Kuriyama, 1988; Maekawa et al., 1991; Vidair et al., 1993). Alternatively, multiple centrosomes/spindle pole bodies can arise from mutations whose primary effect is to cause blockage of chromosomal segregation, e.g., the polo mutation of *Drosophila* (Sunkel & Glover, 1988; L' Lamazares et al., 1991; Clay et al., 1993). In the bnb turkey mutation it is not known whether the multiple centrosome phenotype is the cause or effect of the bn mutation.

The interesting feature of bnb mutant birds is that the mutation is highly cell lineage specific and furthermore is highly differentiation stage specific, apparently occurring specifically at late stages of erythropoiesis. This is inferred from the fact that only a subset (~30%) of erythrocytes express the binucleate or abnormal nuclei phenotype. Any effects of the mutation at early stages, such as BFU-E, would presumably result in mitotic block before the cells reach the terminal differentiation steps. Given this leakiness in the binucleated phenotype the question arose whether indeed p21 represented the bn gene product. In studies carried out in parallel to the research presented here, all individuals of the F<sub>1</sub> generation showed an exact correlation between the expression of p21 and the bnb phenotype. In the F<sub>2</sub> generation of 59 individual birds analyzed, four had apparently normal looking erythrocytes but expressed exclusively p21. By the F<sub>3</sub> generation the correlation between Bn/bn and p23/p21 diverged further and now 12 individuals out of 283 birds examined expressing p23 exhibited the bnb phenotype. This latter result was difficult to reconcile with "leakiness" of binucleation and implied that the two sets of alleles were different (S. Bloom, T. Coleman, E. Lazarides, unpublished observation). The genetic data did

confirm, however that p23 and p21 represent two alleles that are inherited in simple Mendelian fashion. Thus we were left with the intriguing coincidence that p21 appears to represent an aberrant centrosomal associated protein.

Developmental analysis of p23 cytoskeletal associations during chick erythropoiesis to be described in chapter three revealed that this protein is not expressed in early erythroblastic stages but is upregulated around the late polychromatophilic erythroblast stages. However, cytoskeletal associations with the MB and centrosomes do not appear to occur until later, following upregulation of CB6 tubulin and the elaboration of the MB and just prior to the cell becoming postmitotic. It was postulated that these p23 interactions may be induced by lowering of the intracellular  $[Ca^{2+}]$  during these late stages. Having defined this, it would have been interesting to examine whether the truncated p21 form that appears to lack  $Ca^{2+}$  sensitivity, would behave any differently in the timing of its cytoskeletal associations and whether the onset of its expression might correlate with changes in centrosomal number. However, these experiments could not be carried out since mutant birds were no longer available. Subsequent attempts to identify p21-expressing turkeys in local populations were unsuccessful. Such studies could have proven instrumental in defining the consequences of losing  $Ca^{2+}$  sensitivity but not the ability to interact with the MB and centrosomes and may have provided a means to characterize the functional role of the normal p23 protein.

## Figure legends

Fig. 1. Turkey erythrocytes lysates were separated by 20%SDS-PAGE and analyzed by Commassiae Blue staining (A) and Western blotting (B). The nitrocellulose membrane was probed with anti-p23 MAb (20E12B1) at dilution 1:1000. Lane 1, 2 and 3 were lysates from binucleated (bnbn) turkey erythrocytes; lane 3 and 5 were from normal birds (BnBn or Bnbn). The MW of the protein markers are 14 K, 20K, 24K, 29K, 36K, 45K, and 66K, respectively.

Fig. 2. p23 purification by reverse phase FPLC. The affinity column eluants were pooled, adjusted to 0.085%TFA and loaded onto a FPLC ProRPC HR5/10 column. The column was washed with 10ml of 0.1%TFA and then with 10ml of a linear gradient from 0-25% acetonitrile in 0.1%TFA. The column was further eluted with a linear gradient from 25-50% acetonitrile in 50mL scale. The flow rate was 0.3 ml/min and the fractions were monitored at 280nm with 100% O. D. set at 0.05.

Fig. 3. Estimated amino acid composition of turkey p23 and p21. Affinity column eluant was separated by 20%SDS-PAGE and electroblotted onto PVDF membrane. The protein band (observed as a water tracer) was cut out, completely hydrolyzed and analyzed.

Fig. 4. Peptide and cDNA sequence of p23 and p21. The polyadenylated clones encoded a 208 amino acid polypeptide with the first methionine at N-treminus (A). The unpolyadenylated clones encoded a 150 amino acid peptide sequence lacking first methionine of the p23 sequence (B). The partial protein sequence derived from purified

protein, represented by the lines underlying the cDNA sequence, exhibits an exact correlation with the polypeptide sequence of the encoded cDNA clones.

Fig. 5. Protein sequence comparison between turkey p21 and p23 (A) and turkey p23 and chicken p23 (B). The turkey p21 shares 92% homologue with turkey p23 in a 146 amino acid fragment (from amino acid Met<sup>1</sup> to Tyr<sup>146</sup> of p23) and 100% homologue in a 124 amino acid fragment (from amino acid Thr<sup>13</sup> to His<sup>136</sup> of p23) (A). Chicken p23 share 90% homologue with turkey p23 (B).

Fig. 6. Northern blot analysis of p23/p21 size in turkey erythrocytes from 8d embryos. 1 $\mu$ g of poly (A<sup>+</sup>) RNA from Bnbn (lane 1) BnBn (lane 2) and bnb (lane 3) erythrocytes were probed with <sup>32</sup>P radio-labelled p23 gene. The exposure time is 24hr.

Fig.7. Different Ca<sup>2+</sup> effects on p23/p21. Panel A: lysates from normal (lane 1 and lane 3) and binucleated (lane 2) turkey erythrocytes were separated by SDS-PAGE under conditions of either 1mM EGTA or 1mM Ca<sup>2+</sup> included in the sample buffer, gels and running buffer. Distinct double bands were displayed in EGTA-containing SDS-PAGE while the upper band (p23) shifted to Mr of 21 K in the presence Ca<sup>2+</sup>. Panel B: gel filtration of turkey (p23 or p21 containing) erythrocyte lysates which included either 1mM EGTA or 1mM Ca<sup>2+</sup>. In the presence of EGTA, p23 was separated as HMW and LMW fraction while p21 stayed in HMW fractions. In the presence of Ca<sup>2+</sup>, p23 appeared mostly in LMW fractions while p21 were in both HMW and LMW fractions.

Fig. 8. Immunofluorescence localization of p23/p21 in normal (A, B and C) and

binucleated (E, F, G, H and I) turkey erythrocytes using anti-p23 MAb (20E12B1). The marginal band (the peripheral rim), and centrosomes (dots) as well as some discrete sites along the nuclear membrane stained in both normal and binucleated cells. However, multiple dots (3 or more) were shown in binucleated cells while only two dots appeared in normal cells. D is a control. Bar = 10 $\mu$ m.

Fig. 9. Double immunofluorescence labelling with anti-p23 MAb (A) and anti-centrosome antisera (B) in turkey erythrocytes. The dot structures stained by anti-p23 MAb were co-labelled with anti-centrosome antisera. C: cells stained with anti-centrosome antisera alone. Bar = 10 $\mu$ m.

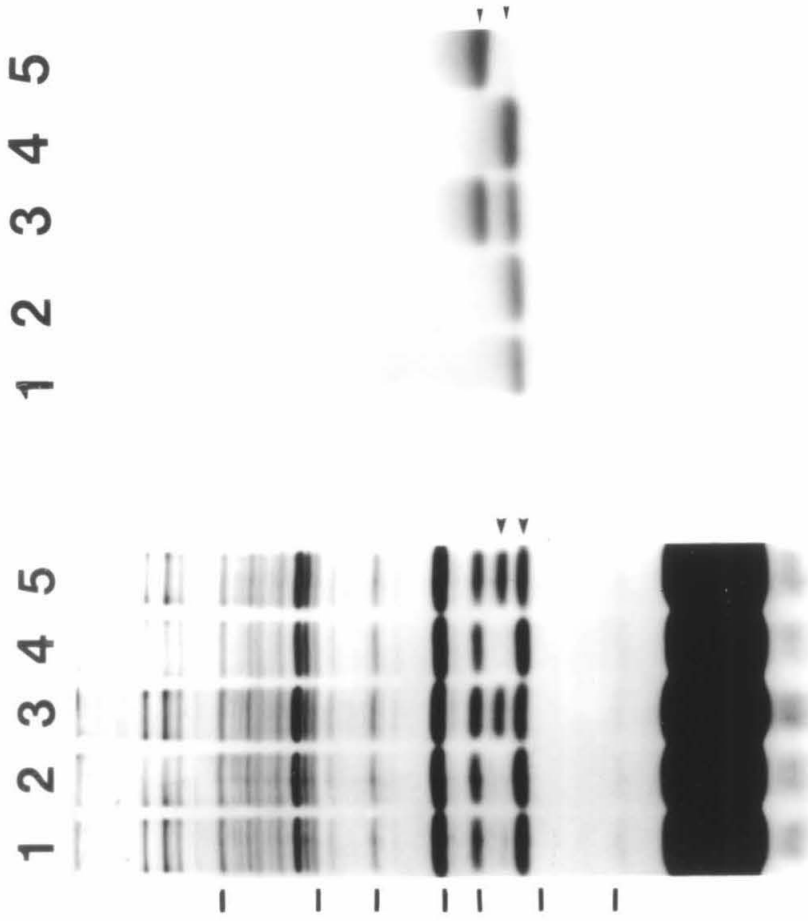


Figure 1

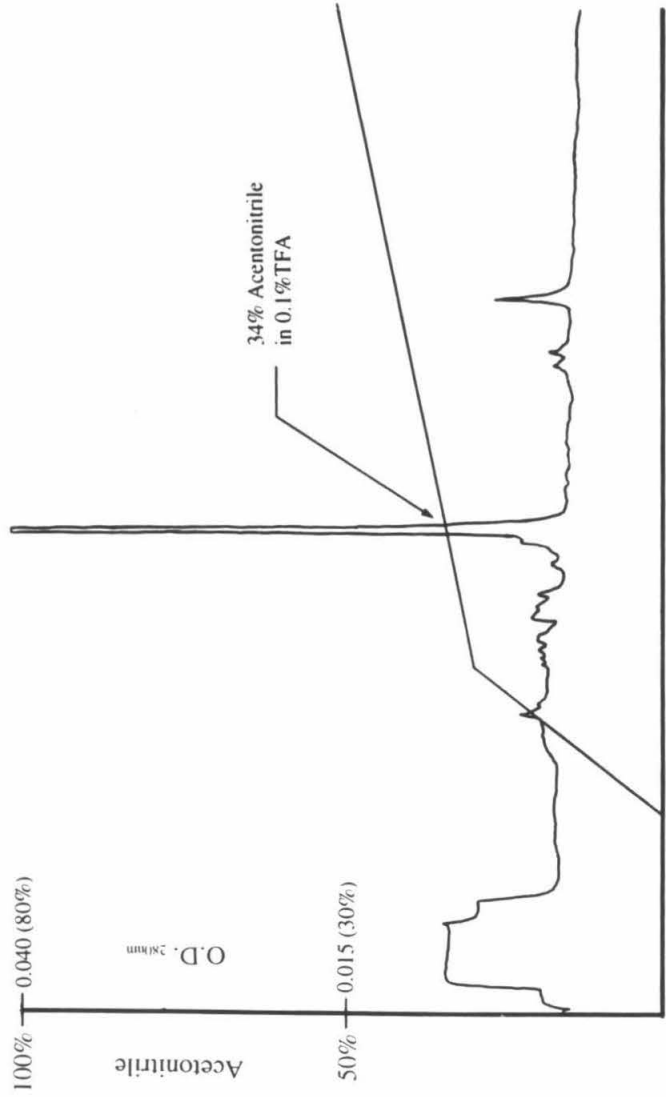


Figure 2

Amino Acid Compositional Analysis

<u>Amino acid</u>	<u>Turkey p23</u>		<u>Turkey p21</u>		<u>Difference</u>	
	<u>MW/AA</u>	<u>No. AA</u>	<u>MW</u>	<u>No. AA</u>	<u>MW</u>	<u>No. AA</u>
Asp	133	6	798	6	798	
Glu	147	11	1617	9	1323	2
Ser	105	14	1470	12	1260	2
Gly	75	23	1725	20	1500	3
His	155	3	465	3	465	
Arg	174	15	2610	12	2088	3
Thr	119	15	1785	15	1785	
Ala	89	26	2314	26	2314	
Pro	115	12	1380	11	1265	1
Tyr	181	3	543	3	543	
Val	117	24	2808	22	2574	2
Met	149	3	447	3	447	
Cys	121	ND		ND		
Ile	131	22	2882	20	2620	2
Phe	165	6	990	6	990	
Lys	146	7	1022	6	876	1
<u>Total</u>		195	23,511	179	21,503	16
						2,008

Figure 3

### A. cDNA sequence and encoded polypeptide of polyadenylated clones

GACGGCGGCGATGGATCGCGATCGGGCGCTGGCGCTGTTCTGGGGGACACCGGAGGACCGGAAAGGAGACGCTGAAGAGGGCGCTGCAGGA 90

M D R D R R V A L F G A T G R T G K E T L K R A L Q E 27

GGGTTTCTCGGTTTCGGCCCTGGTTTCGGAACCCGGCGCTGCTGCCGCCGACCGCGCTCCGTGCCGGGTGGTTTCGCGGGGACGCGCTGCG 180

G F S V S A L V R N P A L L P P D A A P C R V V R G D A L R 57

CCGCGCGATGTGAGCGAGGCGCTCAGGGGGCAGCGCGCTCATCGTCGCCCTGGGGACCCGAGGAGACATCGGTCCCACCACCGTCTCT 270

R A D V S E A V R G Q R A V I V A L G T R G D I G P T T V L 87

GTCAGACAGCACCCGGAACATCGTGGCCGCATGAAGAGCACGCGCTCCGCAAAGTGGTGCATGTCGTCTGCCCTTCTGCTCTGGGA 360

S D S T R N I V A A M K E H G V R K V V A C L S A F L L W D 117

CCCTGACAAGGTCCCGCTGAGGCTGCGGGCGCTGACCGAGGACACCGCGCGATGCACGCGTGTCTGAGCGAGGCTGGGGCTGCAGTACGT 450

P D K V P V R L R A L T E D H A R M H A V L S E A G L Q Y V 147

GGCTGTGATGCCGCCACATCGCGGATGACAAACCGCTGACGGAGGCTACAAGGTGACAGTTGGTGGCACTGGCGGTGGCTCCCGTGT 540

A V M P P H I A D D K P L T E A Y K V T V G G T G G G S R V 177

CATCTCCACGCGCTGACCTGGCGCATTTCTCTGTCGCTGCCTCAGCACCCAGTTCGATGGGAAGAGCGTCTACGTGTGCGGGCACTA 630

I S T P D L A H F L V R C L S T T E F D G K S V Y V C G H Y 207

CGGCTGAGCGGGGACGCGGGGACATCGTGGGACATCGTGGGACATCGTGGGACATCAGGGGACGTTGAGGAGACATCAGGGGGAC 720

G \* 208

ATTGAGGGGACACTGGGGGGACATTTGAGGATATCGAGGGGACATCGGGGGACATTTGTGTGACACCATGGGGACATCAGGGAGGCATC 810

ATGGGGACATCATGGGGACATCATGGGGACGTTGAGGAGACATCATGGGGACATCATGGGGACGTTGAGGAGACATCAGGGGGACATTTG 900

AGGGACACTGGGGGACATTTGTTGGGATATCGAGGGGACACTGGGGACATTTGTGTGACACCATGGGGACATCAGGGAGGCATCATGGGGA 990

CATCATGGGGACATCAGGGGGACGTTGAGGGGGACATCATGGGGGACATCATGGGGGACATCATGGGGAGATTGAGGGGGGACTGGGGGGGG 1080

TCAGGGGGGATTGTTGGGGGGATCGAGGGGGGATTGAGGGGGCTGTGTGACACCAAGGTCCTGAATGCCATTTGGGGGGCTGTTGAAGAAC 1170

ATCGATGATATTAGAGGTGCTTTGGCCAAACTAAGCGAGCTGCATGCTTACATCCTTAGGGTGGACCCAGTGAACCTCAAGCTGCTTTCC 1260

CACTGTATCTCTGCTCCGTGGCTGCCCGCTATCCAGTATTTCACCCAGAGTTCATGCTGCATGGGACAAGTTCCTGTCCACGTTT 1350

CCTCTGTTCTGACTGAGAAGTACAGATAAATGGCTTCCACACTGGGTTAGGGATGTGCACCAATGGCACACAACAGCTGCCAAGTTCCTGG 1440

GGTATTCTCTCATGACGTCCTCCCTCACTGTCTCATGACGGGGCTCAGCCATCTGCAGACCACAATAAATAATCAACTGAAAAA 1530

AAAA 1534

### B. cDNA sequence and encoded polypeptide of unpolyadenylated clones

GGCTATCGCGATCCATCGCGATCGGAGCGTGGCGCTGTTCTGGGTGACCCGGGAGGACCGGAAAGGAGACGCTGAAGAGGGCGCTGCAGGA 90

A I A I H R D R S V A L F G S T G R T G K E T L K R A L Q E 30

GGGTTTCTCGGTTTCGGCCCTGGTTTCGGAACCCGGCGCTGCTGCCGCCGACCGCGCTCCGTGCCGGGTGGTTTCGCGGGGACGCGCTGCG 180

G F S V S A L V R N P A L L P P D A A P C R V V R G D A L R 60

CCGCGCGATGTGAGCGAGGCGCTCAGGGGGCAGCGCGCTCATCGTCGCCCTGGGGACCCGAGGAGACATCGGTCCCACCACCGTCTCT 270

R A D V S E A V R G Q R A V I V A L G T R G D I G P T T V L 90

GTCAGACAGCACCCGGAACATCGTGGCCGCATGAAGAGCACGCGCTCCGCAAAGTGGTGCATGTCGTCTGCCCTTCTGCTCTGGGA 360

S D S T R N I V A A M K E H G V R K V V A C L S A F L L W D 120

CCCTGACAAGGTCCCGCTGAGGCTGCGGGCGCTGACCGAGGACACCGCGCGATGCACGTTGCTGACCAAATCTCAACCCCACTACTA 450

P D K V P V R L R A L T E D H A R M H V V L T K S Q P H Y \* 150

GTCCCTCATGCTGATTCTCCCTCTTATAATCATAGCTAGTCAAGGCCATTTACAGCACGAACCTCACTACGAAAAACAATAATTTATC 540

TCAACCCCTCATCATTAITCAACCAATTTATCATCTAGCCCTTCTCATCAACAGAACTAATATTATTCTACACTCATTTGACGCCACCCCTA 630

Figure 4



**1 2 3**

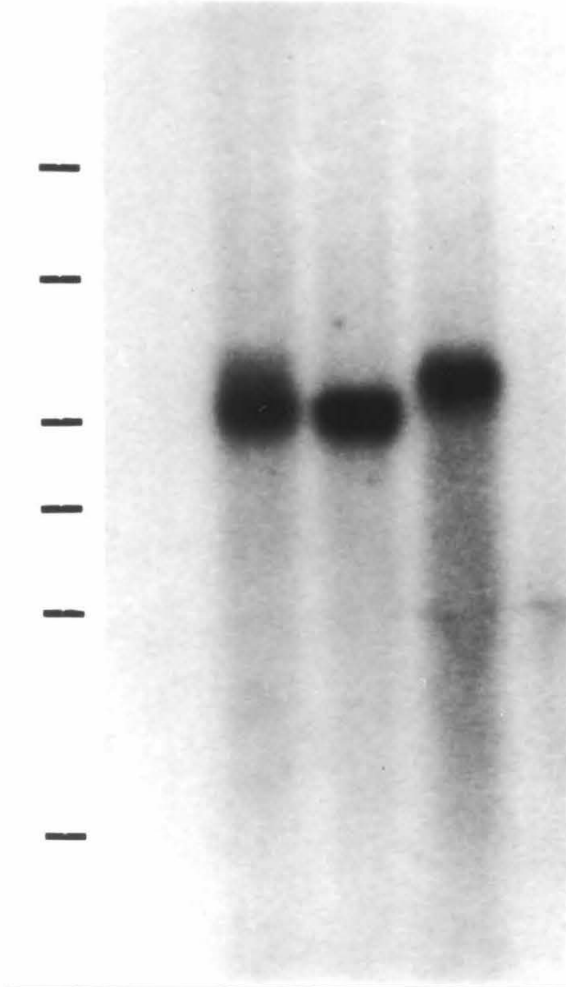
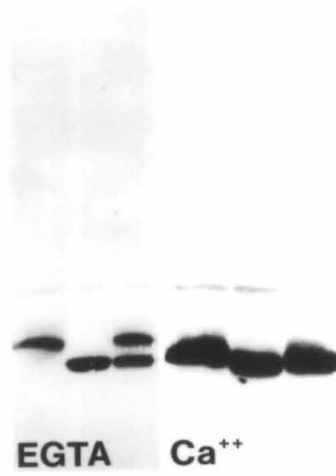


Figure 6

**A**

1 2 3 1 2 3

**B**

EGTA

Ca<sup>++</sup>**P 23****P 21**

Fraction No. →

Fraction No. →

Figure 7

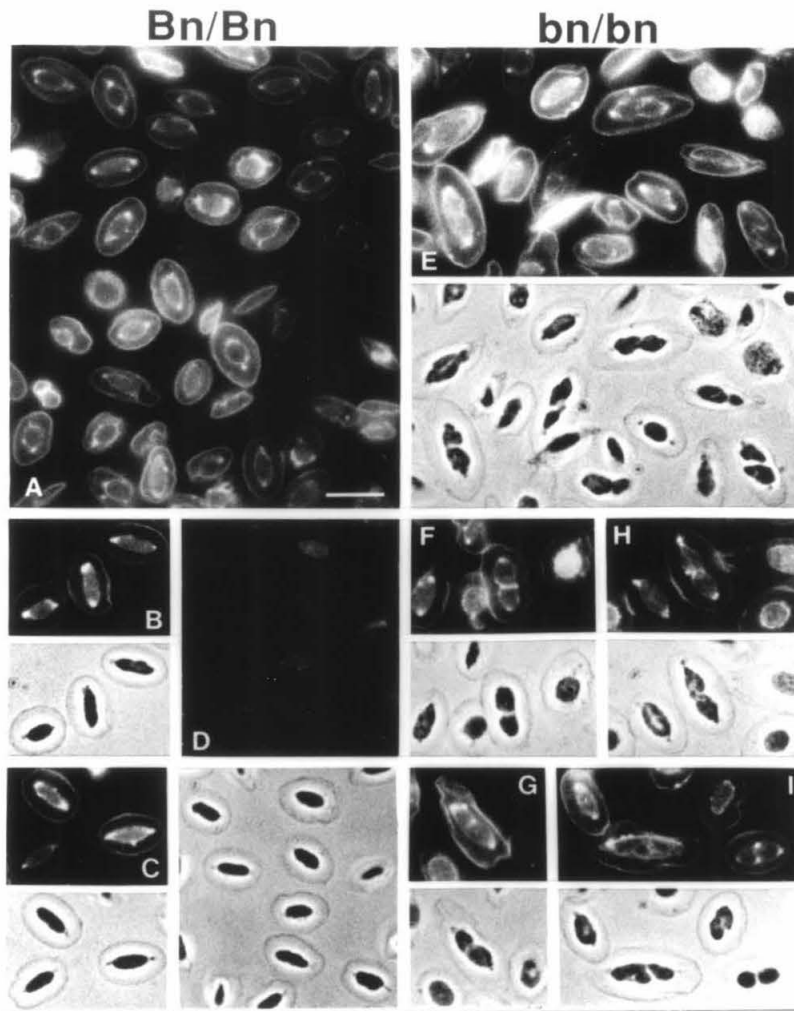


Figure 8

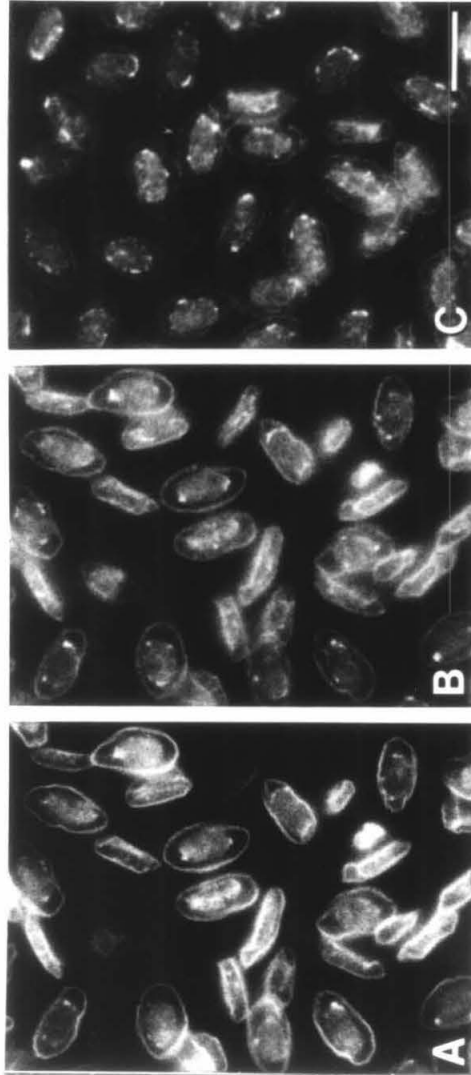


Figure 9

## Chapter Three

### **Identification of a Novel Ca<sup>2+</sup>-Binding Protein that Specifically Associates with the Marginal Band and Centrosomes of Chicken Erythrocytes.**

Jian Zhu, Elias Lazarides and Catherine Woods

Department of Pharmacology, Merck Research Laboratories, West Point PA, 19486

**Abstract.** We have identified a novel Ca<sup>2+</sup>-binding protein, p23, that is expressed specifically in avian erythrocyte and thrombocyte lineages. Sequence analysis of this 23K protein reveals that it bears no homology to any known sequence, in particular, to other Ca<sup>2+</sup>-binding proteins. In mature definitive erythrocytes p23 exists in equilibrium between a soluble and a cytoskeletal bound pool. The cytoskeletal fraction is associated with the marginal band of microtubules (MB), centrosomes and nuclear membrane under conditions of low free [Ca<sup>2+</sup>]. An increase in free [Ca<sup>2+</sup>] to 10<sup>-6</sup>M is sufficient to induce dissociation of >95% of bound p23 from its target cytoskeletal binding sites yet this [Ca<sup>2+</sup>] has little effect on calmodulin-mediated MB depolymerization. Analysis of p23 expression and localization during erythropoiesis in conjunction with heterologous p23 expression in tissue cultured cells demonstrate that p23 does not behave like a typical microtubule associated protein (MAP). Furthermore, p23 association with the MB, centrosome and nuclear membrane occurs specifically in the later stages of embryonic and bone marrow derived erythropoiesis. Strikingly, these interactions do not occur in mature cells of the primitive lineage although p23 is expressed in these cells. A marked stabilization and accumulation of p23 correlates with the onset of p23-cytoskeletal interactions in definitive erythroid cells, even though p23 expression is being markedly

downregulated at this time. We hypothesize that the mechanism of p23 association to the MB and centrosomes may be induced in part by a decrease in intracellular  $[Ca^{2+}]$  during the terminal stages of definitive erythropoiesis.

## Introduction

Microtubules (MTs) are a major class of structural filaments which play a key role in a wide repertoire of cellular events: mitosis and meiosis, ordered vesicle transport, intracellular organization of Golgi and lysosomal vesicles and cell shape and motility to name but a few (for reviews see: Dustin, 1984; Kirschner & Mitchison, 1986). MTs exhibit an inherent property of dynamic instability both *in vitro* (Mitchison & Kirschner, 1984 a,b; Horio & Hotani, 1986) and *in vivo* (Cassimeris et al., 1988; Schulze & Kirschner, 1988) and it is this property that is pivotal for plasticity in cellular MT organization and function. However, highly stable MT configurations exist within some terminally differentiated cell types such as in axonal processes of neurons (Baas & Black, 1990; Reinsch et al., 1991; Tanaka & Kirschner, 1991), polarized epithelial cells (Bré et al., 1990; Wacker et al., 1992), myocytes (Tassin et al., 1985) and in platelets (Kenney & Linck, 1985; Kowit et al., 1988) and the nucleated erythrocytes of non-mammalian vertebrates (Behnke, 1970; Murphy, et al., 1986; Birgbauer & Solomon, 1989). While considerable effort has been directed towards the elucidation of the mechanism and functional significance of dynamic instability the mechanisms underlying the conversion of these normally dynamic structures into highly ordered arrays remain less well defined although MT interactions with MT associated proteins (MAPs) can promote profound changes in MT form and function (for rev. see Olmsted, 1986; Chapin & Bulinski, 1992).

The marginal band of MTs (MB) provides a relatively simple system to study the morphogenesis of stable MT arrays. MBs, found in nucleated nonmammalian erythrocytes and thrombocytes as well as mammalian platelets, consist of a highly ordered, stable MT bundle that underlies the plasma membrane at the equatorial plane of the cell (Behnke, 1970; Barrett and Dawson, 1974; Cohen, 1978; Nemhauser et al., 1980). The MB helps confer and maintain the elliptical shape of these cells as well as aid in resisting the deformation forces experienced during circulation (Barret and Dawson, 1974; Joseph-Silverstein & Cohen, 1984). To understand how the strict temporal and spatial regulation of the biogenesis of this structure is achieved during erythropoiesis several questions need to be addressed. How does the shift from an equilibrium of free tubulin with dynamic MTs towards a predominantly stably polymerized pool of tubulin occur? What factors induce the extensive bundling that occurs prior to the interaction of a MB structure with the plasma membrane? What determines the specific site of MB-plasma membrane interaction? How is the gradual reduction in the number of MTs in cross section within the developing MB and concomitant rigidification of the MB achieved? The answer to the first can be explained in part by the fact that 90-95% of  $\beta$ -tubulin in mature avian erythrocytes consists of an erythrocyte-specific isoform,  $\text{c}\beta 6$  (Murphy & Wallis, 1983a; Murphy et al., 1987), which in vitro polymerizes at a lower critical concentration and forms fewer and longer MTs compared to brain  $\beta$ -tubulin (Murphy & Wallis, 1983b, 1985, 1986). The presence of the MT bundling MAPs, MAP2 and tau (Murphy and Wallis, 1985) and the MAP2-related polypeptide, syncolin (Feick et al., 1991), suggests that the expression of these proteins would both induce bundling and increase MT stability. To address the issue of which factors dictate the precise spatial association of the MB with the membrane, reconstitution studies have been carried out on isolated erythrocyte ghosts prepared after depolymerization of the

endogenous MBs (Miller & Solomon, 1984; Swan & Solomon, 1984). These studies showed that in itself  $\alpha\beta$  tubulin is not essential for the formation of MBs, since brain tubulin can reform MBs (Swan & Solomon, 1984). This indicates the presence of predeterminants at the membrane that nucleate and direct the generation of the new MB. Polypeptides that colocalize to the MB in a manner that is not dependent on intact MB MTs include an 80 kD ezrin-like polypeptide with both MT and actin microfilament association properties (Birgbauer & Solomon, 1989) and the 78 and 48 kD polypeptides which interact with both the spectrin-actin based membrane skeleton and MTs (Stetzkowski-Marden et al., 1991). Whether any of these polypeptides indeed represent the MB predetermining factors remains to be determined. Whilst many facets of MB biogenesis are in the process of being elucidated, the final issue of what are the ultimate steps in erythropoiesis that determine the final MB morphology and rigidity remains unanswered.

The precise arrangement and dynamics of most MTs in eukaryotic cells is mediated by nucleation centers known as MT organizing centers (MTOCs, Pickett-Heaps, 1969; Brinkley, 1985; Mazia, 1987; Kimble and Kariyama, 1992). These MTOCs serve to dramatically lower the critical tubulin concentration required for polymer nucleation and can dictate the orientation and number of MTs emanating out from them (Brenner & Brinkley, 1982; Mitchison & Kirschner, 1984a). Centrosomes generally serve as the major MTOC for cytoplasmic MTs. They typically consist of a pair of centrioles connected by a system of  $\text{Ca}^{2+}$ -activated filaments with the parental centriole being surrounded by a cloud of diffuse pericentriolar material or centrosomal matrix (PCM, Gould & Borisy, 1977). It is this material that contains the MT nucleation sites which can persist (be regenerated) in cells from which centrioles have been

microsurgically removed (Maniotis and Schliwa, 1991). Remarkably, the number of MTs radiating out from the centrosome is relatively constant for any given cell type, with lysed cells free of preexisting MTs directing a similar characteristic number of MTs upon addition of exogenous tubulin (Brenner & Brinkley, 1982). The characterization of auto-antibodies directed against centrosomes and the development of centrosome isolation procedures have enabled the characterization of some of the centrosomal components. Indeed many antigens found in the PCM appear to be conserved in other organisms, for example plant cells, that lack centrioles but contain distinct cytoplasmic MTOCs (Calarco-Gilliam et al., 1983; Vandré et al., 1986; Mogensen & Tucker, 1987). The centrioles consist of a unique tubulin variant  $\gamma$ -tubulin, which exhibits considerable stability against cold and drug induced depolymerization (Oakley and Oakley, 1989; Stearns et al., 1991). Additional centrosomal components include a 51kD GTP/ITP binding protein that has been postulated to be the key component of the MT nucleating granules (Sakai and Ohta, 1991) and a number of  $\text{Ca}^{2+}$ -dependent polypeptides, including a 62-64kD protein (Moudjou et al., 1991) and the homologue of caltractin/centrin, the  $\text{Ca}^{2+}$ -binding contractile protein in *Chlamydomonas* centriolar basal bodies (McFadden et al., 1987; Baron and Salisbury, 1988; Huang et al., 1988a,b). The centrioles and associated pericentriolar material undergo their own cell cycling. In late S and early  $G_2$  phase the centrioles duplicate giving rise to two pairs which at the onset of M phase, separate and migrate to form the axes of the spindle pole (Robbins & Gonatos, 1964; Reider & Borisy, 1982; Mazia, 1987). This centrosomal duplication is critical for entry into the M phase of the cell cycle (Mazia, 1987; Maniotis & Schliwa, 1991). What regulates the block of centrosomal duplication and hence cell cycling observed in many terminally differentiated cell types remains unknown although multiple phosphorylation and  $\text{Ca}^{2+}$ -mediated events are clearly involved (Kimble & Kuriyama, 1992). Furthermore,

it is becoming increasingly evident that in many terminally differentiated cells the MTOC function of the centrosome is also blocked (Tassin, 1985; Mogensen & Tucker, 1987; Tucker et al., 1992). For example, frog and avian nucleated erythrocytes possess a pair of centrosomes which are devoid of any associated cytoplasmic MTs and are associated at each end of the nucleus (Euteneuer, 1985).

We report here the identification and characterization of a new calcium binding protein of  $M_r$  23 kD, p23, that is expressed specifically in avian erythrocytes and thrombocytes. This protein is a  $Ca^{2+}$ -binding protein which exists in equilibrium in soluble and cytoskeletally bound pools in a  $Ca^{2+}$ -dependent manner. The cytoskeletal fraction localizes to the MB, centrosomes and the nuclear membrane of mature erythrocytes in the presence of low free cytoplasmic  $Ca^{2+}$ . As the free  $Ca^{2+}$  levels approach  $10^{-6}M$ , p23 dissociates from these structures and becomes diffusely localized in the cytoplasm. Analysis of the full-length cDNA sequence reveals no homology with any known sequence; in particular it shares no homology with any of the known MAPs. Furthermore, it lacks any conventional consensus sequence for the EF hand  $Ca^{2+}$ -binding domain (Nakayama et al., 1992) or the  $\approx 70$  amino acid stretch of repeat structures encoding the  $Ca^{2+}$ -binding site of the annexin family (Burgoyne & Geisow, 1989) suggesting that p23 may represent a novel third class of  $Ca^{2+}$ -binding proteins. Detailed analysis of p23 expression and localization during erythropoiesis with respect to the development of the MB and the progression through terminal differentiation indicate that its association with both the MB and centrosomes occurs during the final tailoring step of these two structures as the cells become postmitotic. We speculate that this protein may play a regulatory role in a  $Ca^{2+}$ -dependent manner in establishing the extreme stability of these structures in the mature erythrocyte.

## Materials and Methods

### Materials

Anti-chick c $\beta$ 6 erythrocyte tubulin rabbit antisera was generously provided by D. Murphy (Dept. of Cell Biology and Anatomy, John Hopkins Univ. Sch. Med.) and anti-human centrosomal antisera by W. Brinkley (Dept. of Cell Biology, U. of Alabama in Birmingham). anti-chicken  $\beta$ -spectrin rabbit antisera has been characterized previously (Nelson & Lazarides, 1983). The following were obtained commercially:  $\beta$ -actin probe (Clontech); mouse monoclonal anti- $\beta$ -tubulin IgG (Amersham); fertilized chicken eggs (SPAFAS); cell strainer (Falcon); Sephacryl-200, CNBr-activated Sepharose-4B, ProRPC HR5/10, FPLC, oligo-d(T) cellulose spin column, QuickPrep mRNA purification, pSVL (Pharmacia, LKB); RNA ladder standards,  $\lambda$ EHlox<sup>TM</sup> vector (Novagen); endoproteinases (Boehringer Mannheim, Promega); Zeta-Probe nylon membrane (Bio-Rad); alpha-MEM, Lipofectin, Superscript RT (Gibco); alkaline-phosphatase, fluorescein and rhodamine conjugated secondary antibodies (Cappel, Boehringer Mannheim); goat-serum, VectorShield<sup>TM</sup> (Vector Lab); pCDNA1, pRC/RSV (Invitrogen); Decaprime random primer labelling (Ambion); calcium ionophore A23187, nocodazole, GTP (Sigma).

### Methods

#### 1. Preparation of cells

Mature chicken RBCs were collected in 155mM Choline Chloride, 10 mM

HEPES (pH7.6) buffer, washed twice, passed through a cotton plug to remove white blood cells and pelleted at 1000g for 5min. The blood pellet was resuspended with 8 vol of hypotonic lysis buffer (5mM Tris-HCl, pH7.5, 5mM MgCl<sub>2</sub>, 1mM EGTA, 1mM Na<sub>3</sub>N, 5µg/ml PMSF, 5µg/ml leupeptin) for 30 min at 4°C and then centrifuged at 10,000g 30min, 4°C. The pellet was discarded and the SN was stored at -80°C until used.

Bone marrow was expelled from the tibia of 1d-1wk old chicks into α-MEM medium with 1mM GTP, gently dispersed through an 18-gauge needle and the suspension filtered through a cell strainer. Cells were then washed twice and counted.

Erythrocytes were isolated from d2-4 chick embryos by first teasing the blood islands of isolated blastodiscs to release some of the primitive erythrocytes and then further dispersing the blastodisc with an 18g needle. The cell suspension was filtered through a cell strainer and the MEM suspension overlaid on a Percoll cushion (density 1.065 g.ml<sup>-1</sup>). After centrifugation at 800g for 10min, the pellet, consisting predominantly of yolk-free primitive erythrocytes was resuspended in MEM. From 5 day to 18 day of development, the erythrocytes were collected as previously described (Blikstadt & Lazarides, 1983).

Chicken embryonic fibroblast (CEF) primary cultures were made from 10-11d chick embryos as follows: the muscle mass was minced in Hank's buffer, trypsinized at 37°C for 15 mins, filtered through a Falcon cell strainer and pelleted. The cell pellet was resuspended in CEF medium (1% 1Xtryptose phosphate buffer, 0.5% penicillin/streptomycin, 5% chicken serum, 10% newborn calf serum in F10 medium) plated and cells allowed to attach for 1-2 hrs before changing the culture medium to

remove the unattached cells (the bulk of non-fibroblast cells).

Chicken organs were dissected from animals perfused through the left ventricle with heparinized PBS (50U/ml heparin in PBS). The tissues were placed into either 4M guanidinium thiocyanate solution for RNA extraction (Sambook et al., 1989) or tissue lysis buffer ( 50mM Tris-HCl, pH 7.8, 50 mM NaCl, 1% SDS, 0.5% Triton, 100µg/ml PMSF, 1U/ml aprotinin, 10 µg/ml leupeptin, 1mM Na<sub>3</sub>N) for protein preparation and homogenized with Polytron PT 3000 (Brinkmann). Protein lysates were then briefly sonicated.

## **2. Purification of p23**

Turkey or chicken lysates in hypotonic lysis buffer (5mM Tris-HCl, pH 7.8, 1% SDS, 0.5% Triton, 100µg/ml PMSF, 1U/ml aprotinin, 10 µg/ml leupeptin, 1mM Na<sub>3</sub>N) were applied to a Sephacryl-200 column (2cm X 100cm). Fractions containing p23 protein were identified by Western blot analysis, pooled and loaded onto an affinity column made by coupling (NH<sub>4</sub>)<sub>2</sub>SO<sub>4</sub> purified monoclonal antibodies against p23 to CNBr-activated Sepharose-4B. Bound protein was eluted with 100mM Citric acid, pH 3.0. The eluant was adjusted to 0.085%TFA (trifluoroacetic acid) and then loaded onto a ProRPC HR5/10 FPLC column. The column was eluted with a linear gradient to 100% acetonitrile in 0.1% TFA at 0.3 ml/min. p23 came off as a peak at 34% acetonitrile. The final purity was tested by SDS-PAGE, capillary electrophoresis and amino-acid composition analysis.

## **3. Amino-acid compositional analysis and peptide sequence**

FPLC-purified protein was loaded onto a 20% SDS-Polyacrylamide gel, electrophoresed at a 100 volt constant voltage, electroblotted onto a Polyvinylidene Difluoride (PVDF) Membrane™, and hydrolyzed in situ (LeGendre and Matsudaria, 1988). The hydrolyzate was solublized away from PVDF and derivatized prior to amino acid analysis, which was carried out by the protein sequencing facility at the California Institute of Technology.

Initially, for peptide sequencing, initially, partially purified protein (post affinity column) was separated by 20% SDS-PAGE and electroblotted onto nitrocellulose as described (Blikstadt & Lazarides, 1983). The membrane bound protein was subjected to *in situ* trypsin and V-8 protease digestion using the methodology of Aebersold et al.(1987). Subsequently, highly purified protein from the reverse phase column was first lyophilized and then directly cleaved by various endoproteinases (Arg-C, Asp-N, Glu-C, Lys-C). Cleavaged fragment separation and peptide sequencing were carried out by the protein sequencing facility at the California Institute of Technology.

#### **4. Generation of antibodies against p23**

Monoclonal antibodies were made by the monoclonal antibody facility at the California Institute of Technology using crudely purified turkey protein electro-eluted directly from a preparative 20% SDS-gel (Lazarides, 1982). Five different monoclonal antibodies (16F32E1, 16F32H5, 20E12B1, 20E12H5, 20E11B2) were found to have high titer by both Western blotting and immunofluorescence (IF) analysis. Polyclonal antibodies against chick p23 were generated in rabbits using FPLC purified p23 together

with two different synthetic peptides derived from the partial protein sequencing analysis of p23 (turkey and chicken) that were conjugated to KLH (keyhole limpet hemocyanin). The sequences of the three synthetic peptides were: DPEKVPTRLRALTEDHARM, PPHIADDKPLQEAYEVQVGG, TGGSRVISTPDLAHFLVRA. After the fourth injection, a high titer anti-p23 antisera was obtained. The polyclonal antibody was then affinity purified from rabbit serum using purified p23 coupled to Sepharose 4B.

### **5. cDNA cloning and sequencing and 5' RACE**

An expression cDNA library was constructed in  $\lambda$ EH10x™ vector from Poly(A)+ RNA isolated from erythrocytes of 8 day chick embryos. Mixed cocktails of monoclonal antibodies at 1:50 dilution were used to screen the  $1 \times 10^6$  plaques. 28 positive clones were plaque purified to homogeneity and auto-subcloned into pEX10x (Palazzolo et al., 1990). The sequence (16-1461) was determined by dideoxy sequencing of all the clones. The 5' non-coding region (1-16) was cloned by 5' RACE (Loh, 1991). First stand cDNA was primed using a p23 gene-specific antisense oligonucleotide p23-GSP1 ([323-339]: 5'-ACG CCG TGC TCC TTC AT-3'), the tailed cDNA was then amplified by a nested p23-GSP2 ([123-139]: 5'-AGC GCC GGG TTC CGA ACC-3'). The fragment was then blunt-end ligated into pBluescript-KS and sequenced.

### **6. Northern blot hybridization**

Total RNA was isolated from perfused tissues by homogenizing in guanidium isothiocyanate and pelleting through cesium chloride (Sambrook et al., 1989). Poly(A)+ RNA was then isolated using oligo-d(T) cellulose spun columns. Poly(A)+RNA from

cultured cells and erythroid cells was isolated by directly passing the guanidium isothiocyanate lysate over an oligo-(T) spun column by the QuickPrep mRNA purification protocol (Pharmacia). For Northern analysis, RNA was fractionated on 1% agarose gel containing 2.2M formaldehyde and capillary blotted onto Zeta-Probe GT nylon membrane. The blot was UV cross-linked, baked for 1hr at 80°C and hybridized with <sup>32</sup>P-radiolabeled probes at 65°C for 18 hr in 0.25M Na<sub>2</sub>HPO<sub>4</sub>, pH 7.2, 7% SDS. The blot was then washed twice in 20mM Na<sub>2</sub>HPO<sub>4</sub>, 5% SDS for 30 min and twice in 20 mM Na<sub>2</sub>HPO<sub>4</sub>, 1% SDS for 30min before being exposed to film. For reprobing, the blots were stripped with 0.1SSC, 0.5%SDS for 20 min at 95°C before being rehybridized with a second probe.

Two probes were used : a) the reading frame of p23 was generated from the p23 clone in pEXlox by PCR using the two primers: p23-MET-5 (5'-ATG GAT CGC GAT CGG AT-3') and p23-TGA-3 (5'-TCA GCC GTA GTG CCC GC-3'); b) a PCR derived fragment of chicken erythrocyte  $\beta$ -tubulin ( $\beta$ 6) cDNA (Murphy et al., 1987). Two primers were derived from regions of the  $\beta$ 6 gene that are least conserved compared other tubulins:  $\beta$ 6 sense (5'-GAT ATT GCC GGA AAC TAC TGT-3') and  $\beta$ 6 antisense (5'-GAG GAT GGC ATT ATA GGG C-3'). First strand cDNA was synthesized by Poly(A)<sup>+</sup>RNA from bone marrow using SuperscriptRT and then was used as template for PCR. The PCR fragments were agarose gel purified by electroelution, and radiolabeled by Decaprime<sup>TM</sup> random primer labelling.

## **7. Ca<sup>2+</sup>-induced motility shift and Western blot analysis**

Proteins were separated by 20% SDS-PAGE and electroblotted onto

nitrocellulose by the semi-dry method. The nitrocellulose was then blocked with TBST (10 mM Tris-HCl, pH 8.0, 150 mM NaCl, 0.1% Tween-20, 1 mM MgCl<sub>2</sub>, 1 mM EDTA, 1 mM Na<sub>3</sub>N) containing 5% nonfat milk for 1 hr, incubated with first antibody in TBST containing 3% BSA, and then incubated with alkaline-phosphatase conjugated to goat anti-rabbit or goat anti-mouse IgG before being developed with 5-bromo-4-chloroindoxyl phosphate (BCIP) and nitroblue tetrazolium (NBT). The membrane was then kept in TBST containing 10 mM EDTA, 5% nonfat milk.

To study the comparative effects of calcium vs. EGTA on the electrophoretic mobilities of p23 protein in SDS-PAGE, 1 mM CaCl<sub>2</sub> or 1 mM EGTA was included in the sample buffer, running buffer and SDS-gel as described (Burgess et al., 1980)

## 8. Immunofluorescence

Immunofluorescence (IF) was performed essentially as previously described (Granger & Lazarides, 1982), with the following modifications. Erythrocytes from murine primitive lineage, chick primitive lineage, chick definitive lineage, and chick adult were allowed to adhere to coverslips directly; bone marrow cells were allowed to settle on ProNectinF™ coated coverslips; cultured cells were grown on coverslips. Adherent cells were fixed in 2% formaldehyde in TBS (10 mM Tris-HCl, pH 7.8, 150 mM NaCl, 5 mM MgCl<sub>2</sub>, 1 mM EDTA, 1 mM Na<sub>3</sub>N) and permeabilized with 0.5% Triton X-100 in TBS. Polyclonal anti-chicken β-spectrin, anti-chicken cβ6, anti-centrosome, anti-chicken p23, mAb against chicken β-tubulin, or mAb against chicken p23 were added onto the coverslips in TBS, 2% goat serum, and incubated for 1 hr at 37°C. For double labeling, the two different antibodies were mixed and added. After being rinsed in TBS

and incubated in 10% goat serum in TBS, the cells were incubated in fluorescein-conjugated or rhodamine-conjugated secondary antibodies. The coverslips were mounted in VectorShield™ and visualized with a Zeiss Axiophot microscope using a 63X or 100X lens.

### **9. Modulation of free $\text{Ca}^{2+}$ concentration *in vivo***

Mature chicken erythrocytes were allowed to settle on coverslips in PIPES buffer (100 mM PIPES, pH 6.94, 1mM  $\text{MgCl}_2$ , 1mM EGTA, 1 mM ATP). They were then equilibrated with different free  $[\text{Ca}^{2+}]$  using  $\text{Ca}^{2+}$ /EGTA buffers as described (Cande, 1980) in the presence of the calcium ionophore A23187 (5 $\mu\text{M}$ ) at 38°C. Cells were fixed after appropriated time intervals and processed for IF.

### **10. Construction of expression vectors and transient expression**

The reading frame of p23 gene from pEXlox was first subcloned into the adaptor vector CLA 12 NCO (Hughes et al., 1987) to ensure an authentic initiator ATG for p23. The  $\text{ClaI}$ - $\text{HindIII}$  fragment was then subcloned into pSVL, pCDNAI and pRC/RSV vectors. Double  $\text{CsCl}_2$ -banded DNA was introduced into COS, 3T3, and CEF cells by Lipofection or calcium phosphate-mediated transfection. Expression of p23 was monitored by Western blotting and immunofluorescence staining 24-72 hrs after transfection.

## **Results**

## **p23 Purification**

A set of mAbs were identified that reacted with high titer against a single polypeptide in both turkey and chick erythrocyte hypotonic lysates with an apparent  $M_r \approx 23,000$  (Fig. 1A). All five mAbs were able to detect as little as 50pg of the purified antigen which from hereon is designated p23. This antigen was not present in any of the lysates from other tissues obtained from perfused animals (Fig. 1B). Western analysis of different hematopoietic cell types indicated that p23 was not expressed in the buffy coat, purified macrophages, lymphocytes or osteoclasts (data not shown) suggesting that p23 expression is restricted to the erythroid lineage. These antibodies were then coupled to activated Sepharose and used to further purify p23 that had already been partially purified by gel filtration. The affinity-chromatography step yielded 75% pure p23. A final reverse phase FPLC fractionation yielded a single peak of >99% pure p23 eluting at 34%TFA (data not shown). Partial sequence analysis of this polypeptide was obtained for the 39, 20, 53 and 9 amino acid length fragments which are denoted by the heavy lines underlying the cDNA sequence in figure 2.

## **Characterization of p23 cDNA clones**

A cocktail of five mAbs exhibiting the highest titer against both chick and turkey p23 was used to screen the  $\lambda$ EHlox cDNA expression library generated from poly A<sup>+</sup> RNA isolated from developing erythroblasts of 8d chick embryos. Initially turkey erythrocyte p23 was used to raise the mAbs against p23. However, for the subsequent cloning and detailed analysis to be described below, we switched to the chick system

because of the ease of obtaining a steady supply of developing erythroblasts from chick embryos. Turkeys, in contrast, breed only once in the Spring. 28 positive plaques with insert sizes ranging from 1.2 kb to 1.46 kb were obtained from the chick erythroblast EHlox expression library. These were purified, autosubcloned and the inserts sequenced to yield the nucleotide sequence from 16-1461 of the full length sequence shown in figure 1. The 5' non-coding region (1-16) was cloned and sequenced by 5' RACE. The peptide sequence obtained by peptide sequencing of the purified protein (58% of the predicted sequence) showed an exact match with that encoded by the full length cDNA sequence, confirming the identity of the clones. In addition, the amino acid composition calculated from the predicted protein sequence exactly matched that obtained from the purified protein (data not shown). Taken together, these data provide direct evidence that this sequence represents that of the p23 polypeptide recognized by the antibodies. The sequence encodes a basic protein, which is consistent with the basic pI of  $\approx 9.5$  observed by isoelectric focusing of the purified erythrocyte protein (data not shown). The predicted molecular weight is 22,099 which again corresponds well to the observed  $M_r$  of 23 K by SDS-PAGE (Fig. 1). Wisconsin GCG database searches have failed to reveal homology with any other protein in the data base, in particular with other MAPs or  $Ca^{2+}$ -binding proteins (see below).

To determine the transcript size and tissue specificity of p23, the entire coding region of p23 was used to probe a Northern blot of polyA<sup>+</sup> RNA isolated from different tissues of perfused chicks. As shown in Fig 3A, a 1.6Kb band appeared in bone marrow RNA after a short exposure time (6h). This corresponded in size and intensity to the signal observed in RNA isolated from erythroblasts from chick embryos (data not shown). After one week exposure, a faint 1.6 Kb band could be observed in RNA from

brain, kidney and liver with a slightly stronger band in lung RNA. Probing the same blot with a  $\beta$ -actin probe (Fig. 3B) confirmed that these differences were not due to differential loadings of RNA but reflected a true difference in the steady state levels of p23 transcripts between these different cells and tissues. This is in agreement with the Western blot analysis described above and confirms that p23 expression is highly specific to hematopoietic cells.

Southern blot analysis was performed using the full coding region of p23 as the probe. A single band was detected in HindIII digests but with EcoRI one major and two minor bands were also detected (data not shown). These results suggest that although a major single gene exists, p23 may be part of a multigene family.

**p23 associates with the centrosomes, nuclear membrane and marginal band in chick erythrocytes and thrombocytes.**

To analyze the cellular distribution of p23, circulating chick erythrocytes were attached to coverslips and processed for immunofluorescence (IF). When cells were fixed in formaldehyde and subsequently permeabilized with TritonX 100, p23 antibodies were found to localize to the MB (Behnke, 1970). In addition they also reacted with the centrosomes and nuclear membrane (Fig. 4A, B). Cold methanol fixation/permeabilization gives poor images with red cells because of the high hemoglobin content but limits the loss of small cytosolic polypeptides compared to Triton permeabilization. This is evidenced by the efficient retention of hemoglobin. Under these fixation conditions, a high content of diffuse cytosolic p23 reactivity was also observed (data not shown). This suggests that p23 exists in equilibrium in both

insoluble and soluble form. Very bright cells were occasionally observed (indicated by a T in Fig. 4A, B) which on further analysis proved to be thrombocytes, the nonmammalian equivalent of platelets (Spurling, 1981). Indeed, if great care was not taken during collection and handling of the blood prior to fixation to inhibit the clotting cascade, these very bright cells appeared in aggregates. (See also Fig. 3 of Murphy et al., 1986). The p23 antibodies reacted diffusely throughout the cytoplasm and also at the equatorial rim of these thrombocytes, i.e., at the MB. It should be noted that the exposure times in the images shown in Fig. 4 were adjusted to give optimal erythrocyte images, hence thrombocytes appear overexposed. With shorter exposure times the p23 MB localization in thrombocytes could be clearly seen. Interestingly, thrombocytes and platelets are thought to be developmentally related to the erythroid lineage (Lucas and Jamroz, 1961) and are the only other cell types known to express a highly structured marginal band of microtubules. They also are the only other hematopoietic cell type besides erythrocytes to express p23 (see below).

The centrosomal localization of p23 was confirmed by double label immunofluorescence using human autosomal anti-centrosomal antisera and anti-p23 mAbs. The two dots revealed by anti-p23 to be juxtaposed to the the nucleus, generally at the long axis poles, also reacted with the anti-centrosomal antisera (Fig. 4D). Likewise, double immunofluorescence with anti-p23 and either antibodies against general  $\beta$ -tubulin or  $\text{c}\beta 6$ -tubulin (the erythroid specific  $\beta$ -tubulin variant; Murphy & Wallis, 1983a; Murphy et al., 1986) clearly revealed the colocalization of the two antigens at the marginal band (Fig. 4C). Taken together these data indicate that p23 is associated both with the MB microtubules and the centrosomes in these post-mitotic, differentiated cells.

To determine whether the marginal band localization of p23 was dependent on the integrity of the MB microtubules, as is the case with microtubule-associated proteins such as syncolin (Feick et al., 1991), or whether it represents a potential binding site for the MB on the membrane skeleton, as with the 80kD (Birgbauer & Solomon, 1989) or the 78 and 48 kD (Stetzkowski-Marden et al., 1991) MB-associated proteins, we analyzed the effect of destabilizing the MB using a combined treatment of cold (4°C) and the MT-destabilizing drug, nocodazole. Pretreatment of the cells at 4°C for 1h prior to fixation completely depolymerized the microtubules of the MB, as evidenced by the lack of any MB staining with anti-tubulin MAb (data not shown; see also Miller & Solomon, 1984), and also abolished the MB staining by anti- p23 antisera (Fig. 5A). Subsequent rewarming of the cells prior to fixation resulted in the reformation of the MB of microtubules and the restoration of MB staining of p23 (Fig. 5C). MB microtubules are resistant to the destabilizing effect of nocodazole alone (Kim et al., 1987) but the presence of this microtubule destabilizing drug during the rewarming recovery phase to block MT formation prevented restoration of both tubulin and p23 localization at the MB (Fig. 5B). These results indicate the dependence of p23 association at the equatorial plane of the plasma membrane on an intact MB of microtubules. These data also indicate the reversibility of this association. In contrast, centrosomal and nuclear membrane localization of p23 was unaffected by all these treatments (Fig. 5A). This could be either because centriolar  $\gamma$ -tubulin is highly resistant to these MT destabilizing treatments or because p23 interacts with a different binding site at the centrosome whose localization is independent of intact MTs.

**p23 is a  $\text{Ca}^{2+}$ -binding protein which is modulated by  $\text{Ca}^{2+}$  in vivo**

Preliminary studies with turkey p23 suggested that p23 may be a Ca<sup>2+</sup>-binding protein (manuscript in preparation). To test this, chick erythrocyte lysates were electrophoresed by SDS PAGE in the presence of either 1mM Ca<sup>2+</sup> or 1mM EGTA (Burgess et al.,1980). Comparative Western blots of p23 run on these two gel systems revealed that the presence of 1mM Ca<sup>2+</sup> affected the mobility of p23. On regular or EGTA-containing gels p23 migrated with an apparent M<sub>r</sub> of 23,000 while in Ca<sup>2+</sup>-gels there was a shift to an apparent M<sub>r</sub> of ≈20,000 (Fig. 6A). This increased mobility in the presence of 1mM Ca<sup>2+</sup> is characteristic of calcium-binding proteins and has been used to identify a number of such proteins . The increased mobility is graphically illustrated when chick erythrocyte lysates are run alongside turkey erythrocyte lysates since we have observed that in turkeys there appear to be two alleles for p23, one encoding a form that lacks the ability to bind calcium (manuscript in preparation).

Western blot analysis of erythrocyte lysates prepared in the presence or absence of 1mM Ca<sup>2+</sup> in the hypotonic lysis buffer revealed that Ca<sup>2+</sup> also modulates whether p23 exists in soluble form or is associated with the cytoskeleton. When cells were lysed in the presence of EGTA containing buffer, approximately 50% of p23 was found to be soluble and 50% remained with the insoluble cytoskeletal fraction (Fig. 6B). In contrast, the presence of 1mM Ca<sup>2+</sup> caused over 95% of the p23 to become soluble (Fig. 6A). To analyze this effect in greater detail, erythrocyte intracellular [Ca<sup>2+</sup>]<sub>free</sub> was modulated by exposing the cells to different Ca<sup>2+</sup>/EGTA buffers in the presence of the Ca<sup>2+</sup>-ionophore, A23187 at 38°C prior to fixation and processing for IF. As shown in Fig. 7A & B, at low [Ca<sup>2+</sup>]<sub>free</sub> (≤10<sup>-8</sup>), anti-p23 and anti-tubulin staining showed the same pattern as observed in nontreated erythrocytes fixed directly after isolation. When the [Ca<sup>2+</sup>]<sub>free</sub> was increased

to  $10^{-6}$ M the staining of p23 at the centrosomes, nuclear membrane and MB became much weaker (Fig. 7C). Noticeably, at this  $[Ca^{2+}]$  the MB microtubules remained intact as evidenced by anti- $\beta$ -tubulin staining (Fig. 7D). This strongly suggests that  $Ca^{2+}$ -induced dissociation of p23 from the MB occurs before free  $Ca^{2+}$  levels reach concentrations that affect the core MB structure itself. This disruption of all cytoskeletal-bound p23 by  $10^{-6}$  M  $[Ca^{2+}]_{free}$  contrasts to the differences in stability of p23 interaction with these structures observed under MT destabilizing conditions. In cells exposed to free  $Ca^{2+}$  levels of  $10^{-4}$ M, no p23 or tubulin staining was observed (Fig. 7E, F) (Note that with the fixation / permeabilization conditions used, much of the freely soluble proteins were washed away). Thus at these high levels of cytosolic free  $Ca^{2+}$ , p23 becomes completely soluble and the MB fully disassembled. To test the reversibility of these  $Ca^{2+}$  effects, cells were exposed to  $10^{-6}$ M to  $10^{-4}$ M  $[Ca^{2+}]_{free}$  in the presence of A23187 and then restored to  $Ca^{2+}$ -free EGTA buffer for 20 min (all at  $38^{\circ}C$ ) prior to fixation. In cells that had been pre-exposed to  $10^{-6}$ M  $[Ca^{2+}]_{free}$ , the MB and centrosomal localization of p23 was now completely restored. However, in cells preexposed to  $10^{-4}$ M  $[Ca^{2+}]_{free}$ , this effect could not be reversed either for p23 or MB MTs (data not shown). We presume this is because the prolonged exposure of cells to these high cytosolic free  $Ca^{2+}$  levels could have detrimental additional effects such as activation of the  $Ca^{2+}$ -activated protease, Calpain I (see review, Croall & Demartino, 1991), which interfered with the reversibility of the direct  $Ca^{2+}$  effect on p23 and tubulin localization.

### **Transfection and expression of chick p23**

The centrosomal and MB localization of p23 in chick erythrocytes coupled with its ability to interact directly with  $Ca^{2+}$  and the  $Ca^{2+}$ -induced modulation of its localization

led to the question of whether the lineage-restricted expression of p23 to these MB-containing, terminally differentiated cells had any role to play in MB or centrosomal stability. To address the potential function of p23, p23 cDNA was subcloned into pCDNAI, PRC/RSV or pSVL and the resultant constructs transfected into COS or primary CEF cells. IF staining revealed that within the first 36h after transfection in both cell types, p23 was localized predominantly within the nucleus (Fig. 8A,B). Subsequently, p23 became diffusely localized throughout the cytoplasm (Fig. 8C,D). Identical results were obtained for all the constructs. No evidence was seen for any association with either the cytoplasmic or spindle arrays of MTs or with the centrosomes in these cells. In this respect, the behavior of p23 in these mitotic, relatively undifferentiated cells differs markedly from that observed in post-mitotic terminally differentiated erythrocytes and thrombocytes. These studies demonstrate that p23 does not appear competent to interact directly with MTs as has been observed in studies of heterologous expression of MAPs (e.g., Drubin et al., 1985). Nor is p23 competent to interact with the centrosomes in these mitotically active cells. Furthermore, we were unable to detect any consequences of p23 expression on cell behavior.

#### **p23 expression and localization in bone marrow-derived hematopoietic cells:**

The transfection studies demonstrated that p23 expression in heterologous cells failed to recapitulate any of the features of its localization in erythrocytes. One possible explanation is that there is a fundamental difference between the nature of the dynamic interphase MT arrays and MTOC functioning centrosomes in COS and CEF cells and the highly stable MB MTs and the inactive centrosomes/nonreplicating centrioles of differentiated erythrocytes and thrombocytes. Differences in the complement of other

MAPs or in tubulin modifications might also affect the ability of p23 to interact with these structures. In addition, MBs contain a unique  $\beta$ -tubulin variant, c $\beta$ 6 (Murphy & Wallis, 1983a) so the possibility exists that p23 can only interact with erythroid-specific  $\beta$ -tubulin containing MTs. To examine this further we analyzed the expression and localization of p23 throughout erythropoiesis, both in the bone marrow and in developing erythroblasts isolated at different stages of embryonic development.

The first wave of bone-marrow derived erythrocytes are released into circulation 3 weeks after hatching. Between 1-7d after hatching, a large population of progressively maturing erythroblasts can be readily identified. Double immunofluorescent labeling using polyclonal anti- $\beta$ -spectrin as an early erythroid cell marker (Pain et al., 1991) together with anti-p23 mAbs revealed that the large spherical proerythroblasts, readily identified in phase optics by their characteristic morphology (Lucas & Jamroz, 1961), stained positively for  $\beta$ -spectrin but were negative for p23 (see EB marked with a arrow, Fig. 9). In early polychromatophilic erythroblasts (PE), p23 staining appeared diffuse throughout the cytoplasm. p23 only began to localize to the MB and nuclear membrane by the late polychromatophilic stage. All other hematopoietic cell types, including granulocytes, macrophages, osteoclasts and lymphocytes, were noticeably negative for p23 providing a clear indication of the lineage specificity of p23 expression.

To investigate whether p23 association with the MB, nuclear membrane and centrosomes in developing erythroblasts in the bone marrow correlated with the expression of the specific erythroid c $\beta$ 6  $\beta$ -tubulin variant, double immunofluorescent labeling was also carried out using polyclonal anti-c $\beta$ 6 affinity purified IgG and anti-p23 mAbs. As shown in Fig. 9,D,E,F, EBs were also negative for c $\beta$ 6  $\beta$ -tubulin. c $\beta$ 6

expression occurred concurrently with p23 in early PEs, but whereas p23 appeared to be diffusely distributed, c $\beta$ 6 occurred as a continuous bundle encircling the cell periphery and few if any individual cytoplasmic MTs were evident. Since these erythroblastic cells are round, the MB MTs weave in and out of the focal plane and consequently they do not appear continuous in a single plane of focus. At later PE and maturing erythrocyte stages, the MB appeared more consolidated as evidenced by the more compacted ring that no longer weaved in and out of the focal plane; this we interpret to be indicative of a more rigid MB structure and coincides with the cell assuming a more flattened shape. The staining with anti-c $\beta$ 6-tubulin consistently failed to reveal the presence of many individual MTs or to indicate the presence of a centrosomal MTOC connected to the developing MB. Therefore, double immunofluorescence was carried out using anti- $\beta$ spectrin antisera as a marker for erythroid cells (Fig. 10A) together with an antibody recognizing all  $\beta$ -tubulin isoforms (Fig. 10B). This general anti- $\beta$ -tubulin readily revealed the presence of extensive MT arrays emanating from the centrosome/ MTOC in non-erythroid hematopoietic cells. These are not readily apparent in the images presented in Fig. 10 since the exposure times were adjusted to provide optimal images of the extremely bright MT bundles in erythroid cells. Although cytoplasmic arrays are only evident in a few of the non-erythroid cells the centrosomes (which appear as dots) are still clearly visible in all of these cells. With this antibody, it became evident that even up to the PE stage, individual MTs together with loosely coiled MT bundles were present. However, centrosomal centers for the MT arrays were only evident in the EBs that lacked MB-type structures. Taken together, these results suggest that it is unlikely that p23 plays any initiating role in the establishment of the MB structure or that c $\beta$ 6 expression in itself is sufficient to permit direct interactions of p23 with MTs. Therefore, additional factors and /or modifications occurring late in erythroid development are

required for p23 association with the MB, nuclear membrane and centrosomes.

However, upregulation of c $\beta$ 6 expression does correlate with the localization of MT bundles to under the plasma membrane and the loss of cytoplasmic arrays of individual MTs as originally described by Murphy et al.(1986).

### **p23 expression and localization in erythroid cells during chick embryo development.**

Studies with bone marrow derived cells provide a static image of a variety of cells at different stages of development. In contrast, circulating erythroblasts isolated from different stages of chick embryonic development provide a unique system for studying the temporal and spatial control of p23 expression since the initial primitive and subsequent definitive erythrocyte lineage develop as a synchronized cohort (Lucas & Jamroz, 1961; Bruns & Ingram, 1973). This enables an unequivocal analysis of the temporal sequence of events leading up to the formation of the MB and allows for Western and Northern blot analysis of p23 and c $\beta$ 6 expression. The first erythrocytes, the large cells of the primitive lineage, originate in the blood islands and appear 36-48h after fertilization. They undergo synchronous differentiation in circulation, becoming postmitotic around d5. This coincides with the initial appearance of early erythroblasts of the definitive lineage which comprise 1-4% of the cells at d5. By d8, the percent definitive cells rises to 90% with the primitive cells being completely removed from circulation by d16 (Lucas & Jamroz, 1961). The definitive cells differentiate as mitotic cells (corresponding to the progression from early to late polychromatophilic) up until d10. From d11 onwards increasing numbers become postmitotic, with most definitive cells being postmitotic and undergoing their final maturation stages by d14 (Bruns & Ingram, 1973).

D2 circulating primitive erythroblasts were found to be predominantly negative for both p23 and c $\beta$ 6  $\beta$ -tubulin (data not shown). By d3 the primitive cells are at the early polychromatophilic (PE) stage. A few cells (5-10%) now stained positively for p23 which was distributed diffusely throughout the cytoplasm (Fig. 11A,B). A slightly higher percentage ( $\approx$ 25%) were found to be positive for c $\beta$ 6  $\beta$ -tubulin which appeared predominantly in the form of quasi MB structures. Noticeably, the c $\beta$ 6-positive cells appeared to have few, if any, individual cytoplasmic MTs although c $\beta$ 6 antisera did stain the spindle apparatus of the occasional dividing cell (Fig. 11A,C). This indicates that c $\beta$ 6-containing MTs can reorganize to generate a mitotic spindle. At this developmental stage, the quasi MBs tended to weave in and out of the plane of focus around the cell. Staining with the antibody recognizing all  $\beta$ -tubulin isoforms revealed that in fact the majority of cells contained cytoplasmic arrays, with many cells already containing coils of MT bundles within the cell. A few cells contained quasi MBs. Double IF with the two anti-  $\beta$ -tubulin antibodies confirmed that these corresponded to the c $\beta$ 6-positive cells (data not shown). This indicated that MT bundling precedes c $\beta$ 6 expression, but the appearance of c $\beta$ 6-containing MTs coincides with the association of these MT bundles with the plasma membrane as a MB. In polychromatophilic erythroblasts circulating at d4, a much higher proportion of cells stained positively for both p23 and c $\beta$ 6. c $\beta$ 6 appeared to be almost exclusively assembled into consolidating MB structures juxtaposed to the plasma membrane (Fig. 11F). p23 was present in 20-30% of the cells, remaining diffusely localized in the cytoplasm (Fig. 11E). The general anti- $\beta$ tubulin revealed that in many cells the tubulin was localized now almost exclusively in a MB-type structure (Fig. 11ii). Again double IF indicates that these were the c $\beta$ 6-positive cells (data not shown). However, those cells which retained cytoplasmic arrays

corresponded to c $\beta$ 6-negative cells. Again it was noticeable that MT bundling was already occurring in c $\beta$ 6-negative cells. By d5, when the primitive cohort has become postmitotic, there were still a few cells with cytoplasmic MT arrays but a high percentage now possessed MBs, with few cytoplasmic filaments being evident in these MB-containing cells (Fig. 11G,I,iii). As indicated in Fig. 11iii, an occasional cell was observed where staining with the general  $\beta$ -tubulin antibody revealed the presence of the MTOC/centrosome (indicated by the arrow marked ce). We also observed the same array at earlier stages. Thorough searching through many coverslips showed that when such a centrosome was visible it always appeared to be quite distant from the developing MB as shown in Fig. 11iii. It was also noteworthy that in cells expressing loosely coiled bundles encircling the cell, the presumed precursor to the equatorial tight band of the MB, no evidence could be found using the general anti- $\beta$ tubulin for any associated MTOC. Thus at least at this stage, the centrosome did not appear to direct the establishment of the MB.

At d6, the definitive lineage appears in circulation, readily distinguished from the primitive cells on the basis of morphology. These cells noticeably all stained more intensely for p23 than their primitive counterparts, albeit in a diffuse manner. The same cells were negative for c $\beta$ 6 and by general  $\beta$ -tubulin staining lacked any MB structure (Fig. 11J,K,L,iv). Although negative for c $\beta$ 6, these definitive cells had distinct MT bundles in the cytoplasm that again were not connected in any obvious fashion to a centrosomal structure. However, such an association may have been obscured by the high local MT densities. At this stage the primitive cells showed very faint staining for p23 but all expressed mature MBs, manifested as a flat peripheral circle in a single plane of focus. By d7, when more than 50% of the cells were now of the definitive lineage,

little p23 was observed in the remaining primitive cells but p23 was present in all definitive cells, now localizing to the MB as well as in granular form coalescing around the nucleus (Fig. 11M,N,O). By this stage, the majority of cells were c $\beta$ 6-positive although the occasional negative cell was still observed. By general  $\beta$ -tubulin staining these c $\beta$ 6 negative cells contained predominantly loose MT coils encircling the cell (see arrow, Fig. 11v). From d8 onwards the MB localization of c $\beta$ 6 and p23 was identical to that seen at d7. Major changes occurring from d8 to d14 during the final division steps involved the gradual concentration of the granular perinuclear p23 staining around the nucleus, with progressively more cells adopting the double centrosomal localization between d11-14 as progressively more cells become postmitotic. Thereafter, all the cells were postmitotic and all resembled the adult phenotype.

**p23 steady-state levels are determined by stabilization during late stages of definitive erythropoiesis.**

Since the immunofluorescence studies tend to reveal the cytoskeletal-bound fraction of p23, Western and Northern blot analysis was carried out to determine total transcript and protein steady-state levels as a function of erythroid development. As shown in Fig. 12, p23 protein levels are low in circulating primitive cells isolated from d2 embryos but thereafter increase to a maximum at d5. As the primitive lineage in circulation begins to be replaced from d6-7 by the definitive erythroblasts a dramatic increase in p23 protein steady-state levels is seen, reaching a plateau maximal value at d10. c $\beta$ 6  $\beta$ -tubulin expression appears to lag behind p23 but accumulates to a greater extent in the primitive lineage. The total amount of c $\beta$ 6  $\beta$ -tubulin climbs rapidly with the onset of definitive erythroblast release into the circulation, peaking at d7 and declining to

plateau at an intermediate level by d10. This latter event coincides with the time the definitive cells begin to become postmitotic. Quantitative analysis of transcript levels from d4 onwards indicates that  $\text{c}\beta 6$  expression shows a biphasic curve corresponding to the overlapping curves for the two lineages. This correlates with the overall RNA levels which decline rapidly from d9 (data not shown). p23 expression in contrast exhibits a steady decline, without showing a secondary peak around d6-7 coinciding with the release of early erythroblastic stages of the definitive lineage. The surprising conclusion is that p23 expression is highest in early primitive cells despite the lack of any apparent p23-cytoskeletal interactions in these cells. Rather, cytoskeletal interactions are initiated at a time p23 expression is being markedly downregulated. Thus stabilization events occurring specifically in later stages of definitive erythropoiesis must dictate the overall accumulation of p23 protein.

## **Discussion**

### **p23 is a novel $\text{Ca}^{2+}$ -binding protein.**

We have identified and characterized a novel  $\text{Ca}^{2+}$ -binding protein in chick, p23, whose expression is restricted to the erythrocyte and thrombocyte lineages. Immunofluorescent localization of p23 reveals that a fraction of the antigen is associated in a  $\text{Ca}^{2+}$ -dependent manner with the MB, centrosomes and nuclear membrane of mature erythrocytes and thrombocytes. Analysis of the full length cDNA indicates that p23 lacks homology with any previously described polypeptide sequence and in particular with regard to the following two features. First, the p23 sequence lacks any of the structural features conferring MT binding properties that have been found in those MAPs

that have been analyzed in structural detail. For example the carboxyl terminal regions of MAP2 and tau share considerable homology, containing imperfect repeat stretches of 18 residues with spacer sequences of about 13-14 amino acids that together comprise the MT binding domain. This region is highly basic enabling interactions with the acidic region of tubulin that contains the MAP binding sites (Goedert et al., 1991; Brandt and Lee, 1993). p23 is also highly basic (pI~9.5) but lacks these repeat sequences that might promote changes in MT morphology. This might explain why we have failed to find any gross effect of p23 on purified tubulin properties (unpublished results) although there are reports that highly basic proteins lacking such motifs can induce MT lateral association through simple charge interactions. These include both specific MT binding proteins such as the Stable Tubulin Only Protein (STOP; Pirollet et al., 1989) and the homologous myelin basic protein which induce MT stabilization in a  $\text{Ca}^{2+}$ /calmodulin-dependent manner (Dyer and Benjamins, 1989; Pirollet et al., 1992), as well as nonspecific proteins such as histones and RNase (Erickson and Voter, 1976; Centoze and Sloboda, 1986; Multigner et al., 1992). Second, although p23 exhibits a gel shift in apparent  $M_r$  in the presence of  $\text{Ca}^{2+}$ , a diagnostic feature of direct  $\text{Ca}^{2+}$  binding proteins, it lacks any homology with the two known classes of  $\text{Ca}^{2+}$  binding proteins. p23 contains none of the consensus sequence that can generate the pair of helix-loop-helix structural motif that constitutes the binding site of the "EF hand" family typified by calmodulin (Kretsinger, 1980). Nor does p23 contain the repeated  $\text{Ca}^{2+}$  binding site consensus sequence contained in a conserved 70 amino acid stretch characteristic of the annexin family (Burgoyne and Geisow, 1989). p23 also differs functionally from these previously characterized  $\text{Ca}^{2+}$ -binding proteins in one major respect. Binding to its target skeletal binding sites requires low  $[\text{Ca}^{2+}]$ , with concentrations of  $10^{-6}\text{M}$  being sufficient to induce maximal p23 dissociation. Interestingly, this  $[\text{Ca}^{2+}]$  is not high enough to induce

MT depolymerization, a process known to be mediated by calmodulin (Marcum et al., 1978). This can be interpreted to indicate that p23 exhibits a higher affinity for  $\text{Ca}^{2+}$  than the prototypic  $\text{Ca}^{2+}$ -binding protein, calmodulin. If this is the case it would be reasonable to expect that significant structural differences exist in the p23  $\text{Ca}^{2+}$  binding site(s) compared to those of classical  $\text{Ca}^{2+}$ -binding proteins to accommodate a higher affinity for  $\text{Ca}^{2+}$ .

**p23 specifically associates with the MB but does not exhibit typical MAP activity.**

The transfection studies indicate that p23 expression in itself is not sufficient for interaction of this protein with centrosomal MT arrays in the proliferating cell types used. This is in marked contrast with heterologous expression studies of known MAPs. For example, tau not only rapidly associates with preexisting MTs but also induces profound changes in MT organization and stability when expressed in highly divergent cell types (Drubin et al., 1985; Kanai et al., 1992). 90-95% of the  $\beta$ -tubulin subunits in the MB consist of a unique, erythroid-specific isoform,  $\text{c}\beta 6$  (Murphy & Wallis, 1983a; Murphy et al., 1987).  $\text{c}\beta 6$  exhibits 17% divergence from other  $\beta$ -tubulins and tends to form longer and more stable MTs *in vitro* in comparison with brain tubulin (Murphy and Wallis, 1983b; Murphy et al., 1987). The possibility that p23 may serve as a  $\text{c}\beta 6$ -MT-specific MAP is rendered unlikely by the observation that although both polypeptides are coexpressed in primitive erythroid cells, p23 shows little if any association with the MB in this lineage. Taken together, these observations are in accordance with preliminary experiments which suggest that p23 does not modify either brain or erythrocyte tubulin MT characteristics *in vitro* in any readily definable manner (data not shown).

To date, proteins that have been described to localize specifically to the MB fall into two general categories; those MAPs, e.g., syncolin (Feick et al., 1991), MAP2 and tau (Murphy & Wallis, 1985) whose localization is dependent on an intact MB and proteins such as the ezrin-like protein (Birgbauer and Solomon, 1989) and the 78 and 48K proteins (Stetzkowski-Marden et al., 1991) whose localization is independent of an intact MB and which may be involved in the tethering of the MB to the plasma membrane at the equatorial plane of the cell. Although p23 resembles the former in that disruption of the MB MTs disrupts p23 MB localization it does not appear to function as a classical MAP, at least in a simple binary complex.

### **p23 and MB biogenesis.**

The detailed IF analysis of p23 association with the MB provided some insight into the mechanisms underlying the elaboration of the MB during erythropoiesis and the potential significance of p23-MB interactions during this process. Similarly to observations made by others, we observed that a high degree of MT bundling early in development precedes the association of an MB-like structure with the equatorial rim of the cell (Kim et al., 1987; Murphy et al., 1986). The MB-membrane association occurs coordinately with upregulation in the erythroid-specific  $\text{c}\beta 6$   $\beta$ -tubulin during the late polychromatophilic stage (our results; Murphy et al., 1986). Throughout this time in both lineages p23 expression is high but p23 protein fails to accumulate and shows no evidence of any MB association. Since p23 fails to bind to the MB of definitive erythroid cells until well after the bundled MTs have coalesced into a coherent, membrane-bound MB, it is evident that p23 cannot be playing any role in the biogenesis of the MB structure per se. This is underscored by the fact that in primitive erythrocytes

where the MB is also fully formed and membrane-bound, p23 exhibits little if any detectable association with the MB. This implies that p23-MB interactions are induced specifically in the late stages of definitive erythropoiesis. Indeed it is striking that in these late stages marked accumulation of p23 protein occurs at a time when p23 biosynthesis is in rapid decline. Therefore, a pronounced stabilization of p23 against catabolism is induced specifically at this time. This would be analogous to the mechanisms regulating the accumulation of the membrane skeleton during erythropoiesis where preferential stabilization against catabolism ultimately regulates the extent of a  $\beta$ -spectrin, ankyrin and protein 4.1 accumulation specifically in later stages of erythropoiesis (Lazarides, 1987; Woods & Lazarides, 1988). It remains to be seen whether p23 MAP activity is induced by posttranslational regulatory modifications, or whether p23-MB interactions involve a tertiary interaction, such as the case with the protein 4.1 enhanced interaction of spectrin with actin in the erythroid membrane skeleton (Byers & Branton, 1985) or whether these interactions are indirect, involving a cascade of binding sites for example as occurs in linking the actin network to adhesion plaques (Geiger & Ginsberg, 1991). Whichever the case, the interlinking mechanism must be developmentally regulated and restricted to the definitive lineage.

In considering the potential significance of p23-MB interactions it is interesting to consider one unique feature of terminally differentiated erythrocytes compared to other terminally-differentiated cell types. Following the final mitosis, transcriptional and translational activity is downregulated and much of the intracellular organelles are eliminated. This is of particular importance to the definitive lineage which has to survive much longer (~30d) than the primitive lineage in circulation. Thus, unlike other terminally differentiated cell types, for example neurons, where newly synthesized

tubulin / MTs are continually being incorporated into the preexisting arrays (Baas & Black, 1990; Reinsch et al., 1991; Tanaka & Kirschner, 1991; Ahmad et al., 1993), the erythrocyte MB MTs cannot be replenished and have to exhibit extreme stability. Given that p23 association with the MB occurs late in erythropoiesis, it is tempting to speculate that p23 may be providing the ultimate stabilizing factor analogous to the late incorporation of membrane skeletal cross-linking proteins that also occurs in the postmitotic stages of erythrocyte maturation (Lazarides, 1987; Woods & Lazarides, 1988).

**p23 association with the centrosome and nuclear membrane is restricted to late stages of definitive erythropoiesis.**

Our studies indicate that p23 also acts as a novel centrosomal-associated protein uniquely in the erythrocyte and thrombocyte lineages. Centrosomes typically are composed of a pair of centrioles connected by caltractin-like  $\text{Ca}^{2+}$ -activated filaments together with a cloud of PCM that contains the MT nucleating activity (Gould & Borisy, 1977; Rieder & Borisy, 1982; McFadden et al., 1987; Huang et al., 1988a,b). Although these two centrosomal elements are generally intimately associated and oscillate in function in parallel, they are structurally and functionally distinct (Mazia, 1987). At the structural level analyzed in this study, it cannot be definitively shown whether p23 is associated with the centriolar or PCM component of the erythrocyte centrosome. The size and  $\text{Ca}^{2+}$ -binding properties of p23 are reminiscent of the properties of caltractin/centrin in *Chlamydomonas* basal bodies (McFadden et al., 1987; Huang et al., 1988 a, b) and the related cdc31 yeast spindle body protein (Baum et al., 1986), core proteins of the  $\text{Ca}^{2+}$ -activated filaments connecting the centrioles and controlling their

orientation. However, structural sequence analysis revealed no homology between p23 and these proteins.

Despite the absence of ultrastructural detail, several interesting conclusions can still be drawn regarding the nature of p23-centrosomal interactions which emerged by analyzing developmental changes in p23 localization during both primitive and definitive erythropoiesis. First, despite high levels of p23 expression in primitive erythrocytes, p23 fails to associate with the centrosome, not only when the centrosome still functions as an active MTOC (see Fig. 1 iii) but also when the centrosome becomes inactive as an MTOC and its own duplication cycle is blocked. Likewise in definitive erythroblasts, p23 association with the centrosome is not simply a function of whether the centrosome is functioning as an active MTOC, either for interphase MT or spindle apparatus arrays. Thus its association with the centrosome is not linked to the cycling functional role of the PCM. Therefore, even under conditions of high expression, p23 is not a constitutive component of the centrosome but rather one whose binding to this structure is conditionally linked to as yet unknown factors operative only in the late stages of definitive erythropoiesis. At present the timing of p23 association with the centrosome in definitive cells cannot be precisely described. However, around d7 there is an abrupt change from diffuse p23 localization to MB and granular perinuclear localization which, as mentioned earlier, correlates with a dramatic increase in p23 stabilization, manifested by marked p23 accumulation. Hence accumulation occurs concomitantly with induction of p23-cytoskeletal interactions. During these stages a classical interphase MTOC corresponding to a centrosome could not be identified as a focal point of MT arrays. Although it cannot be ruled out that the local high MT densities in these small round erythroblast cells may have obscured such evidence, it has

been noted that use of centrosomal antisera failed to demonstrate centrosomal links to the developing MB (Miller & Solomon, 1984). Our evidence and that of others supports the hypothesis that membrane stabilizing factors (predeterminants) most likely serve a localized MTOC function since the temporal sequence of membrane association correlates with the time that these MTs lose their sensitivity to cold and drug induced destabilization (Kim et al., 1987). In other terminally differentiated cell types highly stable MT arrays are thought to arise from dispersed MT nucleating activity rather than from classical centrosomes (Tassin et al., 1985; Mogensen, 1987; Baas and Ahmad, 1992). In such cases the PCM may become quite dispersed. It can be hypothesized that these anti-p23 reactive granular perinuclear aggregates represent dispersed PCM material, which would then suggest that p23 is associating specifically with non-MTOC functioning PCM material in these definitive cells. Only after definitive erythroid cells become postmitotic is p23 unambiguously associated with the centrosomes. Interestingly, avian and amphibian definitive erythrocytes contain a pair of centrosomes, located at the ends of the long axis of the nucleus (results described here; Searle & Bloom, 1979 ; Eutenauer et al., 1985). This centrosomal localization is characteristic of early prophase, which indicates that following the final mitosis, chromatin and centrosomal replication cycles must fall out of synchrony. Mature nucleated erythrocytes are blocked in the G<sub>1</sub><sub>D</sub> stage of the cell cycle (Darzynkiewicz, 1987). In these cells it is evident that the centrosomal cycle has proceeded up to the point of specifying the spindle poles but the centrosomes are blocked from assuming the MTOC activity that would normally follow. In this context it has been demonstrated that the PCM may encircle the nucleus prior to complete establishment of the spindle poles (Mazia, 1987). Thus the nuclear membrane staining observed with anti-p23 may represent this dispersed stage. However, p23-centrosomal interactions can not simply be conditional on withdrawal

from the centriolar cycle since when primitive erythroblasts withdraw into the G1<sub>D</sub> stage this is not accompanied by p23 association with the centrosomes.

### **Ca<sup>2+</sup> changes may regulate p23-cytoskeletal associations in erythroid development.**

Given that initiation of p23 interactions with quite disparate cytoskeletal structures, the MB, centrosome and nuclear membrane, occur at the same developmental stage and that p23 association with these structures appears to be independent of their functional state, these associations must be effected by some global change(s) occurring specifically in the definitive lineage in these late stages of terminal differentiation. Since p23 appears to be a Ca<sup>2+</sup>-binding protein whose cytoskeletal interactions are regulated by [Ca<sup>2+</sup>]<sub>free</sub> it seems reasonable to speculate that changes in [Ca<sup>2+</sup>]<sub>free</sub> might be one of the major determinants. As mentioned earlier, the Ca<sup>2+</sup>-binding properties of p23 differ from those of classical Ca<sup>2+</sup>-binding proteins. Whereas the EF-hand and annexin families of proteins bind to their target polypeptides under conditions of elevated [Ca<sup>2+</sup>]<sub>free</sub>, p23 does so under low Ca<sup>2+</sup> conditions. Furthermore, we have demonstrated that Ca<sup>2+</sup>-induced dissociation of p23 from all its cytoskeletal sites occurred at lower free [Ca<sup>2+</sup>] than that required for Ca<sup>2+</sup>/calmodulin induced MB MT disassembly, suggesting that p23 exhibits a higher affinity for Ca<sup>2+</sup>. One of the late events during the differentiation of nucleated definitive erythrocytes is the down regulation / elimination of most intracellular organelles, analogous to the complete elimination of intracellular organelles that occurs in enucleate mammalian erythrocytes (Parmley, 1988). For example, only one mitochondrion is typically observed per mature avian erythrocyte (Searle & Bloom, 1979; Granger and Lazarides, 1982). This is reflected in the decrease in mitochondrial respiratory activity in definitive erythrocytes (Lucas and Jamroz, 1961). Since

mitochondria and the ER act as the major reservoirs of intracellular  $\text{Ca}^{2+}$  in most cell types, this could result in lower than normal  $[\text{Ca}^{2+}]_{\text{free}}$  in erythrocytes. Indeed intracellular levels of 60nM have been recorded in non-aged human erythrocytes (Aiken et al., 1992). With the improved methodology now available to measure intracellular  $[\text{Ca}^{2+}]$  it should be possible to compare the resting free  $[\text{Ca}^{2+}]$  in primitive and definitive erythroid cells. This would resolve the issue of whether the onset of p23 association with the erythroid cytoskeleton is induced simply by the lowering of intracellular  $\text{Ca}^{2+}$  levels during the final erythroid stages or whether additional factors specific to these late definitive stages are also required.

## Figure legends

Figure 1. Western blot analysis. Panel A: Turkey (T) and chicken (C) erythrocyte lysates separated by 20% SDS-PAGE before being transferred to nitrocellulose and probed with the anti-turkey p23 mAb, 20E12B1. Panel B: Western blot analysis of tissue extracts from perfused chicks compared with erythrocyte and bone marrow cell lysates. 50µg total protein per lane was separated by 20% SDS-PAGE. After transfer the blot was probed with rabbit polyclonal anti-chick p23. Er, erythrocyte; BM, bone marrow; Br, brain; Ki, kidney; Li, liver; He, heart; Lu, lung.

Figure 2. Peptide and cDNA sequence of p23. The nucleotide sequence between 16 and 1461, which includes the full coding sequence, was sequenced directly from positive clones isolated from the chick erythroblast λEX10x library. Nucleotide sequence 1- 16 was obtained by 5'RACE. The underlined stretches of the amino acid sequence predicted from the cDNA denote the sequences obtained by direct sequencing of the purified p23 protein. An exact match is seen between the observed and predicted sequence for these polypeptide stretches. This sequence is filed with the GenBank under accession number L11171.

Figure 3. Northern blot analysis of p23 expression in different chick cell and tissue types. 1µg of poly A<sup>+</sup> RNA from tissues isolated from perfused chicks was separated by formaldehyde gel electrophoresis and probed with the full length reading frame of p23 (panel A). The same blot was reprobed with a β-actin probe as a control (panel B). The tissues include bone marrow (BM), brain (Br), kidney (Ki), heart (He),

liver (Li), lung (Lu) and muscle (Mu). The exposure time shown for the BM lane in panel A is 6hr, whereas that for the remaining lanes is 6d. The exposure time for the  $\beta$ -actin blot is 30min. Note that cardiac tissue contains the cross reactive  $\gamma$ -actin species but muscle actin does not cross react with this  $\beta$ -actin probe.

Figure 4. Immunofluorescent localization of p23 in mature chick erythrocytes and thrombocytes. Panel A represents immunostaining with anti-p23 mAb with the corresponding phase in panel B. Both the MB (arrows) and centrosomes (seen as two dots shown by arrowheads on eachside of the nucleus in most cells) were stained as well as the nuclear membrane. The MB p23 localization is confirmed by anti-tubulin staining (panel C) and the centrosomal localization by anti-human centrosome staining (D). The very bright cells were identified as thrombocytes (shown as T) on the basis of their morphology and tendency to aggregate. Bar, 10  $\mu$ m.

Figure 5. Effect of MT destabilization on p23-MB localization. Mature chick erythrocytes were preteated for 1hr at 4°C prior to immunofluorescent staining with anti-p23 (A) or allowed to rewarm at 37°C for 30 min. in the presence (B) or absence (C) of 5 $\mu$ M of the MT destabilizing drug, nocodazole. Note that MB but not centrosomal (see double arrowheads) p23 staining is abolished by cold preteatment. Bar, 10  $\mu$ m.

Figure 6.  $\text{Ca}^{2+}$  effects on p23. Panel A: direct effects of  $\text{Ca}^{2+}$  on p23 mobility in SDS-PAGE. Chick erythrocyte lysates were run under conditions of either 1mM EGTA (lane 1) or 1mM  $\text{Ca}^{2+}$  (lane 2) included in the sample buffer, 20% SDS-PAG and running buffer. Molecular weight markers run alongside each erythrocyte lane are designated. These all showed no shift in apparent  $M_r$  under either conditions. Panel B:

the effect of on the p23 solubility including EGTA (set 1) or 1mM Ca<sup>2+</sup> (set 2) alone in the hypotonic lysis buffer. S, the soluble fraction; P, the insoluble pellet.

Figure 7. Immunofluorescent analysis of the effects of modulating intracellular [Ca<sup>2+</sup>]<sub>free</sub> on anti-p23 and anti-tubulin staining. Cells were incubated in different Ca<sup>2+</sup>/EGTA buffers in the presence of the Ca<sup>2+</sup> ionophore, A23187, 1μM prior to fixation and processing for double immunofluorescence with anti-p23 (A, C, E) or anti-tubulin (B, D, F). [Ca<sup>2+</sup>] of 10<sup>-8</sup>M (A, B), 10<sup>-6</sup>M (C, D) and 10<sup>-4</sup>M (E, F) are shown. Bar, 10μm.

Figure 8. Immunofluorescent analysis of p23 localization following transient transfection of the p23 cDNA into COS cells. The fluorescent and corresponding phase images obtained 36hr (A, B) and 48hr (C, D) after transfection are shown. Bar, 20 μm.

Figure 9. p23 expression and localization in bone marrow hematopoietic cells. Double immunofluorescence was carried out either using anti-p23 (B) together with anti-β-spectrin (A) as an early erythroid marker or with anti-p23 (E) together with affinity purified anti-cβ6 β-tubulin (D). The corresponding phase images are shown in the bottom panels (C, F). Cell types/stages are indicated as follows: E, mature erythrocyte; EB, early erythroblast; PE, polychromatophilic erythroblast; L, lymphocyte and G, granulocyte. Bar, 10μm.

Figure 10. Double immunofluorescent staining of bone marrow cells with anti-β-spectrin (A) and anti-general β-tubulin (B) antisera with the corresponding phase image (C). EB, early erythroblasts; PE, polychromatophilic erythroblast; E, mature erythrocyte and G, granulocyte. Bar, 10μm.

Figure 11. Timing of p23-cytoskeletal associations during embryonic erythropoiesis. Double immunofluorescent analysis of p23 (B, E, H, K, N) and c $\beta$ 6  $\beta$ -tubulin (C, F, I, L, O) localization together with general  $\beta$ -tubulin localization (i, ii, iii, iv, v) in circulating erythrocytes isolated at the different days of embryonic development shown. The phase images correspond to those of the adjacent two fluorescent images. An active centrosome in the 5d erythroid population is indicated by ce in iii; an early definitive erythroblast (de) at 6d is compared with a primitive erythrocyte (pe) in panels J, K and L and at 7d in panels M, N and O. Arrowhead in panel iv indicates bundles of MTs encircling the cell. Bar, 10 $\mu$ m.

Figure 12. Relative changes in p23 transcript and protein levels during development. Western and Northern analysis were carried out with 10<sup>5</sup> and 5 X 10<sup>6</sup> cell equivalents respectively of circulating erythroid cells isolated from successive days of embryonic development. The same blots were probed for both p23 and c $\beta$ 6  $\beta$ -tubulin and the resulting signals scanned with a Molecular Dynamics densitometer and expressed in relative units. The data represent the values obtained from one experiment. Three independent experiments gave similar results.

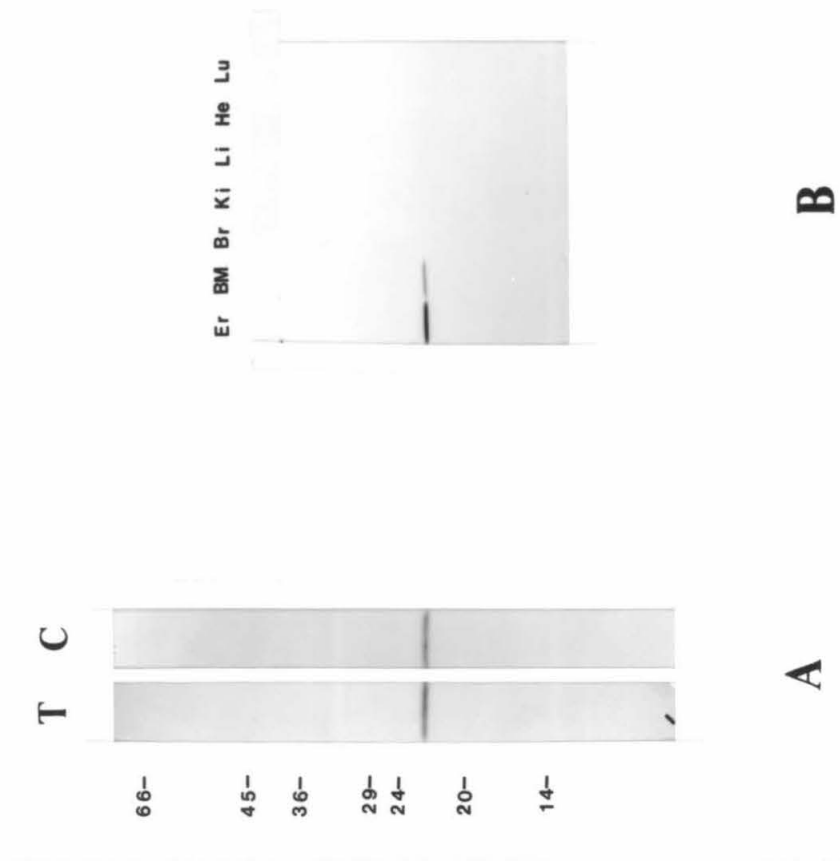


Figure 1

### cDNA Sequence of Chicken p23

```

TGGTGTTCACGACGGCGCGATGGATCGCGATCGGATCGTGGCGCTGTTTCGGGGCCACCGGGAGGAGCGGCCGGGAGGCGCTGCGGAGG 90
      M D R D R I V A L F G A T G R S G R E A L R R 23
GCGCTGCGGGAGGGCTACGCGGTATCGGCTCTGGTTCGGAAACCGGGCGCTGTGCGGCCCGACGCGCGCCGTGCGGGTGGTCCGCGGG 180
A L R E G Y A V S A L V R N P A L L P P D A A P C R V V R G 53
GACGCGCTGCGCGCCGCGACGTCAGCGCCACCGTGC GG GGCAGCGCGCCGTCATCGTCACTTGGGAACGCGCGGAGACATCGGTCCC 270
D A L R A A D V S A T V R G Q R A V I V T L G T R G D I G P 83
ACCACCGTCTATCAGACAGCACCCGCAACATCGTGGCCGATGAAGGAGCACGCGCTGCCAAAGTGGTGGCGTGTCTGTCCGCTTC 360
T T V L S D S T R N I V A A M K E H G V R K V V A C L S A F 113
CTCTTATGGGATCCTGAGAAGTCCCCACGCGGCTGCGGGCGCTGACGGAGGACCACGCGCGGATGCACGCCGTGCTGAGCGGGGCCGGG 450
L L W D P E K V P T R L R A L T E D H A R M H A V L S G A G 143
CTGGATTACGTGGCCGTCATGCGCCCCACATCGCCGACGACAAGCCGCTGACGGAGGCATACGAGGTACGGTCCGTGGCACCGCGCGT 540
L D Y V A V M P P H I A D D K P L T E A Y E V T V G G T G G 173
GGCTCGCGGGTTCATCTCCACGCGGACCTGGCCCATTTCTCCTGCGCTGCCTCAGCACCACCGGTTTCGACGGGAAGAGCGTCTACGTC 630
G S R V I S T P D L A H F L V R C L S T T A F D G K S V Y V 203
TGCGGGCACTACGGCTGAGGGGGGGCAGCGGGGGCATGGGGGCAGTGGGGGCATGGGGGCAGTGGGGGCAGTGGGGTCAATAGGGAC 720
C G H Y G * 208
ATGAGGTCATTGGGGATATTGGGGTCAATGAGGGCAATGGGGGCAGTGGGGCAATAGGGACATTGAGGTCATTGGGGGCATTGGGGTTC 810
AATGAGGGCATTGGGGGCATTGGGGTCAATGGGGCAATGGAGGCAGTGGGGCATTGGGACACATGGGGACATGGGGGCATTGGCGTTC 900
AATGGGGACATTGGGGGCAATGGAGGCAATGGGGAATGGGGGGCAATGGGGGCAGTGGGGACATGGGGGTCAATGGGGACATGGGAGGC 990
AATGGGGGCAATGGGGACATTGGGGGCATTGGGGGCAATGGGGGCATGGGGGCAATGGAGGCAATGGGGACATTGGGGTCAATGGGGTTC 1080
AATGGGGCAATGGGGCAATGGGGTCAATGGGGTCAATGGGGTCAATGGGGTCAATGGGGTCAATGGGGTCAATGGGGTCAATGGGGTCA 1170
CAATGGGGTCAATGGGGACATGGGGTCAATGGGGACACATGGGGCAATGGGGTCAATGGGGTCAATGGGGTCAATGGGGTCAATGGGGTCA 1260
GCCAATGGGGTCAATGGGGACACAAATGGGGCAATGGGGACATAATGGGGCAATGGGGTCAATGGGGCAATGGGGTCAATGGGGTCAATGGGGTCA 1350
CCAAAATGGCGTAGATTTGACCCCAAAAAAGCCCCACTTTTCCCCCCCCCGAATCCCAACGCGGCCGTGGTATAAACTTCAATAAG 1440
GCCGAAAAAAAAAAAAAAAAAAAA 1461

```

Figure 2

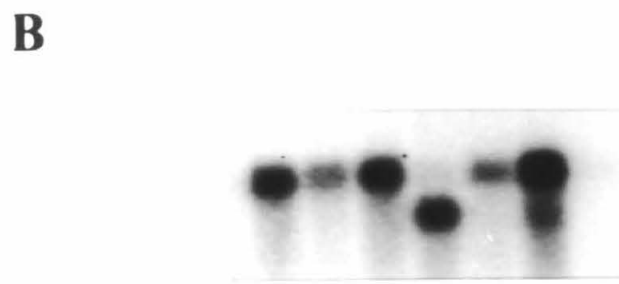
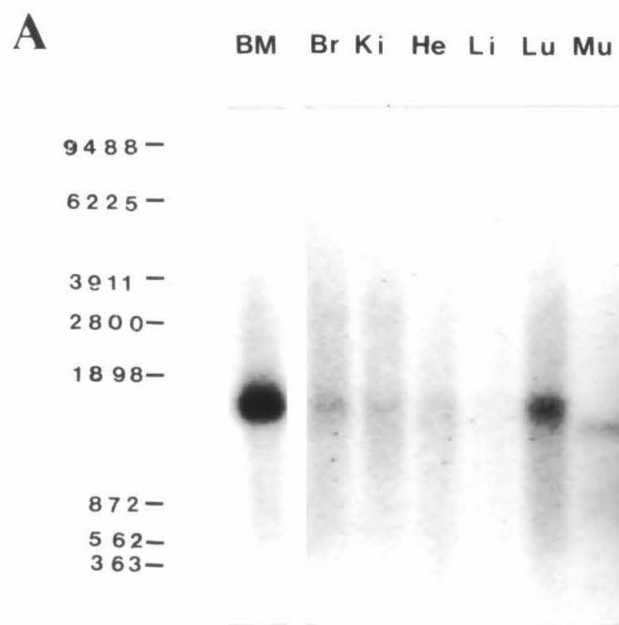


Figure 3

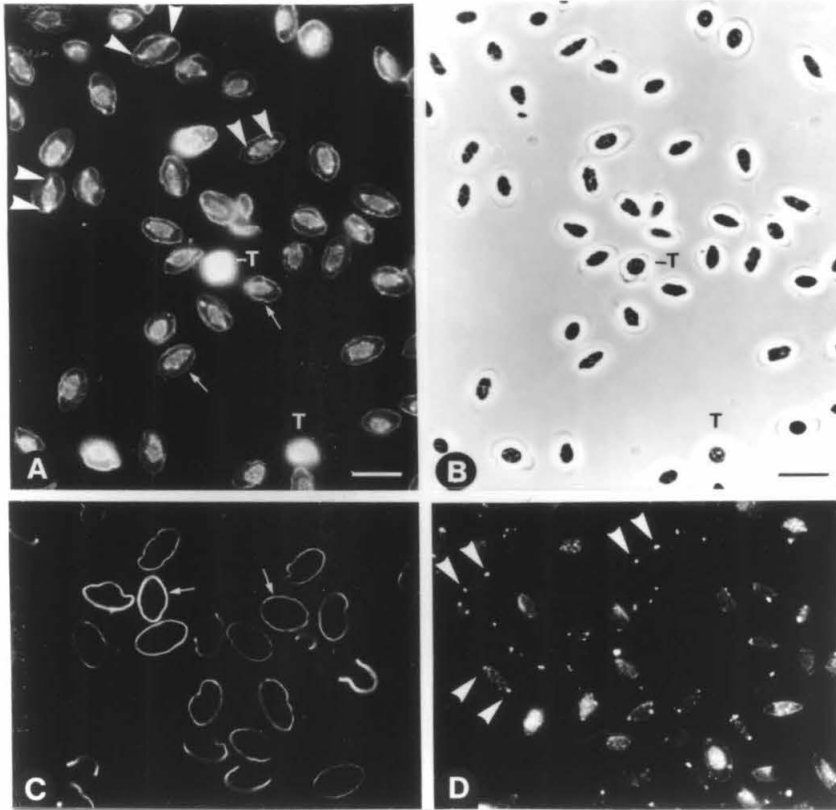


Figure 4

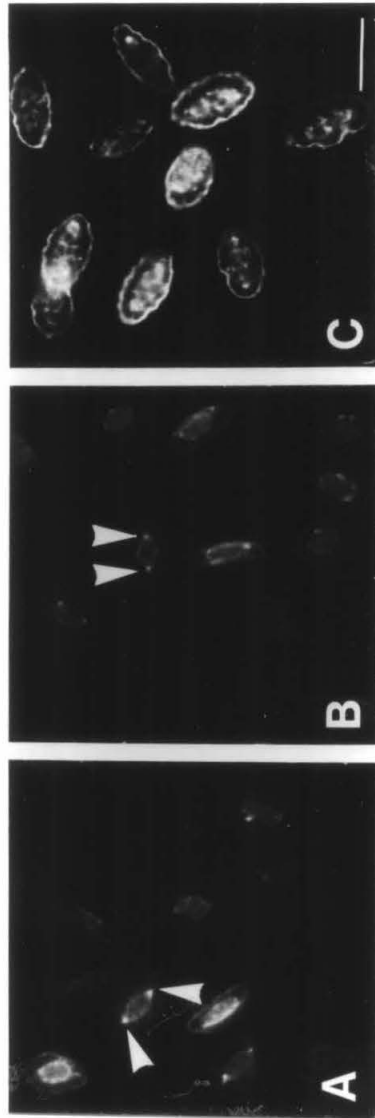


Figure 5

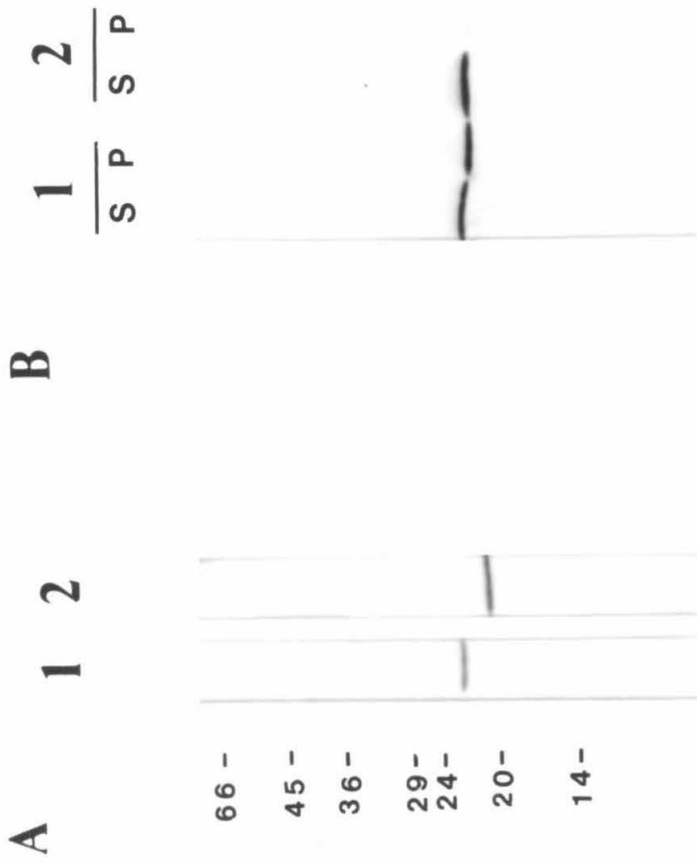


Figure 6

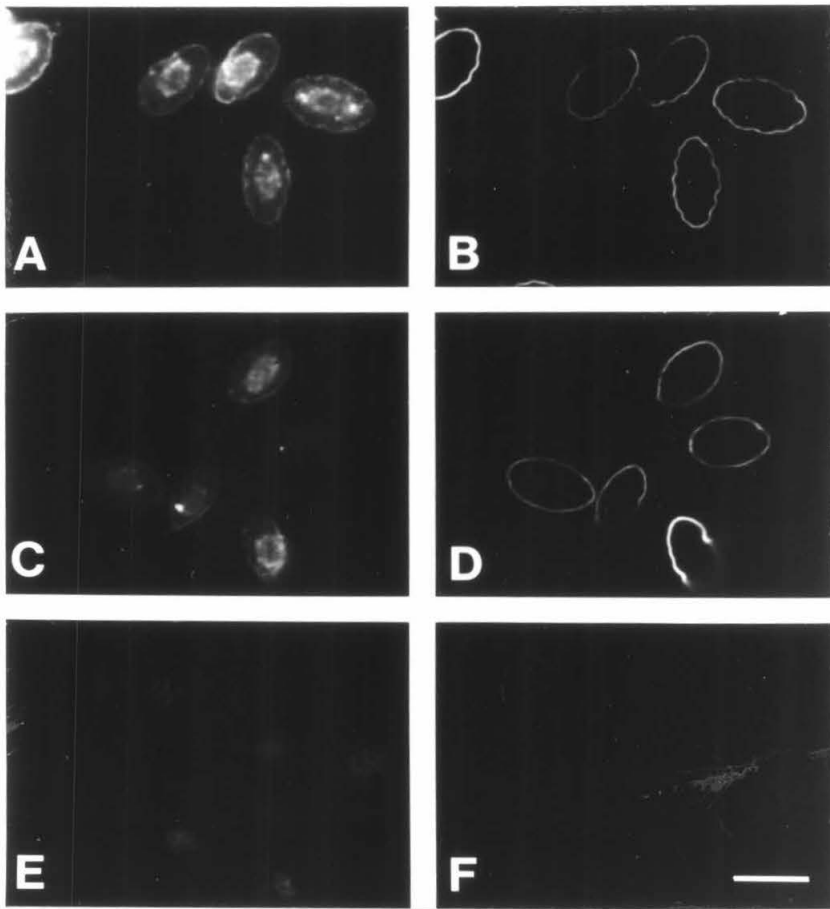


Figure 7

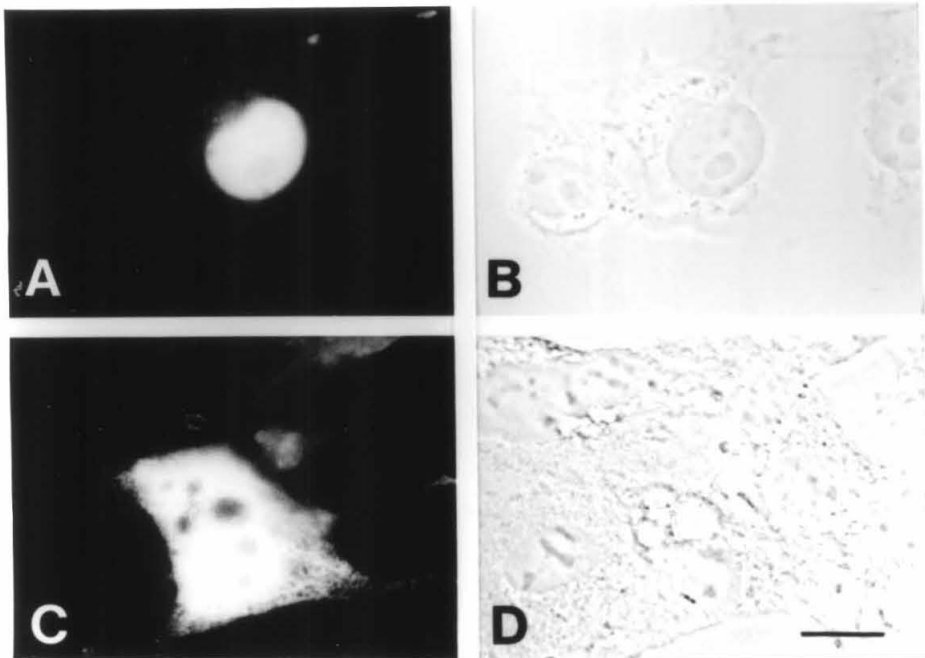


Figure 8

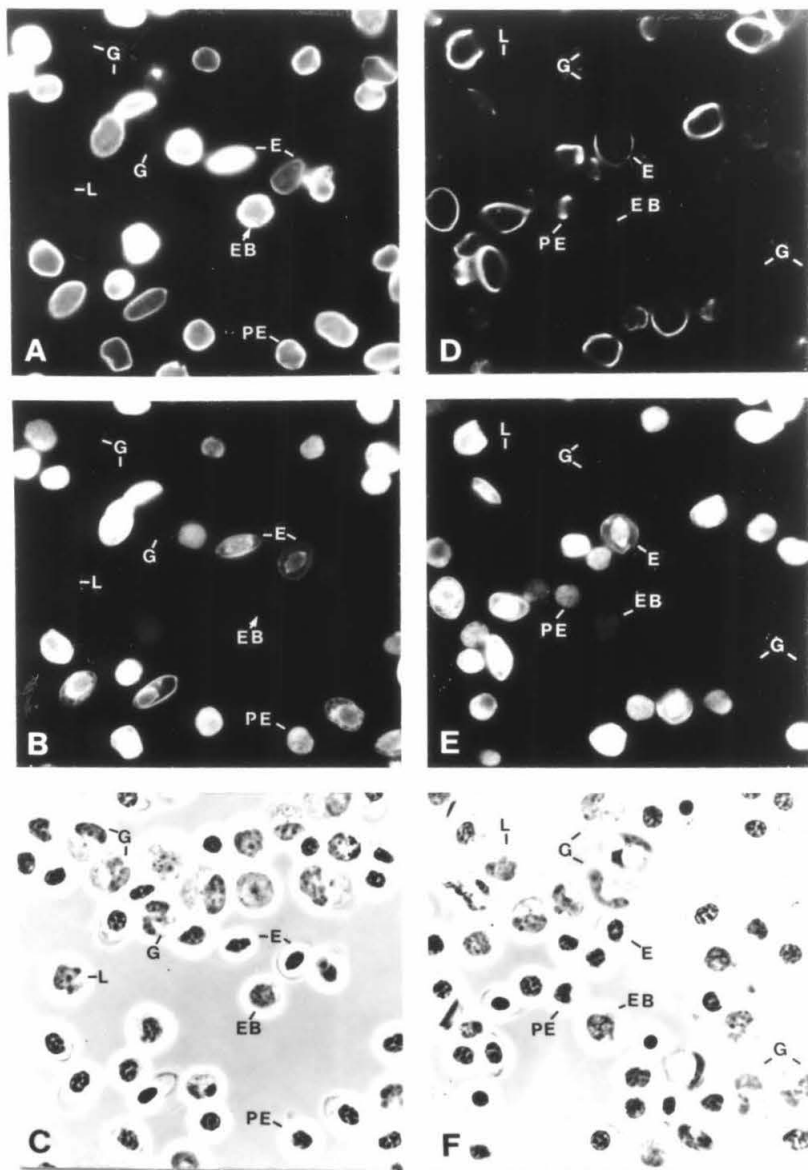


Figure 9

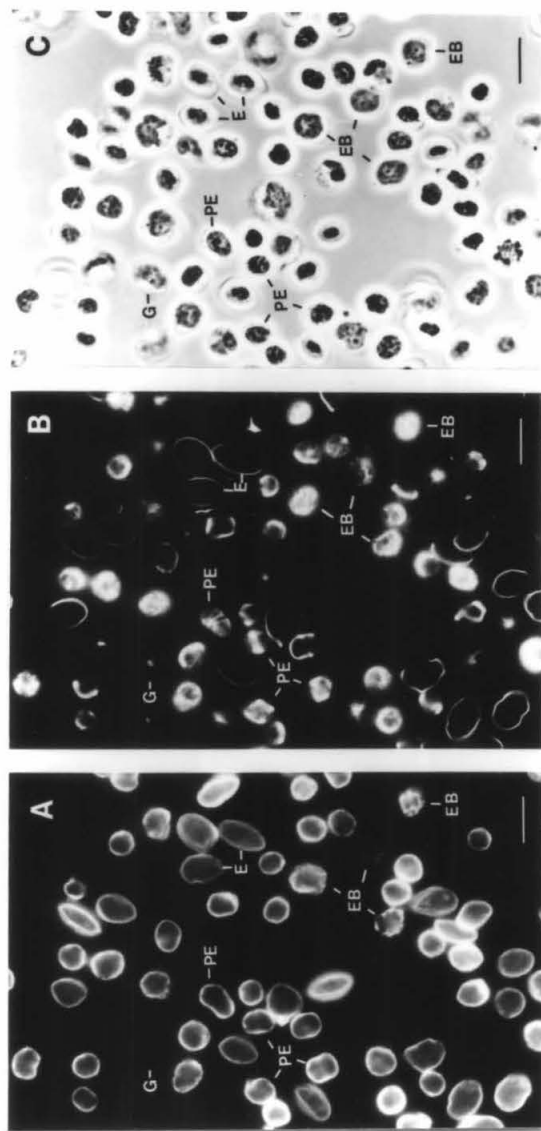


Figure 10

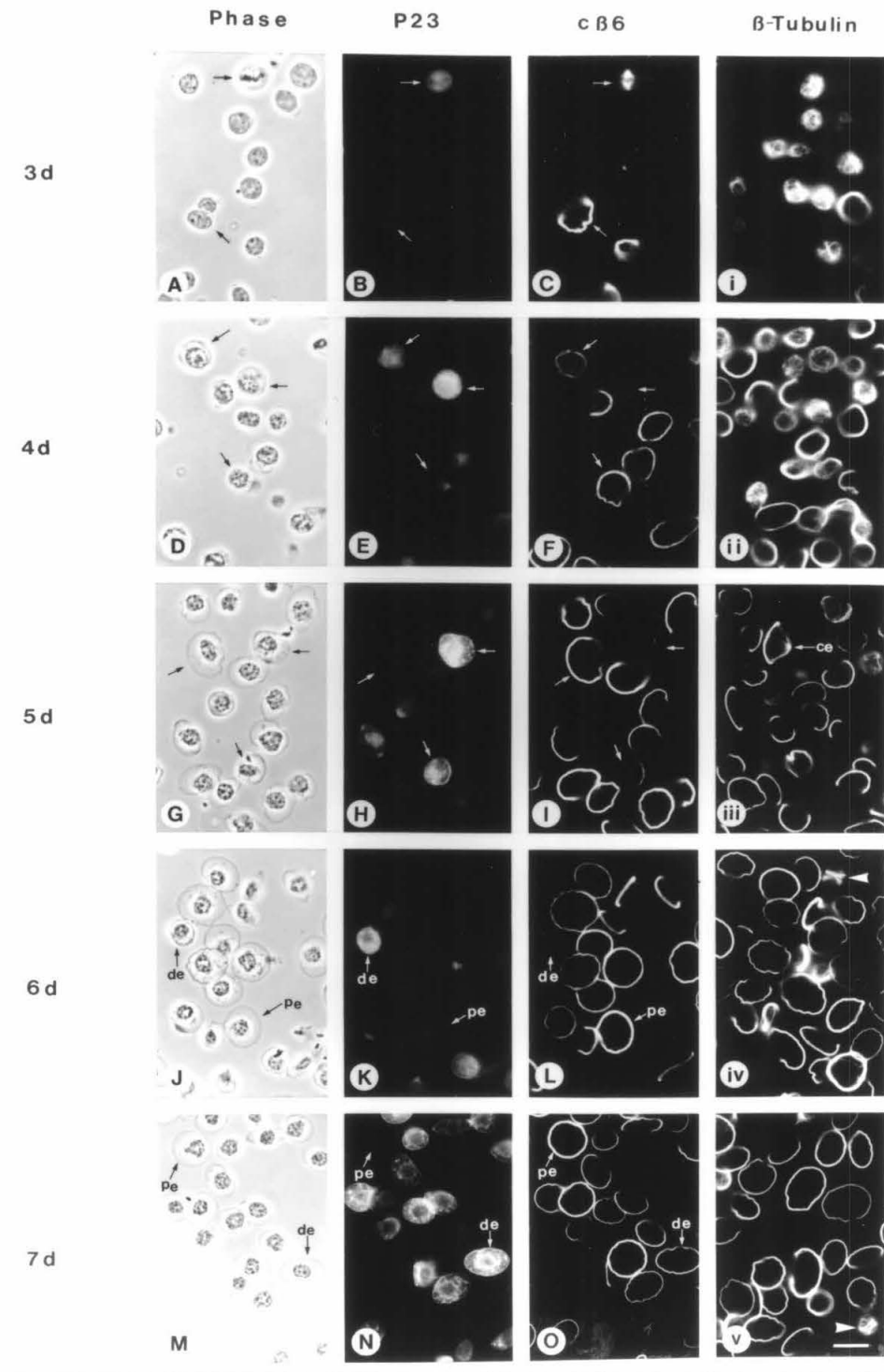


Figure 11

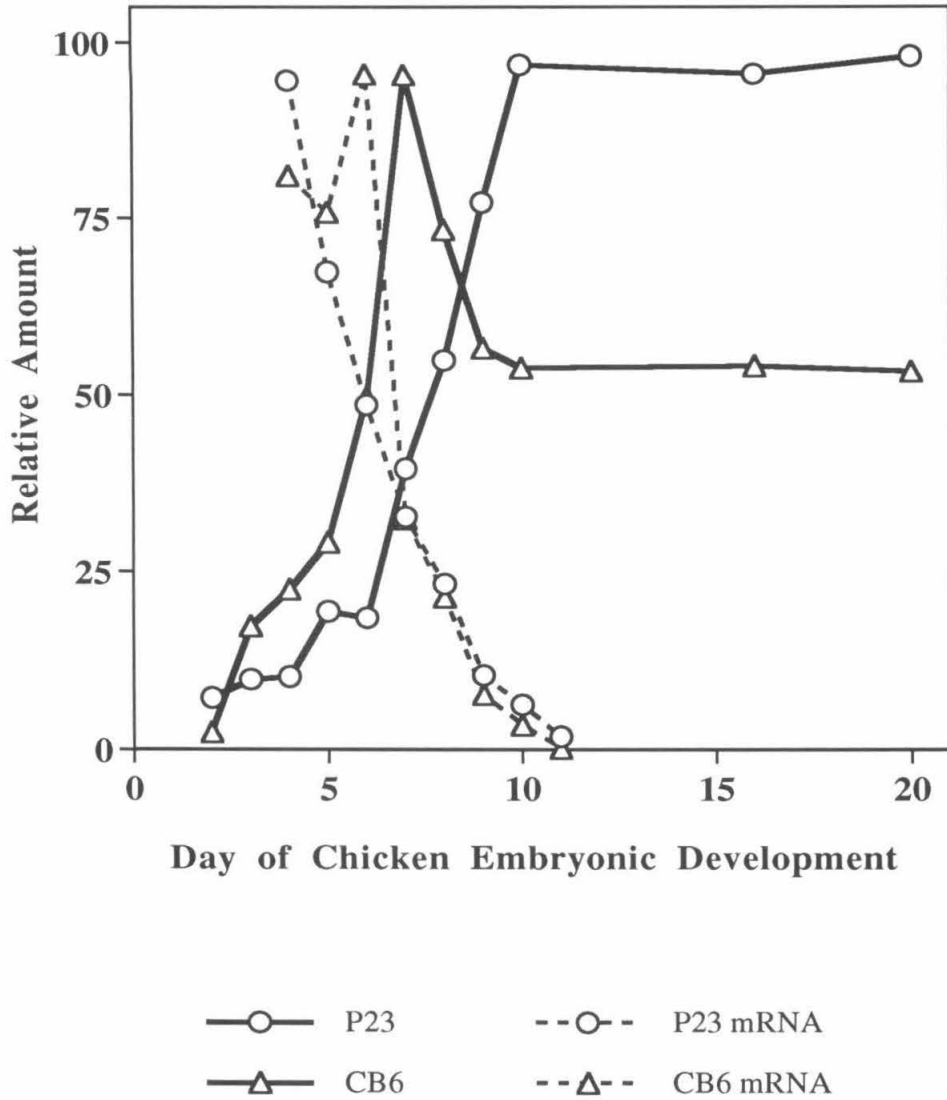


Figure 12

## Chapter Four

### P23 Fails to Interact Directly with Microtubules

#### Introduction

In earlier experiments, we identified a novel calcium binding protein in mature avian erythrocytes (chicken and turkey) with MW of 23 kDa (p23). p23 is a highly basic protein with a pI > 9.5. It localizes to centrosomes and discrete sites around the nuclear membrane as well as the marginal band (MB), a microtubule (MT) based structure which encircles the equatorial rim of these nucleated erythrocytes under the cytoplasmic face of the plasma membrane (Behnke, 1970; Barret and Dawson, 1974; Cohen, 1978; Nemhauser et al., 1980). MB microtubules (MT) are composed of a unique erythroid  $\beta$ -tubulin variant, c $\beta$ 6 (Murphy & Wallis, 1983a,b; Murphy et al., 1987), which exhibits different properties to those of other tubulins (e.g., brain tubulin). MT formation of erythroid tubulin in vitro is characterized by a lower critical concentration for nucleation and a tendency to form fewer but longer more stable MTs than brain tubulin (Murphy & Wallis, 1983b, 1985; Trinczek et al., 1993). Since immunofluorescence and developmental analysis of p23 expression and localization revealed that p23 appears to be associated with the c $\beta$ 6-MT containing MB structure (Chapter 3), the question arose whether p23 functioned as a microtubule-associated protein (MAP).

Classically MAPs have been defined as proteins which consistently copurify with tubulin during successive cycles of assembly and disassembly and modulate MT

properties. The structural MAPs, which include MAP1 (380 kDa), MAP2 (280 kDa), MAP4 (200kDa) and tau protein (50~70 kDa), are actively involved in MT assembly, stabilization and bundling (see reviews, Olmsted, 1986; Matus, 1988; Tucker, 1990; Goedert, 1991). In addition to these major MAPs, it has been reported that some basic proteins with low molecular weight (LMW, <50 kDa, such as histone H1 (34 kDa) and RNase A (14 kDa)) can also facilitate the assembly and bundling of MTs *in vitro* (Erickson & Voter, 1978; Centones & Sloboda, 1986). The phenomena was hypothesized to be the result of a non-specific electrostatic interaction between LMW basic proteins and acidic tubulins (Erickson & Voter, 1978). Recently, the hypothesis of nonspecific, artifactually-induced interactions between these proteins and MTs has been challenged by the unexpected discovery that histone H1 appears to localize in sea urchin sperm flagella and be involved in the stabilization of axonemal MTs (Multigner et al., 1992). The 20 kDa Stable Tubulin Only Protein (STOP), which was initially characterized as being associated with cold-stable MTs from bovine brain, was subsequently identified as myelin basic protein (Pirollet et al., 1989). STOP has been shown to increase MT stability in a Ca<sup>2+</sup>/calmodulin dependent manner (Pirollet et al., 1992). Whether or not these interactions occur specifically *in vivo* remains to be determined.

Given the basic nature of p23 and its apparent association with the c $\beta$ 6-MT containing MB structure, we suspected that p23 may function as a c $\beta$ 6-specific MAP. Alternatively, p23 could belong to the family of LMW basic proteins that can also act to augment MT assembly, bundling and stabilization. To further investigate the issue, we tested a) the ability of p23 to copurify with erythroid tubulin through successive cycles of assembly and disassembly; b) the ability of p23 to induce and/or augment MT

polymerization from purified brain and erythroid tubulins; c) the ability of p23 to induce MT bundling by electron microscopy. From these experiments p23 did not appear to interact directly with either brain or erythroid tubulins. Therefore, p23 does not behave as a classical MAP and does not exert any direct effect on MT assembly or bundling properties at least in a simple binary fashion.

## **Materials & Methods**

### **Protein preparation**

Chicken p23 was isolated by gel filtration and affinity chromatography as previously described (Chapter 2 & 3). The eluants from the affinity column (in 100mM Citric acid buffer, pH 3.0) were immediately adjusted to pH ~7.0 by adding 1/10 volume of 1M HEPES buffer (pH 8.4) and pooled into a dialysis bag (MW cut 8,000) and concentrated with Aquacide II. Once the pooled fractions were reduced to 1/10 vol of original volume, the bag was removed from Aquacide II, washed, and left in dialysis buffer (100mM MES, pH 6.75, 1mM EGTA, 1mM MgCl<sub>2</sub>, 10 g/ml leupeptin, three times changes) for 24 hr at 4°C. The solution was then aliquoted, rapidly frozen in liquid nitrogen (LN<sub>2</sub>) and stored at -80°C until use.

Bovine brain tubulin was prepared according to the method of Asnes & Wilson (1979) with the following modifications: 1) the phosphat-glutamate buffer was replaced by MES buffer (100mM MES, pH 6.75, 1mM EGTA, 1mM MgCl<sub>2</sub>); 2) the brain tissue was homogenized in a Waring blender instead of a Teflon glass homogenizer with MES buffer containing 1mM DTT and 10 g/ml PMSF; 3) following the second assembly cycle,

the microtubule pellet was frozen in LN<sub>2</sub> and stored at -80°C until use.

Chicken erythrocyte tubulin (c $\beta$ 6, Murphy et al., 1983a; 1985) was purified according to Murphy (1991) except MES buffer was substituted for phosphate-glutamate buffer. The c $\beta$ 6-microtubule pellet from the third cycle was frozen in LN<sub>2</sub> and stored at -80°C.

Before conducting MT assembly experiments, the whole pellet was resuspended in MES buffer for 20 min at 0°C prior to centrifugation at 200,000g for 20min to remove any cold-insoluble debris. The protein concentration was determined by the Bicichoninic Acid (BCA) Protein Assay.

### **Protein gel electrophoresis & immunoblotting**

Proteins were separated by 20% SDS-PAGE as previously described (Chapter3). Since the microtubule pellet was resuspended in one-tenth the original supernatant (SN) volume, the pellet suspension used for SDS-PAGE was diluted ten times in order to have equivalent SN-pellet loadings. Immunoblotting was carried out as previously described (chapter 3).

### **Turbidity measurement in MT assembly**

Turbidity measurements were carried out essentially as described by Gaskin et al. (1974) and adapted for 96 well micro titer plate reading at 340nm with a ThermoMax microplate reader. Reactions were carried out in a 200 $\mu$ l volume containing 1mg/ml

tubulin, 1mM MgCl<sub>2</sub>, 1mEGTA, either in the presence or absence of 100mg/ml p23, mixed with 6μl of 25mM GTP and incubated for 30 min at 37°C. Absorbance readings were taken every 30s.

### **Electron microscopy**

MT polymerization was initiated either in the presence or absence of p23 as described above. After incubation was complete, 3μl of reaction mixture was placed on 400-mesh copper grids that had been previously coated with colloidon (1.5%) and carbon. After 10s, the sample was drawn off with filter paper and the grids were stained with 0.5% uranyl acetate as described (McEwen and Edelstein, 1977). Grids were examined using a Philips CM12 transmission electron microscope at 13,500 X..

### **Results**

As a first step to ascertain the mechanism by which p23 associates with the MB, we sought to determine whether p23 would copurify with erythroid tubulin through successive rounds of MT depolymerization and polymerization. This is a classical approach to determine whether a protein is a *bone fide* MAP. The first cycle was carried out by incubating chicken erythrocyte lysate with 1mM GTP for 45 min to induce MT polymerization and subsequent centrifugation at 25,000g for 90 min at 37°C to pellet MTs. The pellet (H<sub>1</sub>P) was resuspended in one-tenth the supernatant volume to maintain a similar tubulin concentration in MES buffer as used in the first cycle and subjected to a second assembly cycle. The pellet of the second cycle (H<sub>2</sub>P) was again resuspended in 1/10 of the supernatant volume. The suspension was then centrifuged at 200,000g for 45

min at 5°C to remove actin-spectrin and cold-insoluble tubulin aggregates (C<sub>2</sub>P). The supernatant (C<sub>2</sub>S) was subjected to a third assembly cycle. This time the sample was layered on a sucrose cushion or directly loaded into tube and was centrifuged at 200,000g for 60 min at 30°C to pellet assembled MTs. As shown in Fig. 1, almost all the p23 was co-pelleted with H<sub>1</sub>P in the first cycle. This pellet contained polymerized MT, actin-spectrin complexes as well as other components (Murphy, 1991). However, in the second cycle, only 20% of p23 stayed in the pellet (H<sub>2</sub>P) while 80% remained in supernatant (H<sub>2</sub>S). 10% of pelleted p23 was in the cold insoluble fraction (C<sub>2</sub>P). After the third cycle, the tubulin was over 80% pure and p23 was no longer found in the MT pellet (H<sub>3</sub>P). Therefore, the amount of p23 copurifying with the MT pellet decreased dramatically during successive cycles of MT assembly and disassembly cycle. This suggests p23 exhibits weak, if any, direct binding to MTs.

An alternative approach towards understanding the significance of p23 association with MTs is to investigate whether p23 can induce MT assembly or bundling. One method to assay this is to look for increases in turbidity under conditions favoring polymerization of tubulin into MTs when p23 is added in assembly reaction. Both bovine and erythroid tubulins were used to see if the effect is cβ6 specific. Purified chicken p23 was either mixed with bovine or erythrocyte tubulins in a molar ratio of 1:5 (p23:tubulin) in MES buffer. (Note: the maximum concentration of p23 that could be obtained was 100µg/ml). The protein mixtures were incubated at 37°C in the presence or absence of 1mM GTP and absorbance was recorded every 30s. Tubulin alone and tubulin with GTP in the absence of p23 were used as control. As shown in Fig. 2, in the absence of GTP, p23 alone is incompetent to initiate MT assembly. Even under conditions promoting tubulin polymerization into MTs (i.e., in the presence of GTP),

p23 does not affect the extent of tubulin polymerization. Thus p23 did not augment either c $\beta$ 6-MT or bovine brain tubulin MT assembly. EM analysis (Fig. 3) provided further evidence that no assembly occurred when p23 was incubated with tubulin in the absence of GTP. In addition, no evidence of p23 effects on MT bundling in the p23, tubulin and GTP mixture was observed.

## Discussion

Previously IF analysis had demonstrated that p23 localized to the centrosomes and marginal bands (MBs) of mature chicken and turkey erythrocytes. Developmental analysis showed that the localization of p23 succeeded the formation of MBs in the late erythropoiesis stages. It was also observed that the localization of p23 relied on the integrity of MBs and cytoplasmic [Ca<sup>2+</sup>] (Chapter3). These results suggested that p23 may interact with MB microtubules after MBs are formed. In the assembly/disassembly experiments presented here, close to 100% of p23 was found in the pellet of first assembly pelleting cycle. However, since the pellet obtained after the first round of MT polymerization is also known to contain considerable amounts of contaminating proteins, e.g., actin-spectrin complexes (Murphy, 1991) in addition to MTs, the presence of p23 in the pellet is not conclusive of an MT-association. During the second and third cycles of tubulin polymerization, the purity of tubulin increases considerably but now p23 fails to follow the same soluble-insoluble cycle exhibited by tubulins. These data suggest that either 1) p23 is not a MAP; 2) the interactions between p23 and MTs are either indirect or very weak or 3) another component may be required for the localization of p23 to MB in a calcium dependent manner.

The turbidity of polymerization reaction solutions is a reliable measure of the mass of high molecular MTs assembled from soluble protein (Gaskin et al., 1974). Our results showed that p23 alone cannot induce the assembly or increase the extent of assembly. Nor could it cause the bundling of MTs under conditions favoring MT assembly. However, the turbidity measurement is a steady-state value of the MT mass and does not accommodate the dynamic nature of MTs. To ascertain whether p23 has a more subtle effect on supramolecular organization, we analyzed whether p23 had any effect on the resultant supramolecule structure of MTs by EM. However we were unable to detect any effects of p23 on average MT length or bundling. From the results presented here, we cannot exclude the possibility that p23 may affect MT stability by changing the growth or shrinking rate of MTs. Moreover, since p23 is only 75% pure in the eluant from the affinity column, and from the purification schemes used the tubulin preparations still contain MAPs, it could be that contaminants in the protein mixture may have affected the result. However, despite the possibility that contaminating proteins may mask any direct effect p23 may have on MT supramolecular organization, the experiments reported here suggest it is more likely that p23 is not directly, or sufficient in itself to affect MT polymerization and bundling. Therefore, the answer to the issue of what p23 associates with in the MB and centrosomes, and the functional significance of these associations awaits further experimentation.

## Figure legends

Figure 1. P23 distribution during successive assembly and disassembly cycles of chicken erythrocyte  $\beta$ -tubulin.  $H_NP$ ,  $H_NS$ ,  $C_NP$  and  $C_NS$ : purification fractions obtained after n cycles from assembly - disassembly. C denotes fractions from 4°C centrifugations and H, fractions from 30°C centrifugations; S, supernatant; P, pellet.

Figure 2. Turbidity measurement of microtubule assembly from bovine (A) and erythrocyte (B) tubulin in either the presence or absence of p23. No polymerization was measured in the tubulin mixture without GTP, irregardless of the presence of p23. In the presence of GTP, the degree of polymerization when p23 was included was almost the same as that without p23.

Figure 3. MT assembly examined by electron microscopy under conditions of (A) with GTP alone; (B) with GTP and p23; (C) with p23 alone. No MT bundling was shown in the presence of p23. All micrographs were recorded at 13,5000 X.

H<sub>1</sub>S H<sub>1</sub>P H<sub>2</sub>S H<sub>2</sub>P C<sub>2</sub>S C<sub>2</sub>P H<sub>3</sub>S H<sub>3</sub>P

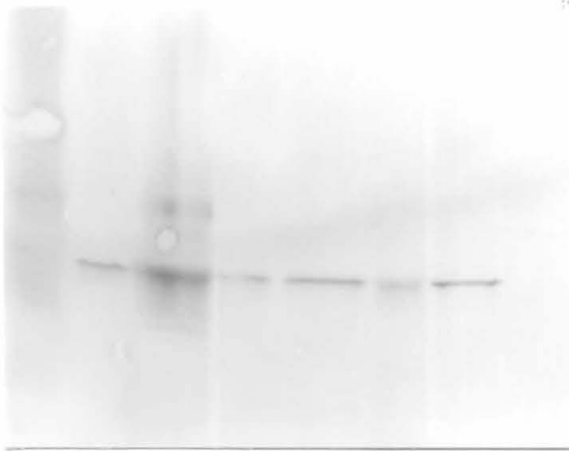


Figure 1

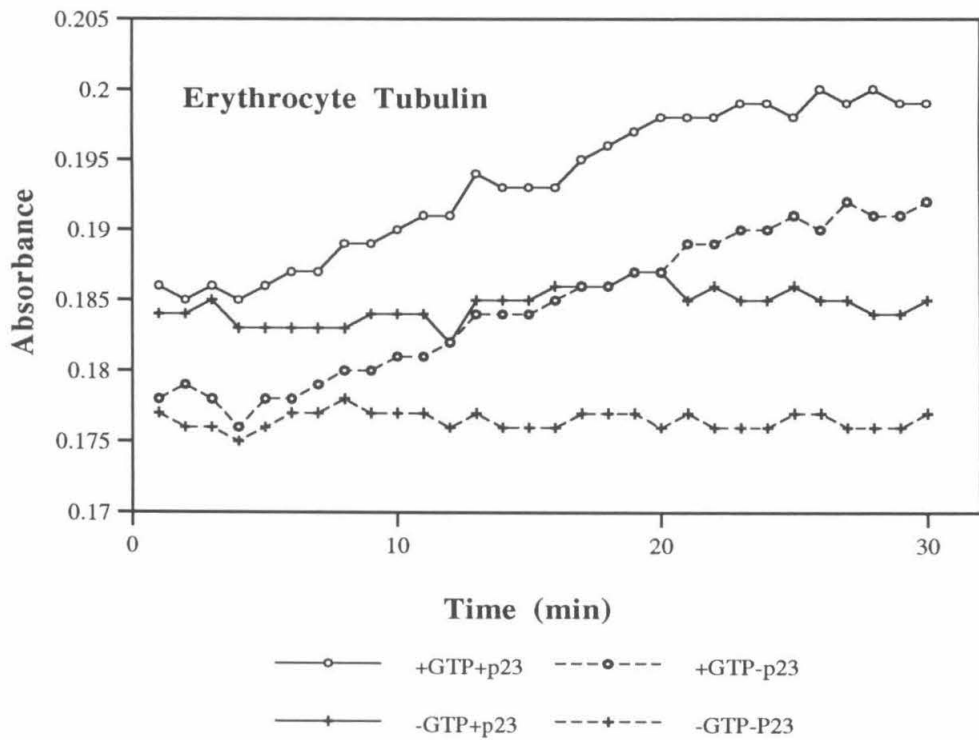
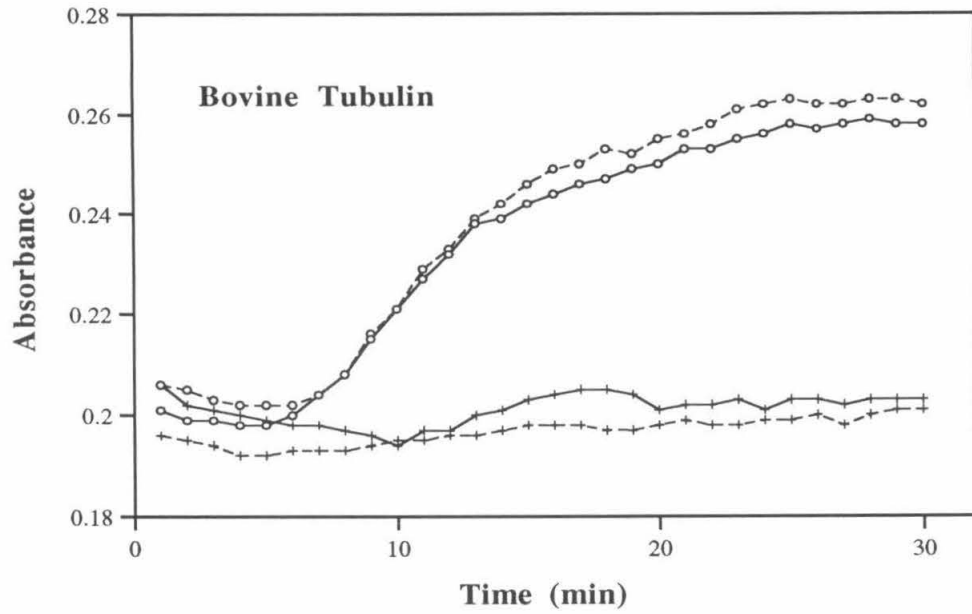


Figure 2

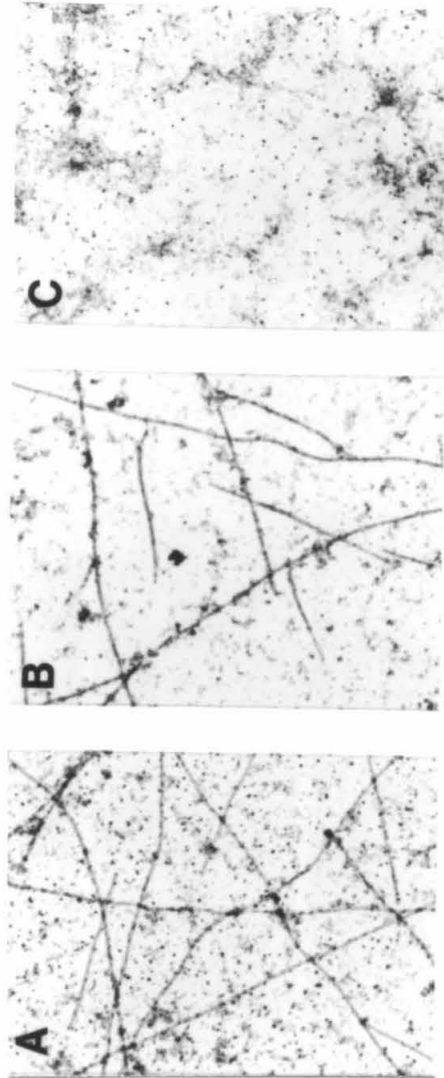


Figure 3

## Chapter Five

### Search for p23 Homologues in Other Species

#### Introduction

Marginal bands (MBs), continuous peripheral bundles of MTs encircling the equatorial rim of the cells (Behnke, 1970; Barret and Dawson, 1974; Cohen, 1978; Nemhauser et al., 1980), have been suggested to be involved in determining cell morphology and maintaining cell shape against deformity during circulating (Barrett and Dawson, 1974; Joseph-Silverstein & Cohen, 1984). These MB structures have been found in nonmammalian erythrocytes and thrombocytes (Behnke, 1970; Murphy et al., 1986; Birgbauer & Solomon, 1989), mammalian platelets (Kenney & Linck, 1985; Kowitz et al., 1988), and in rudimentary form in mammalian nucleated, primitive erythrocytes (Sangiorgi et al., 1990). The data presented previously describe a novel  $\text{Ca}^{2+}$  binding protein, p23, which localizes to the MBs of avian erythrocytes and thrombocytes. The protein was also hypothesized to be involved in MB stabilization, following MB formation, in a  $\text{Ca}^{2+}$  dependent manner. Since p23 is expressed exclusively in avian erythrocytes and thrombocytes that are both MB-containing cell types, we reasoned that p23 homologues may be present in MB-containing cells of other species. We demonstrate here by immunofluorescence staining that antigenically-related p23 homologues exist in goldfish and *Xenopus* erythrocytes, human platelets, and primitive mouse erythrocytes. Further analysis using cross-species Southern blots suggests that p23 may belong to a multigene family that is expressed in a variety of species.

## Materials & Methods

### Cells

Primitive erythroid cells of 9d mouse embryos were isolated as previously described (Sangiorgi et al., 1990). Goldfish and frog RBCs were collected and washed in heparinized Ringer's solution as described by Cohen and Ginsburg (1986). Human platelet-rich plasma was separated from red and white blood cells by centrifugation (200g, 15min) of freshly collected whole blood in sodium citrate. The platelets were freed of plasma by two cycles of pelleting at 1200g for 15min and resuspended in modified Tyrode's medium ( $Mg^{2+}$ - $Ca^{2+}$  free Hank's buffered salt solution, 5 mM  $MgCl_2$ , 5 mM HEPES, 1 mM EGTA, 0.5% BSA, 500 nM PGE1[prostaglandin E1]) (Kenney and Linck, 1985).

### Antibody preparation

Rabbit polyclonal antisera were generated against chicken p23 as described (Chapter 3). Filtered rabbit antisera containing one tenth volume of 10XTBS (100mM Tris-HCl, pH 8.0, 1.5M NaCl, 10mM EGTA) were loaded onto an affinity column made by coupling purified chicken p23 to CNBr-activated Sephadex-4B. Specifically-bound IgG was then eluted with citric buffer (100mM Citric Acid, pH 3.0, 20mM NaCl). The eluant was adjusted to ~pH 7, concentrated by Aquacide II (Calbiochem), and dialyzed against 1 X TBS for 24hrs at 4°C. The antibody concentration (~100 $\mu$ g/ml) was determined by BCA protein assay (Pierce). The solution was then aliquoted and stored at

- 80°C until use.

### **Immunofluorescence analysis**

Immunofluorescence (IF) staining was carried out as previously described (Chapter 3). The cells were double-labelled with rabbit polyclonal anti-chicken p23 (diluted 1:10) and mouse monoclonal anti-chicken  $\beta$ -tubulin (diluted 1:100) and were visualized using Zeiss Axiophot microscope with a 63 X lens. The IF images were photographed using Kodak TP (ISO 100) film with an ISO setting of 200 and developed in D-19 developer. The phase images were photographed using Kodak TP (ISO 100) films and developed in HC-110 developer.

### **Southern and Northern blotting**

Freshly prepared or commercially purchased genomic DNAs from different species were digested by either EcoRI or HindIII, separated on a 0.7% agarose gel in TBE (89mM Tris-HCl, pH 8.3, 89mM boric acid, 20mM EDTA), transferred to Zeta-probe GT nylon membrane (Biorad) and blocked (Sambrook et al., 1989). The multiple species Southern blot, as well as the multiple tissue Northern blots (MTN) of human and mouse, were then hybridized by a  $^{32}$ P radio-labelled chicken p23 probe as previously described (Chapter 3) with the following slight modification: 80mM  $\text{NaH}_2\text{PO}_4$  pH7.2 (equivalent to 0.5 X SSC) was substituted for 20mM  $\text{NaH}_2\text{PO}_4$ .

## **Results**

Fig. 1 shows the results of double labelling using polyclonal anti-p23 and monoclonal anti- $\beta$ -tubulin in human platelets (A, B, C), mouse primitive erythrocytes (D, E, F), goldfish erythrocytes (G, H, I) and *Xenopus* erythrocytes (J, K, L). The polyclonal anti-chicken p23 appeared to stain the MBs in both fish and frog erythrocytes. Anti-p23 also reacted with dot structures presumed to be the centrosomes. IF also demonstrated that cross-reactive proteins to p23 also could be observed in mouse primitive erythrocytes and human platelets. However, in these cells the staining appeared diffuse rather than being localized to MB or MT structures. Under the same staining conditions, no positive signal was found in mouse definitive erythrocytes and bone marrow cells (data not shown).

Since components antigenically related to p23 were detected in MB containing cells of other species, multiple species Southern blot analysis was performed to verify p23 gene homologues existed in other species. When the blot was hybridized with  $^{32}\text{P}$  labelled chicken p23 probe and washed under medium stringency (80 mM  $\text{NaH}_2\text{PO}_4$ ) conditions, several positive bands were observed in *C. elegans*, *S. cerevisiae*, *Xenopus* and mouse genomic DNA (Fig. 2). When human and mouse multiple tissue Northern (MTN) blots were probed, double bands were detected in both human (2.0Kb and 1.8Kb) and mouse (1.8 Kb and 1.4 Kb) liver mRNA; a single band (1.8 Kb) was detected in mouse lung mRNA (Fig. 2).

## Discussion

The data presented here reveal that antigenically-related p23 homologues appear to be expressed in MB-containing cells of other vertebrate species. p23 homologues

were found to localize to the MBs of fish and *Xenopus* erythrocytes in an identical manner to chicken and turkey p23. Mammalian human platelets and mouse nucleated primitive erythrocytes also stained positively with anti-p23 sera. However, in these cells the staining was distributed diffusely in cytoplasm. Given that chicken p23 is diffuse in developing erythrocytes before the formation of MBs, p23-like proteins in these cells may be behaving in an analogous fashion to avian early erythroblast stages. The diffuse pattern could be caused by too high cytoplasmic  $[Ca^{2+}]$  or lack of linkage components to couple p23 to the MB and centrosomal structure.

These immunoreactive antigens in other vertebrate species have yet to be shown conclusively to be p23 homologues. Western blot analysis revealed a band of  $M_r \sim 23$  K in the lysate of fish erythrocytes but no immunoreactive bands were detected in the lysates of other cells (data not shown). This may reflect the possibility that fish p23 is antigenically closer to chicken p23 than other species. This is supported by the fact that anti-p23 IF staining of fish erythrocytes appeared much brighter than with the other cell types tested.

The Southern and Northern analysis support the hypothesis that p23 homologues exist in other species. The heterogeneity in the transcript size not only between species but within a given species may indicate that p23 is a multigene family. Comparative analysis of variants found in different cell types and different species, in particular of the lower species, may greatly extend our understanding of the function of p23 and how it may have evolved to exhibit such cell-lineage specificity in its expression.

## Figure legends

Fig. 1. Double immunofluorescence staining with anti-chicken p23 antisera (A, D, G, J) and anti- $\beta$ -tubulin MAbs (B, E, H, K) in marginal band-containing cells of other species: human platelet (A, B, C); mouse primitive erythrocytes (D, E, F); fish erythrocytes (G, H, I) and *Xenopus* erythrocytes (J, K, L). C, F, I, and L were the phase images of these cells. Bar = 10  $\mu$ m.

Fig. 2. Cross species Southern and Northern blots. The genomic DNAs from *S.cerevisiae*, *C. elegans*, *Drosophila*, *Xenopus*, turkey, chicken, mouse and human were digested with HindIII and EcoRI, separated on 0.7% agarose gels, blotted to nylon membrane and hybridized with <sup>32</sup>P-labelled chicken p23 probe (A). Multiple tissue Northern (MTN) blots from mouse and human (Clontech) were also hybridized with the same probe (B). Exposure time was 48 hr.

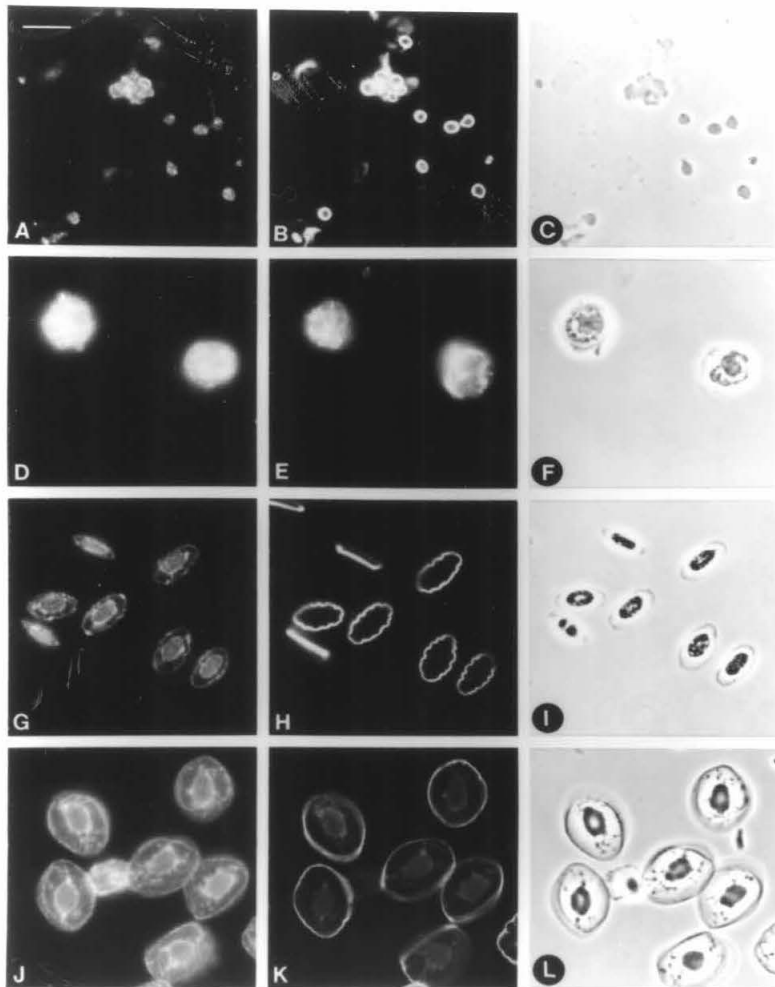


Figure 1

**SOUTHERN**

**NORTHERN**

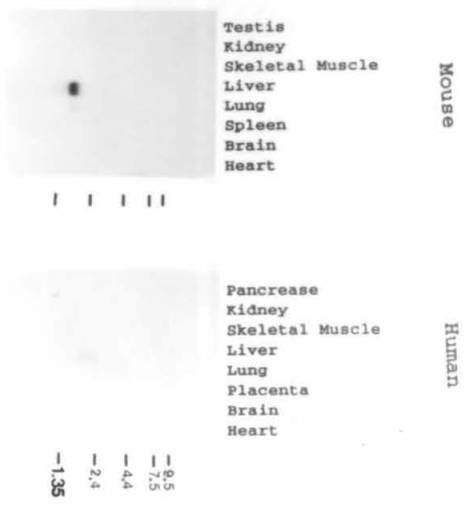
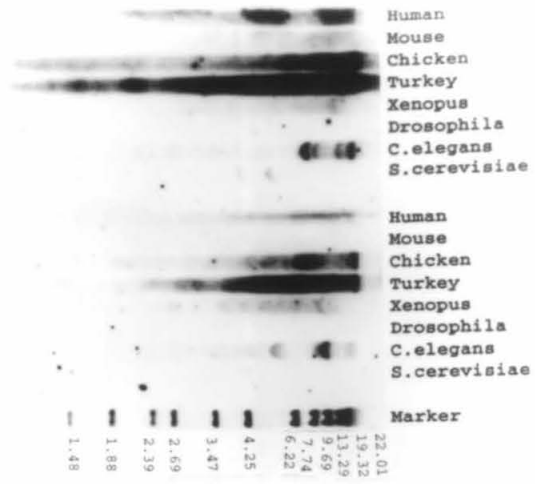


Figure 2

## Chapter Six

### Conclusions

During the study of the binucleated mutation in turkey erythrocytes, which has been suggested to be caused by non-disjunction of chromosomes during the final division of definitive erythropoiesis, we found a protein of Mr ~23 K (p23) always appeared in normal (BnBn) erythrocytes while a truncated form of p23 with Mr~21 K (p21) existed in bnbN erythrocytes. Both p23 and p21 localized to the marginal bands, centrosomes, and discrete sites around the nuclear membrane. p23 appears to be a Ca<sup>2+</sup>-binding protein and its polymeric state is modulated by Ca<sup>2+</sup>. In contrast, p21 is not Ca<sup>2+</sup>-binding protein and is insensitive to [Ca<sup>2+</sup>]. Molecular cloning yielded the entire coding region of the p23 gene but only a partial coding region of p21. We suspected that the failure to clone the whole p21 gene might be caused by marked secondary structure at the 5' end. The data also show that p21 has a 62 amino deletion at its C-terminus but must therefore have acquired an additional ~40 amino acids at the N-terminus when compared to p23. p23 does not have homologous sequence to any other known sequence in the database. Neither does it exhibit a Ca<sup>2+</sup>-binding motif. Despite the apparent differences between p23 and p21, the p23/p21 allelism did not exhibit an absolute correlation with the Bn/bn genotype. Unfortunately, further analysis was prevented due to the closure of the turkey farm.

Extensive studies of the protein were carried out with chicken erythrocytes because chick erythroblastic cells were readily available. Chicken erythrocytes and

thrombocytes express a p23 homologue that share over 90% homology to turkey p23. Like the turkey protein, chicken p23 exhibits a  $\text{Ca}^{2+}$ -induced shift in Mr under  $\text{Ca}^{2+}$ -SDS-PAGE. Developmental analysis indicated that chicken p23 is diffusely distributed in bone marrow derived definitive erythroblasts but localizes to its target subcellular structures only in maturing erythrocytes after they become postmitotic. p23 is expressed in primitive erythrocytes but it fails to associate with any subcellular organelles. Interestingly, p23 interaction with its target structures can be modulated by intracellular  $[\text{Ca}^{2+}]$ . An increase in  $[\text{Ca}^{2+}]$  to  $10^{-6}\text{M}$  is sufficient to dissociate p23 from these structures. We have postulated from these data that p23 interaction with the marginal band and centrosomes may be induced in part by intracellular  $[\text{Ca}^{2+}]$  during the terminal differentiation of definitive ery\*throid cells and p23 may play a regulatory role in a  $\text{Ca}^{2+}$ -dependent manner in the stabilization of the marginal band structure.

The observation that p23 is a basic protein and localizes to the marginal bands led to the speculation of possible interaction between p23 and marginal band microtubules. It was shown that chicken p23 did not co-purify with erythrocyte-specific microtubules during assembly and disassembly cycles and could not affect microtubule assembly or bundling directly. But these results cannot rule out the possibility that p23 may still be involved in marginal band function, for example, help to maintain the high degree of stability of MBs. This idea has been further emphasized by the discovery that antigenically related p23 homologues are present in MB-containing cells of other species. It remains to be determined whether the p23 homologues in other species indeed belong to a p23 multigene family.

The function of p23 is still unclear, despite several attempts to elucidate it. It is

hypothesized in this thesis that p23 could be involved in stabilization of marginal bands after its formation. This hypothesis, however, is based solely on p23 localization studies. More specific indications about its function will require more detailed biochemical analysis. Alternatively, if p23 homologues are identified in other more easily manipulable genetic systems, such as yeast or *C. elegans*, the disruption of such p23 homologous genes in these systems could yield more insight into p23 function. Another approach is to search for any components p23 may interact with. p23 failed to show any direct interaction with microtubules both *in vivo* and *in vitro*. However, *in vivo* p23 may bind to microtubule-associated proteins, or membrane components that colocalize to the marginal position or some unknown proteins rather than directly with the core MT components. Finding the direct target component may give clues to the role of p23. Finally, it will be interesting to understand further the molecular structure of p23, how it binds to  $\text{Ca}^{2+}$  through its unique 3D structure and how p23 exercises its function in a  $\text{Ca}^{2+}$ -dependent manner *in vivo*.

## References

- Adoutte, A., Elgado, P., Fleury, A., Levilliers, N., Laine, M., Marty, M., Boisvieux-Ulrich, E., and Sandoz, D. (1991). Microtubule diversity in ciliated cells: evidence for its generation by post-translational modification in the axonemes of *Paramecium* and quail oviduct cells. *Biol. Cell* 71, 227-245.
- Aebersold, R. H., Leavitt, J., Saavedra, R. A., Hood, L. E., and Kent, S. B. H. (1987). Internal amino acid sequence analysis of proteins separated by one- or two-dimensional gel electrophoresis after *in situ* protease digestion on nitrocellulose. *Proc. Natl. Acad. Sci. USA* 84, 6970-6974.
- Ahmad, F. J., Pienkowski, T. P., and Baas, P. W. (1993). Regional differences in microtubule dynamics in the axon. *J. Neurosci.* 13, 856-866.
- Aiken, N. R., Satterlee, J. D., and Galey, W. R. (1992). Measurement of intracellular  $Ca^{2+}$  in young and old human erythrocytes using F-NMR spectroscopy. *Biochim. Biophys. Acta.* 1136, 155-160.
- Alfa, C. E., Ducommun, B., Beach, D., and Hyams J. S. (1990). Distinct nuclear and spindle pole body populations of cyclin-cdc2 in fission yeast. *Nature* 347, 680-682.
- Algrain, M., Turunen, O., Vaheri, A., Louvard, D., and Arpin, M. (1993). Ezrin contains cytoskeleton and membrane binding domains accounting for its proposed role as a membrane-cytoskeleton linker. *J. Cell Biol.* 120, 129-139.
- Arce, C. A., Rodriguez, J. A., Barra, H. S. and Caputto, R. (1978). Capability of tubulin and microtubules to incorporate and to release tyrosine and phenylalanine and the effect of incorporation of these amino acids on tubulin assembly. *J. Neurochem.* 31, 205-210.

- Arce, C. A. and Barra, H. S. (1983). Association of tubulinyl-tyrosine carboxypeptidase with microtubules. *FEBS Lett.* 157, 75-78.
- Asnes, C. F. and Wilson, L. (1979). Isolation of bovine microtubule protein without glycerol: polymerization kinetics change during purification cycles. *Anal. Biochem.* 98, 64-73.
- Baas, P. W. and Ahmad, F. J. (1992). The plus ends of stable microtubules are the exclusive nucleating structures for microtubules in axons. *J. Cell Biol.* 116, 1231-1241.
- Baas, P. W., Pienkowski, T. P., and Kosik, K. S. (1991). Processes induced by tau expression in sf9-cells have an axon-like microtubule organization. *J. Cell Biol.* 115, 1333-1344.
- Baas, P. W. and Black, M. M. (1990). Individual microtubules in the axon consist of domains that differ in both composition and stability. *J. Cell Biol.* 111, 495-509.
- Bailly, E. and Bornens, M. (1992). Centrosome and cell division. *Nature*, 300-301.
- Bailly, E., Doree, M., Nurse, P., and Bornens, M. (1989). P34<sup>cdc2</sup> is located in both nucleus and cytoplasm: part is centrosomally associated at G<sub>2</sub>/M and enters vesicles at anaphase. *EMBO J.* 8, 3985-3995.
- Baron, A. T. and Salisbury, J. L. (1988). Identification and localization of a novel, cytoskeletal, centrosome-associated protein in PtK<sub>2</sub> cells. *J. Cell Biol.* 107, 2669-2678.
- Baron, A. T., Greenwood, T. M., and Salisbury, J. L. (1991). Localization of the centrin-related 165,000-Mr protein of PtK<sub>2</sub> cells during the cell-cycle. *Cell Motil.* 18, 1-14.
- Barra, H. S., Arce, C. A., Rodriguez, J. A., and Caputto, R. (1973). Incorporation of phenylalanine as a single unit into rat brain protein: reciprocal inhibition by

phenylalanine and tyrosine of their respective incorporations. *J. Neurochem.* 21, 1241-1251.

Barrett, L. A. and Dawson, R. B. (1974). Avian erythrocyte development: microtubules and the formation of the disk shape. *Dev. Biol.* 36, 72-81.

Baum, P., Furlong, C., and Byers, B. (1986). Yeast gene required for spindle pole body duplication: homology of its product with Ca<sup>2+</sup>-binding proteins. *Proc. Natl. Acad. Sci.* 83, 5512-5516.

Baum, P., Yip, C., Goetsch, L., and Byers B. (1988). A yeast gene essential for regulation of spindle pole duplication. *Mol. Cell Biol.* 8, 5386-5397.

Behnke, O. (1970). A comparative study of microtubules of disk-shaped blood cells. *J. Ultrastruct. Res.* 31, 61-75.

Beltramo, D. M., Arce, C. A., and Aarra, H. S. (1989). Tyrosination-detyrosination of tubulin and microtubules during the development of chick erythrocytes. *Mol. Cell Biochem.* 89, 47-56.

Bernhardt, R. and Matus, A. (1984). Light and electron-microscopic studies of the distribution of microtubule-associated protein-2 in rat brain: a difference between dendritic and axonal cytoskeletons. *J. Comp. Neur.* 226, 203-221.

Binder, L. I., Frankfurter, A., and Rebhun, L. I. (1985). The distribution of tau in the mammalian central nervous-system. *J. Cell Biol.* 101, 1371-1378.

Birgbauer, E. and Solomon, F. (1989). A marginal band-associated protein has properties of both microtubule- and microfilament-associated proteins. *J. Cell Biol.* 109, 1609-1620.

Blikstad, I. and Lazarides, E. (1983). Vimentin filaments are assembled from a soluble precursor in avian erythroid cells. *J. Cell Biol.* 96, 1803-1808.

- Bloom, S. E., Buss, E. G., and Strother, G. K. (1970). Cytological and cytophotometric analysis of binucleated red bloodcell mutants (bn) in turkeys (*Meleagris gallopavo*). *Genetics* 65, 51-63.
- Brandt, R. and Lee, G. (1993). Functional organization of microtubule-associated protein tau. Identification of regions which affect microtubule growth, nucleation and bundle formation *in vitro*. *J. Biol. Chem.* 268, 3414-3419.
- Bré, M. H., Pepperkok, R., Hill, A. M., Levilliers, N., Ansorge, W., Stelzer, E. H. K., and Karsenti, E. (1990). Regulation of microtubule dynamics and nucleation during polarization in MDCK II cells. *J. Cell Biol.* 111, 3013-3021.
- Brenner, S. L. and Brinkley, B. R. (1982). Tubulin assembly sites and the organization of microtubule arrays in mammalian cells. *Cold Spring Harbor Symp. Quant. Biol.* 46, 241-254.
- Brewis, N. D., Street, A. J., Prescott, A. R., Cohen, P. T. W. (1993). PPX, a novel protein serine threonine phosphatase localized to centrosomes. *EMBO J.* 12, 987-996.
- Brinkley, B. R. (1985). Microtubule organizing centers. *Ann. Rev. Cell Biol.* 1, 145-172.
- Brinkley, B. R. and Stubblefield, E. (1970). Ultrastructure and interaction of the kinetochore and the centriole in mitosis and meiosis. *Adv. Cell Biol.* 1, 119-185.
- Brose, N., Petrenko, A. G., Sudhof, T. C., and Jahn, R. (1992). Synaptotagmin: a calcium sensor on the synaptic vesicle surface. *Science* 256, 1021-1025.
- Bruns, G. A. P. and Ingram, V. M. (1973). The erythroid cells and haemoglobins of the chick embryo. *Philos. Trans. R. Soc. Lond. B. Biol. Sci.* 226, 225-305.

- Buckley, K. M., Floor, E., and Kelly, R. B. (1987). Cloning and sequence analysis of cDNA encoding p38, a major synaptic vesicle protein. *J. Cell Biol.* 105, 2447-2456.
- Bulinski, J. C. and Gundersen, G. G. (1991). Stabilization and post-translational modification of microtubules during cellular morphogenesis. *Bioessays* 13, 285-293.
- Burgess, W. H., Jemiolo, D. K., and Kretsinger, R. H. (1980). Interaction of calcium and calmodulin in the presence of sodium dodecyl sulfate. *Biochim. Biophys. Acta.* 623, 257-270.
- Burgoyne, R. D. and Geisow, M. J. (1989). The annexin family of calcium-binding proteins. *Cell Calcium* 10, 1-10.
- Byers, T. J. and Branton, D. (1985). Visualization of the protein associations in the erythrocyte membrane skeleton. *Proc. Natl. Acad. Sci. USA* 82, 6153-6157.
- Calarco-Gillam, P. D., Sisbert, M. C., Hubble, R., Mitchison, T., and Kirschner, M. (1983). Centrosome development in early mouse embryos as defined by an autoantibody against pericentriolar material. *Cell* 35, 621-629.
- Cande, W. Z. (1980). A permeabilized cell model for studying cytokinesis using mammalian tissue culture cells. *J. Cell. Biol.* 87, 326-335.
- Cassimeris, L. U., Walker, R. A., Pryer, N. K., and Salmon, E.D. (1987). Dynamic instability of microtubules. *Bioessays* 7, 149-154.
- Cassimeris, L., Pryer, N. K., and Salmon, E. D. (1988). Real-time observations of microtubule dynamic instability in living cells. *J. Cell Biol.* 107, 2223-2231.
- Centonze, V. E. and Sloboda, R. D. (1986). A protein factor from *Bufo marinus* erythrocytes cross-bridges microtubules *in vitro*. *Exp. Cell Res.* 167, 471-483.

- Centonze, V. E. and Borisy G. G. (1990). Nucleation of microtubules from mitotic centrosomes is modulated by a phosphorylated epitope. *J. Cell Sci.* 95, 405-411.
- Chandra, R., Salmon, E. D., Erickson, H. P., Lockhart, A., and Endow, S. A. (1993). Structural and functional domains of the *Drosophila ncd* microtubule motor protein. *J. Biol. Chem.* 268, 9005-9013.
- Chapin, S. J. and Bulinski, J. C. (1992). Microtubule stabilization by assembly-promoting microtubule-associated proteins: a repeat performance. *Cell Motil. Cyto.* 23, 236-243.
- Chen, Y. D. and Hill, T. L. (1983). Use of *monte-carlo* calculations in the study of microtubule subunit kinetics. *Proc. Natl. Aca. Sci. USA* 80, 7520-7523.
- Chen, J., Kanai, Y., Cowan, N. J., and Hirokawa, N. (1992). Projection domains of MAP2 and tau determine spacings between microtubules in dendrites and axons. *Nature* 360, 674-677.
- Chretien, D. and Wade, R. H. (1991). New data on the microtubule surface lattice. *Biol. Cell* 71, 161-174.
- Clay, F. J., Mcewen, S. J., Bertoncello, I., Wilks, A. F., and Dunn, A. R. (1993). Identification and cloning of a protein kinase-encoding mouse gene, *Plk*, related to the *polo* gene of *Drosopila*. *Proc. Natl. Aca. Sci. USA* 90, 4882-4886.
- Cleveland, D. W. and Sullivan, K. F. (1985). Molecular-biology and genetics of tubulin. *Ann. Rev. Biochem.* 54, 331-365.
- Cohen, W. D. (1978). Observations on the marginal band system of nucleated erythrocytes. *J. Cell Biol.* 78, 260-273.
- Coling, D. E. and Salisbury, J. L. (1992). Characterization of the calcium-binding contractile protein centrin from *Tetraselmis striata* (Pleurostrophyceae). *J. Protoz.* 39, 385-391.

- Croall, D. E. and Demartino, G. N. (1991). Calcium-activated neutral protease (calpain) system: structure, function, and regulation. *Physiol. Rev.* 71, 813-847.
- Darzynkiewicz, Z. (1987). Cytochemical probes of cycling and quiescent cells applicable to flow cytometry. In *Techniques in Cell Cycle Analysis* (ed. J. W. Gray and Z. Darzynkiewicz). Human Press, Clifton, NJ. 255-290.
- Debec, A., Szollosi, A., and Szollosi, D. (1982). A *Drosophila melanogaster* cell-line lacking centriole. *Bio. Cell* 44, 133-138.
- Debec, A. and Montmory, C. (1992). Cyclin-B is associated with centrosomes in *Drosophila* mitotic cells. *Biol. Cell* 75, 121-126.
- DeBello, W. M., Beta, H., and Augustine, G. J. (1993). Synaptotagmin and neurotransmitter release. *Cell* 74, 947-950.
- Decamilli, P., Moretti, M., Donini, S. D., Walter, U. and Lohmann, S. M. (1986). Heterogeneous distribution of the cAMP receptor protein II in the nervous-system: evidence for its intracellular accumulation on microtubules, microtubule-organizing centers, and in the area of the Golgi-complex. *J. Cell Biol.* 103, 189-203.
- Dessev, G., Iovchevadessev, C., Bischoff, J. R., Beach, D., and Goldman, R. (1991). A complex containing p34<sup>cdc2</sup> and cyclin-B phosphorylates the nuclear lamin and disassembles nuclei of clam oocytes *in vitro*. *J. Cell Biol.* 112, 523-533.
- Donato, R. (1991). Perspectives in S-100 protein biology. *Cell Calcium* 12, 713-726.
- Drechsel, D. N., Hyman, A. A., Cobb, M. H., and Kirschner, M. W. (1992). Modulation of the dynamic instability of tubulin assembly by the microtubule-associated protein tau. *Mol. Biol. Cell* 3, 1141-1154.
- Drubin, D. G., Feinstein, S. C., Shooter, E. M., and Kirschner, M. W. (1985). Nerve growth factor-induced neurite outgrowth in PC12 cells involves the coordinate

- induction of microtubule assembly and assembly-promoting factors.. *J. Cell Biol.* 101, 1799-1807.
- Dustin, P. (1984). *Microtubules*. 2d ed. New York: Springer.
- Dyer, C. A. and Benjamins, J. A. (1989). Organization of oligodendroglial membrane sheets. I. Association of myelin basic protein and 2',3'-cyclic nucleotide 3'-phosphohydrolase with the cytoskeleton. *J. Neurosci Res.* 24, 201-211.
- Eddé, B., Rossier, J., Lecaer, J.P., Prome, J. C., and Desbruyeres, E. (1992). Polyglutamylated alpha-tubulin can enter the tyrosination detyrosination cycle. *Biochem.* 31, 403-410.
- Eddé, B., Jeantet, C. and Gros, F. (1981). One beta-tubulin subunit accumulates during neurite outgrowth in mouse neuroblastoma cells. *Bioc. Biop. Rev.* 103, 1035-1043.
- Endow, S. A., Henikoff, S., and Solerniedziela, L. (1990). Mediation of meiotic and early mitotic chromosome segregation in *Drosophila* by a protein related to kinesin. *Nature* 345, 81- 83.
- Enos, A. P. and Morris, N. R. (1990). Mutation of a gene that encodes a kinesin-like protein blocks nuclear division in *Aspergillus nidulans*. *Cell* 60, 1019-1027.
- Erickson, H. P. and Voter, W. A. (1976). Polycation-induced assembly of purified tubulin. *Proc. Natl. Acad. Sci. USA* 73, 2813-2817.
- Euteneuer, U., Ris, H., and Borisy, G. G. (1985). Polarity of marginal-band microtubules in vertebrate erythrocytes. *Eur. J. Cell Biol.* 37, 149-155.
- Evans, L., Mitchison, T., and Kirschner, M. (1985). Influence of the centrosome on the structure of nucleated microtubules. *J. Cell Biol.* 100, 1185-1191.

- Febvre-Chevalier, C. and Febvre, J. (1992). Microtubule disassembly *in vivo*: intercalary destabilization and breakdown of microtubules in the heliozoan *Actinocoryne contractilis*. *J. Cell Biol.* 18, 585-594.
- Feick, P., Foisner, R., and Wiche, G. (1991). Immunolocalization and molecular properties of a high molecular weight microtubule-bundling protein (syncolin) from chicken erythrocytes. *J. Cell Biol.* 112, 689-699.
- Fulton, C. and Dingle, A. D. (1971). Basal bodies, but not centrioles, in *Naegleria*. *J. Cell Biol.* 51, 826-836.
- Gambino, J., Ross, M. J., Weatherbee, J. A., Gavin, R. H., and Eckhardt, R. A. (1985). *Xenopus* marginal band disassembly by calcium-activated cytoplasmic factors. *J. Cell Sci.* 79, 199-216.
- Gard, D. L. and Kirschner, M. W. A. (1985). Polymer-dependent increase in phosphorylation of beta-tubulin accompanies differentiation of a mouse neuroblastoma cell-line. *J. Cell Biol.* 100, 764-774.
- Gard, D. L., Hafezi, S., Zhang, T., and Doxsey, S. J. (1990). Centrosome duplication continues in cycloheximide-treated *Xenopus* blastulas in the absence of a detectable cell-cycle. *J. Cell Biol.* 110, 2033-2042.
- Gaskin, F., Cantor, C. R., and Shelanski, M. L. (1974). Turbidimetric studies of the *in vitro* assembly and disassembly of porcine neurotubules. *J. Mol. Biol.* 89, 737-758.
- Geiger, B. and Ginsberg, D. (1991). The cytoplasmic domain of adherens-type junctions. *Cell Motil.* 20, 1-6.
- Geiger, B. and Ayalon, O. (1992). Cadherins. *Annu. Rev. Cell Biol.* 8, 307-332.
- Gelfand, V. I. and Bershady, A. D. (1991). Microtubule dynamics: mechanism, regulation, and function. *Annu. Rev. Cell Biol.* 7, 93-116.

- Ginsburg, M. F., Twersky, L. H., and Cohen, W. D. (1989). Cellular morphogenesis and the formation of marginal band in amphibian splenic erythroblasts. *Cell Motil. Cyto.* 12, 157-168.
- Goedert, M., Crowther, R. A., and Garner, C. C. (1991). Molecular characterization of microtubule-associated proteins tau and MAP2. *TINS* 14, 193-199.
- Gonzalez, C., Casal, J., and Ripoll, P. (1988). Functional monopolar spindles caused by mutation in *mgr*, a cell-division gene of *Drosophila melanogaster*. *J. Cell Sci.* 89, 39-47.
- Gonzalez, C., Saunders, R. D. C., Casal, J., Molina, I. and Carmena, M. (1990). Mutations at the *asp* locus of *drosophila* lead to multiple free centrosomes in syncytial embryos, but restrict centrosome duplication in larval neuroblasts. *J. Cell Sci.* 96, 605-616
- Gould, R. P. and Borisy, G. G. (1977). The pericentriolar material in Chinese hamster ovary cells nucleates microtubule formation. *J. Cell Biol.* 73, 601-615.
- Granger, B. L. and Lazarides, E. (1982). Structural association of synemin and vimentin filaments in avian erythrocytes revealed by immunoelectron microscopy. *Cell* 30, 263-275.
- Gundersen, G. G. and Bulinski, J. C. (1986). Microtubule arrays in differentiated cells contain elevated levels of a post-translationally modified form of tubulin. *Eur. J. Cell* 2, 288-294.
- Gundersen, G. G., Khawaja, S., and Bulinski, J. C. (1987). Post polymerization detyrosination of alpha-tubulin: a mechanism for subcellular differentiation of microtubules. *J. Cell Biol.* 105, 251-264.
- Gupta, R. S. (1990). Microtubules, mitochondria, and molecular chaperones: a new hypothesis for *in vivo* assembly of microtubules. *Biochem. Cell Biol.* 68,

1352-1363.

- Hagan, I. and Yanagida, M. (1990). Novel potential mitotic motor protein encoded by the fission yeast *cut7+* gene. *Nature* 347, 563-566.
- Hagan, I. and Yanagida, M. (1992). Kinesin-related *cut7* protein associates with mitotic and meiotic spindles in fission yeast. *Nature* 356, 74-76.
- Heizmann, C. W. and Schafer, B. W. (1990). Internal calcium-binding proteins. *Seminars in Cell Biol.* 1, 277-282.
- Hill, T. L. and Chen, Y. (1984). Phase-changes at the end of a microtubule with a GTP cap. *Proc. Natl. Aca. Sci. USA* 81, 5772-5776.
- Horio, T. and Hotani, H. (1986). Visualization of the dynamic instability of individual microtubules by dark-field microscopy. *Nature* 321, 605-607.
- Horio, E., Uzawa, S., Jung, M. K., Oakley, B. R., Tanka, K., and Yanagida, M. (1991). The fission yeast-tubulin is essential for mitosis and is localized at microtubule organizing centers. *J. Cell Sci.* 99, 693-700.
- Hoyle, H. D. and Raff, E. C. (1990). 2 *Drosophila* beta tubulin isoforms are not functionally equivalent. *J. Cell Biol.* 111, 1009-1026.
- Hoyt, M. A., He, L., Loo, K. K., and Saunders, W. S. (1992). 2 *Saccharomyces cerevisiae* kinesin-related gene products required for mitotic spindle assembly. *J. Cell Biol.* 118, 109-120.
- Huang, B., Watterson, D. M., Lee, V. D., and Schibler, M. J. (1988a). Purification and characterization of a basal body-associated  $Ca^{2+}$ -binding protein. *J. Cell Biol.* 107, 121-131.
- Huang, B., Mengersen, A., and Lee, V. D. (1988b). Molecular cloning of cDNA for caltractin, a basal body-associated  $Ca^{2+}$ -binding protein: homology in its protein

- sequence with calmodulin and the yeast CDC31 gene product. *J. Cell Biol.* 107, 133-140.
- Hughes, S. H., Greenhouse, J. J., Petropoulos, C. J., and Sutrave, P. (1987). Adaptor plasmids simplify the insertion of foreign DNA into helper-independent retroviral vectors. *J. Virology* 61, 3004-3012.
- Johnson, G. V. W. (1992). Differential phosphorylation of tau by cyclic-AMP dependent protein-kinase and Ca<sup>2+</sup> calmodulin-dependent protein kinase-II: metabolic and functional consequences. *J. Neurochem.* 59, 2056-2062.
- Joseph-silverstein, J. and Cohen, W. D. (1984). The cytoskeletal system of nucleated erythrocytes. III. Marginal band function in mature cells. *J. Cell Biol.* 98, 2118-2125.
- Joshi, H. C., Palacios, M. J., McNamara, L., and Cleveland, D. W. (1992).  $\gamma$ -tubulin is a centrosomal protein required for cell cycle-dependent microtubule nucleation. *Nature* 356, 80-83.
- Kallenbach, R. J. (1982). Continuous hypertonic conditions activate and promote the formation of new centrioles within cytastess in sea urchin eggs. *Cell Biol. Int. Rep.* 6, 1025-1031.
- Kanai, Y., Takemura, R., Oshima, T., Mori, H., and Ihara, Y. (1989). Expression of multiple tau isoforms and microtubule bundle formation in fibroblasts transfected with a single tau cDNA. *J. Cell Biol.* 109, 1173-1184.
- Kanai, Y., Chen, J., and Hirokawa, N. (1992). Microtubule bundling by tau proteins *in vivo*: analysis of functional domains. *EMBO J.* 11, 3953-3961.
- Karsenti, E., Kobayashi, S., Mitchison, T., and Kirschner, M. (1984). Role of the centrosome in organizing the interphase microtubule array: properties of cytoplasts containing or lacking centrosomes. *J. Cell Biol.* 98, 1763-1776.

- Karsenti, E., Bravo, R., and Kirschner, M. (1987). Phosphorylation changes associated with the early cell-cycle in *Xenopus*. *Dev. Biol.* 119, 442-453.
- Kellog, D. R. and Alberts, B. M. (1992). Purification of a multiprotein complex containing centrosomal proteins from the *Drosophila* embryo by chromatography with low-affinity polyclonal antibodies. *Mol. Biol. Cell.* 3, 1-11.
- Kelly, R. B. (1993). Storage and release of neurotransmitters. *Cell* 72, 43-53.
- Kelly, R. B. and Grote, E. (1993). Protein targeting in the neuron. *Ann. Rev. Neur.* 16, 95-127.
- Kenney, D. M. and Linck, R. W. (1985). The cytoskeleton of unstimulated blood platelets: structure and composition of the isolated marginal microtubular band. *J. Cell Sci.* 78, 1-22.
- Keryer, G., Rios, R. M., Landmark, B. F., Skalhegg, B., and Lohmann, S. M. (1993). A high-affinity binding-protein for the regulatory subunit of cAMP-dependent protein kinase-II in the centrosome of human-cells. *Exp. Cell Rev.* 204, 230-240.
- Kim, S., Magendantz, M., Katz, W., and Solomon, F. (1987). Development of a differentiated microtubule structure: formation of the chicken erythrocyte marginal band *in vivo*. *J. Cell Biol.* 104, 51-59.
- Kim, J. M., Ljungdahl, P. O., and Fink, G. R. (1990). *Kem* mutations affect nuclear-fusion in *Saccharomyces cerevisiae*. *Genetics* 126, 799-812.
- Kimble, M. and Kuriyama, R. (1992). Functional components of microtubule-organizing centers. *Intl. Rev. Cyto.* 136, 1-50.
- Kimble, M. and Curch, K. (1983). Meiosis and early cleavage in *Drosophila melanogaster* eggs: effects of the claret-non-disjunctional mutation. *J. Cell Sci.* 62, 301-318.

- Kirschner, M. W. (1989). Biological implications of microtubule dynamics. The Harvey Lectures. Series 83, 1-20.
- Kirschner, M. and Mitchison, T. (1986). Beyond self-assembly: from microtubules to morphogenesis. *Cell* 45, 329-342.
- Knowles, B. A. and Hawley, R. S. (1991). Genetic-analysis of microtubule motor proteins in *Drosophila*: a mutation at the *ncd* locus is a dominant enhancer of *nod*. *Proc. Natl. Aca. Sci. USA* 88, 7165-7169.
- Kotani, S., Nishida, E., Kumagai, H., and Sakai, H. (1985). Calmodulin inhibits interaction of actin with MAP2 and tau, 2 major microtubule-associated proteins. *J. Biol. Chem.* 260, 779-783.
- Kowit, J. D., Linck, R. W., and Kenney, D. M. (1988). Isolated cytoskeletons of human blood platelets: dark-field imaging of coiled and uncoiled microtubules. *Biol. Cell* 64, 283-291.
- Kretsinger, R. H. (1980). Structure and evolution of calcium-modulate proteins. *CRC Crit. Rev. Biochem.* 8, 119-174.
- Kristofferson, D., Mitchison, T., and Kirschner, M. (1986). Direct visualization of steady-state microtubule dynamics *in vitro*. *Ann. N. Y. Acad.* 466, 664-665.
- Kumar, N. and Flavin, M. (1981). Preferential action of a brain detyrosinating carboxypeptidase on polymerized tubulin. *J. Cell Biol.* 256, 7678-7680.
- Kuriyama, R. Keryer, G., and Borisy, G. G. (1984). The mitotic spindle of Chinese-hamster ovary cells isolated in taxol-containing medium. *J. Cell Sci.* 66, 265-275.
- Kuriyama, R. and Borisy, G. G. (1981). Centriole cycle in Chinese hamster ovary cell as determined by whole mount electron microscopy. *J. Cell Biol.* 91, 814-821.

- Kyhse-Andersen, J. (1984). Electrophoretic transfer of multiple gels: a simple apparatus without buffer tank for rapid transfer of proteins from polyacrylamide to nitrocellulose. *J. Biochem. Biophys. Meth.* 10, 203-209.
- Lazarides, E. (1987). From genes to structural morphogenesis: the genesis and epigenesis of a red blood cell. *Cell* 51, 345-356.
- Lazarides, E. (1982). Antibody production and immunofluorescent characterization of actin and contractile proteins. *Meth. Cell Biol.* 24, 313-331.
- Ledizet, M. and Piperno, G. (1987). Identification of an acetylation site of *Chlamydomonas* alpha-tubulin. *Proc. Natl. Aca. Sci. USA* 84, 5720-5724.
- Lee, Y. C. and Wolff, J. (1984). The calmodulin-binding domain on microtubule-associated protein 2. *J. Biol. Chem.* 259, 8041-8044.
- LeGendre, N. and Matsudaira, P. (1988). Direct protein microsequencing from Immobilon-P transfer membrane. *BioTechniques* 6, 154-159.
- L'Hernault, S. W. and Rosenbaum, J. L. (1985). *Chlamydomonas* alpha-tubulin is posttranslationally modified by acetylation on the epsilon-amino group of a lysine. *Biochem* 24, 473-478.
- Liu, B., Marc, J., Joshi, H. C., and Palevitz, B. A. A. (1993). Gamma-tubulin-related protein associated with the microtubule arrays of higher-plants in a cell cycle-dependent manner. *J. Cell Sci.* 104, 1217-1228.
- L'Lamazares, S., Moreira, A., Tavares, A., Girdham, C., and Spruce, B. A. (1991). *Polo* encodes a protein-kinase homolog required for mitosis in *Drosophila*. *Gene Dev.* 5, 2153-2165.
- Loh, E. (1991). Anchored PCR: amplification with single-sided specificity. *Methods* 2, 11-19.

- Lucas, A. M. and Jamroz, C. (1961). Atlas of avian hematology. Agriculture monograph 25, U.S. Department of Agriculture, Washington.
- MacRae, T. J. (1992). Microtubule organization by cross-linking and bundling proteins. *Biochim. Biophys. Acta.* 1160, 145-155.
- Maekawa, T., Leslie, R., and Kuriyama, R.. (1991). Identification of a minus end-specific microtubule-associated protein located at the mitotic poles in cultured mammalian-cells. *Eur. J. Cell* 54, 255-267.
- Maniotis, A. and Schliwa, M. (1991). Microsurgical removal of centrosomes blocks cell reproduction and centriole generation in BSC-1 cells. *Cell* 67, 495-504.
- Marcum, J. M., Dedman, J. R., Brinkley, B. R., and Means, A. R. (1978). Control of microtubule assembly-disassembly by calcium-dependent regulator protein. *Proc. Natl. Acad. Sci. USA* 75, 3771-3775.
- Marchesi, V. T. and Ngo, N. (1993). *In vitro* assembly of multiprotein complexes containing alpha-tubulin, beta-tubulin, and gamma-tubulin, heat-shock protein hsp70, and elongation factor-1-alpha. *Proc. Natl. Acad. Sci. USA* 90, 3028-3032.
- Margolis, R. L. and Wilson, L. (1978). Opposite end assembly and disassembly of microtubules at steady state *in vitro*. *Cell* 13, 1-8.
- Matus A. (1988). Microtubule-associated proteins: their potential role in determining neuronal morphology. *Ann. Rev. Neur.* 11, 29-44.
- May, G. S., Mcgoldrick, C. A., Holt, C. L., and Denison, S. H. (1992). The *bimB3* mutation of *Aspergillus-nidulans* uncouples DNA-replication from the completion of mitosis. *J. Biol. Chem.* 267, 5737-5743.
- Mazia, D. (1987). The chromosome cycle and the centrosome cycle in the mitotic cycle. *Intl. Rev. Cyto.* 100, 49-92.

- McDonald, H. B. and Goldstein, L. S. B. (1990). Identification and characterization of a gene encoding a kinesin-like protein in *Drosophila*. *Cell* 61, 991-1000.
- McDonald, H. B., Stewart, R. J. and Goldstein, L. S. B. (1990). The kinesin-like *ncd* protein of *Drosophila* is a minus end-directed microtubule motor. *Cell* 63, 1159-1165.
- McEwen, B. and Edelman, S. J. (1977). Evidence for a mixed lattice in microtubules reassembled *in vitro*. *J. Mol. Biol.* 139, 123-145.
- McFadden, G. I., Schulze, D., Surek, B., Salisbury, J. L., and Melkonian, M. (1987). Basal body reorientation mediated by a Ca<sup>2+</sup>-modulated contractile protein. *J. Cell Biol.* 105, 903-912.
- McGrew, J. T. Goetsch, L., Byers, B., and Baum, P. (1992). Requirement for *esp1* in the nuclear division of *Saccharomyces cerevisiae*. *Mol. Biol. Cell* 3, 1443-1454.
- McIntosh, J. R. and Euteneuer, U. (1984). Tubulin hooks as probes for microtubule polarity: an analysis of the method and an evaluation of data on microtubule polarity in the mitotic spindle. *J. Cell Biol.* 98, 525-533.
- McIntosh, J. R. and Pfarr, C. M. (1991). Mitotic motors. *J. Cell Biol.* 115, 577-585.
- Meluh, P. B. and Rose, M. D. (1990). *Kar3*, a kinesin-related gene required for yeast nuclear-fusion. *Cell* 60, 1029-1041.
- Miller, M. and Solomon, F. (1984). Kinetics and intermediates of marginal band reformation: evidence for peripheral determinants of microtubule organization. *J. Cell Biol.* 99, 70-75.
- Mitchison, T. and Kirschner, M. (1984a). Microtubule assembly nucleated by isolated centrosomes. *Nature* 312, 232-237.
- Mitchison, T. and Kirschner, M. (1984b). Dynamic instability of microtubule growth. *Nature* 312, 237-242.

- Mogensen, M. M. and Tucker, J. B. (1987). Evidence for microtubule nucleation at plasma membrane-associated sites in *Drosophila*. *J. Cell Sci.* 88, 95-107.
- Mogensen, M. M., Tucker, J. B., and Stebbings, H. (1989). Microtubule polarities indicate that nucleation and capture of microtubules occurs at cell-surfaces in *Drosophila*. *J. Cell Biol.* 108, 1445-1452.
- Moudjou, M., Paintrand, M., Vigues, B., and Bornens, M. (1991). A human centrosomal protein is immunologically related to basal body-associated proteins from lower eucaryotes and is involved in the nucleation of microtubules. *J. Cell Biol.* 115, 129-140.
- Multigner, L., Gagnon, J., Dorsselaer, A. V., and Job, D. (1992). Stabilization of sea urchin flagellar microtubules by histone H1. *Nature* 360, 33-39.
- Muresan, V., Joshi, H. C., and Besharse, J. C. (1993). Gamma-tubulin in differentiated cell-types: localization in the vicinity of basal bodies in retinal photoreceptors and ciliated epithelia. *J. Cell Sci.* 104, 1229-1237.
- Murphy, D. B. and Wallis, K. T. (1983a). Brain and erythrocyte microtubules from chicken contain different  $\beta$ -tubulin polypeptides. *J. Biol. Chem.* 258, 7870-7875.
- Murphy, D. B. and Wallis, K. T. (1983b). Isolation of microtubule protein from chicken erythrocytes and determination of the critical concentration for tubulin polymerization *in vitro* and *in vivo*. *J. Biol. Chem.* 258, 8357-8364.
- Murphy, D. B. and Wallis, K. T. (1985). Erythrocyte microtubule assembly *in vitro*. *J. Biol. Chem.* 260, 12293-12301.
- Murphy, D. B., Grasser, W. A., and Wallis, K. T. (1986). Immunofluorescence examination of beta tubulin expression and marginal band formation in developing chicken erythroblasts. *J. Cell Biol.* 102, 628-635.

- Murphy, D. B., Wallis, K. T., Machlin, P. S., Ratrie III, H., and Cleveland, D. W. (1987). The sequence and expression of the divergent  $\beta$ -tubulin in chicken erythrocytes. *J. Biol. Chem.* 262, 14305-14312.
- Murphy, D. B. (1991). Purification of tubulin and tau from chicken erythrocytes - tubulin isotypes and mechanisms of microtubule assembly. *Meth. Enzym.* 196, 235-246
- Nakayama, S., Moncrief, N. D., and Kretsinger, R. H. (1992). Evolution of EF-hand calcium-modulated proteins. II. Domains of several subfamilies have diverse evolutionary histories. *J. Mol. Evol.* 34, 416-448.
- Nelson, W. J. and Lazarides, E. (1983). Switching of subunit composition of muscle spectrin during myogenesis *in vitro*. *Nature* 304, 364-368.
- Nemhauser, I., Ornberg, R., and Cohen, W. D. (1980). Marginal bands in blood cells of invertebrates. *J. Ultrastruct. Res.* 70, 308-317.
- Nigg, E. A., Schafer, G., Hilz, H., and Eppenberger, H. M. (1985). Cyclic-AMP-dependent protein-kinase type-II is associated with the Golgi-complex and with centrosomes. *Cell* 41, 1039-1051.
- Norbury, C. and Nurse, P. (1992). Animal-cell cycles and their control. *Ann. Rev. Biochem.* 61, 441-470.
- Nurse, P. (1990). Universal control mechanism regulating onset of M-phase. *Nature* 344, 503 -508.
- Oakley, B. R. and Morris, N. R. (1981). A  $\gamma$ -tubulin mutation in *Aspergillus nidulans* that blocks microtubule function without blocking assembly. *Cell* 24, 837-845.
- Oakley, B. R. and Morris, N. R. A. (1983). Mutation in *Aspergillus nidulans* that blocks the transition from interphase to prophase. *J. Cell Biol.* 96, 1155-1158.

- Oakley, B. R., Oakley, C. E., Kniepkamp, K. S., and Rinehart, J. E. (1985). Isolation and characterization of cold-sensitive mutations at the *benA*, beta-tubulin, locus of *Aspergillus nidulans*. *Mol. G. Genet.* 201, 56-64.
- Oakley, C. E. and Oakley, B. R. (1989). Identification of  $\gamma$ -tubulin, a new member of the tubulin superfamily encoded by *mipA* gene of *Aspergillus nidulans*. *Nature* 338, 662-664.
- Oakley, B. R., Oakley, C. E., Yoon, Y., and Jung, M. K. (1990).  $\gamma$ -tubulin is a component of the spindle pole body that is essential for microtubule function in *Aspergillus nidulans*. *Cell* 61, 1289-1301.
- Ohta, K., Toriyama, M., Miyazaki, M., Murofushi, H., and Hosoda, S. T. (1990). The mitotic apparatus-associated 51-kDa protein from sea-urchin eggs is a GTP-binding protein and is immunologically related to yeast polypeptide elongation factor-1-alpha. *J. Biol. Chem.* 265, 3240-3247.
- Ohta, K., Shiina, N., Okumura, E., Hisanaga, S., Kishimoto, T., Endo, S., Gotoh, Y., Nishida, E., and Sakai, H. (1993). Microtubule nucleation activity of centrosomes in cell-free extracts from *Xenopus* eggs: involvement of phosphorylation and accumulation of pericentriolar material. *J. Cell Sci.* 104, 125-137.
- Olmsted, J. B. (1986). Microtubule-associated proteins. *Ann. Rev. Cell Biol.* 2, 421-457.
- Oosawa, F. and Kasai, M. (1962). A theory of linear and helical aggregations of macromolecules. *J. Mol. Biol.* 4, 10-21.
- Pain, B., Woods, C. M., Saez, J., Flickinger, T., Raines, M., Peyrol, S., Moscovici, C., Moscovici, M. G., Kung, H.-J., Jurdic, P., Lazarides, E., and Samarut, J. (1991).

- EGF-R as a hemopoietic growth factor receptor: the *C-erbB* product is present in chicken erythrocytic progenitors and controls their self-renewal. *Cell* 65, 37-46.
- Palazzolo, M. J., Hamilton, B. A., Ding, D., Martin, C. H., Mead, D. A., Mierendorf, R. C., Raghavan, K. V., Meyerowitz, E. M., and Lipshitz, H. D. (1990). Phage lambda cDNA cloning vectors for subtractive hybridization, fusion-protein synthesis and Cre-*loxP* automatic plasmid subcloning. *Gene* 88, 25-36.
- Parmley, R. T. (1988). Mammals. *In* Vertebrate Blood Cells (ed. A. F. Rowley and N.A. Ratcliffe). Cambridge University Press. 337-425.
- Peck, B. K., Duborgel, F., Huttenlauch, I., and Haller, G. D. (1991). The membrane skeleton of Pseudomicrothorax. *J. Cell Sci.* 100, 693-706.
- Persechini, A., Moncrief, N. D., and Kretsinger, R. H. (1989). The EF-hand family of calcium-modulated proteins. *TINS* 12, 462-467.
- Phillips, S. G. and Rattner, J. B. (1976). Dependence of centriole formation on protein synthesis. *J. Cell Biol.* 70, 9-19.
- Picard, A., Harricane, M. C., Labbe, J. C., and Doree, M. (1988). Germinal vesicle components are not required for the cell-cycle oscillator of the early starfish embryo. *Dev. Biol.* 128, 121-128.
- Pickett-Heaps, J. D. (1969). The evolution of the mitotic apparatus: An attempt at comparative ultrastructural cytology in dividing plant cells. *Cytobios* 3, 257-280.
- Pirollet, F., Rauch, C. T., Job, D., and Margolis, R. L. (1989). Monoclonal antibody to microtubule-associate STOP protein: affinity purification of neuronal STOP activity and comparison of antigen with activity in neuronal and nonneuronal cell extracts. *Biochem.* 28, 835-842.

- Pirollet, F., Margolis, R. L., and Job, D. (1992).  $\text{Ca}^{2+}$ -calmodulin regulated effectors of microtubule stability in neuronal tissues. *Biochim. Biophys. Acta.* 1160, 113-119.
- Raff, E. C. (1984). Genetics of microtubule systems. *J. Cell Biol.* 99, 1-10.
- Raff, J. W. and Glover, D. M. (1988). Nuclear and cytoplasmic mitotic-cycles continue in *Drosophila* embryos in which DNA-synthesis is inhibited with aphidicolin. *J. Cell Biol.* 107, 2009-2019.
- Raff, J. W. Kellogg, D. R., and Alberts, B. M. (1993). *Drosophila* gamma-tubulin is part of a complex containing 2 previously identified centrosomal MAPs. *J. Cell Biol.* 121, 823-835.
- Rattner, J. B., Lew, J., and Wang, J. H. (1990). p34<sup>cdc2</sup> kinase is localized to distinct domains within the mitotic apparatus. *Cell Motil.* 17, 227-235.
- Rattner, J. B. (1991). Hsp70 is localized to the centrosome of dividing HeLa-cells. *Exp. Cell Re.* 195, 110-113.
- Reinsch, S. S., Mitchison, T. J., and Kirschner, M. (1991). Microtubule polymer assembly and transport during axonal elongation. *J. Cell Biol.* 115, 365-379.
- Rieder, C. L. and Borisy, G. G. (1982). The centrosome cycle in PK<sub>2</sub> cells: asymmetric distribution and structural changes in pericentriolar material. *Biol. Cell* 44, 117-132.
- Riederer, B. and Matus, A. (1985). Differential expression of distinct microtubule-associated proteins during brain-development. *Proc. Natl. Aca. Sci. USA* 82, 6006-6009.
- Robbins, E. and Gonatos, N. K. (1964). The ultrastructure of a mammalian cell during the mitotic cycle. *J. Cell Biol.* 21, 429-463.

- Romisch, J. and Paques, E. P. (1991). Annexins: calcium-binding proteins of multi-functional importance. *Med. Microbiol. Immunol.* 180, 109-126.
- Roof, D. M., Meluh, P. B., and Rose, M. D. (1992). Kinesin-related proteins required for assembly of the mitotic spindle. *J. Cell Biol.* 118, 95-108.
- Rose, M. D. and Fink, G. R. (1987). *Kar1*, a gene required for function of both intranuclear and extranuclear microtubules in yeast. *Cell* 48, 1047-1060.
- Sakai, H., and Ohta, K. (1991). Centrosome signalling at mitosis. *Cell Signalling* 3, 267-272.
- Salmon, E. D., Leslie, R. J., Saxton, W. M., Karow, M. L., and McIntosh, J. R. (1984). Spindle microtubule dynamics in sea-urchin embryos: analysis using a fluorescein-labeled tubulin and measurements of fluorescence redistribution after laser photobleaching. *J. Cell Biol.* 99, 2165-2174.
- Sambrook, J., Fritsch, E. F., and Maniatis, T. (1989). *Molecular Cloning: A Laboratory Manual* (Cold Spring Harbor, New York: Cold Spring Harbor Laboratory Press).
- Sammak, P. J., Gorbisky, G. J., and Borisy, G. G. (1987). Microtubule dynamics *in vivo*: a test of mechanisms of turnover. *J. Cell Biol.* 104, 395-405.
- Sammak, P. J. and Borisy, G. G. (1988a). Direct observation of microtubule dynamics in living cells. *Nature* 332, 724-726.
- Sammak, P. J. and Borisy, G. G. (1988b). Detection of single fluorescent microtubules and methods for determining their dynamics in living cells. *Cell Motil.* 10, 237-245.
- Sanchez, I., Twersky, L. H., and Cohen, W. D. (1990). Detergent-based isolation of marginal bands of microtubules from nucleated erythrocytes. *Eur. J. Cell Biol.* 52, 349-358.

- Saunders, W. S. and Hoyt, M. A. (1992). Kinesin-related proteins required for structural integrity of the mitotic spindle. *Cell* 70, 451-458.
- Saxton, W. M., Stemple, D. L., Leslie, R. J., Salmon, E. D., and Zavortink, M. (1984). Tubulin dynamics in cultured mammalian-cells. *J. Cell Biol.* 99, 2175-2186.
- Scaife, R. M., Wilson, L., and Purich, D. L. (1992). Microtubule protein ADP-robisylation in vitro leads to assembly inhibition and rapid depolymerization. *Biochem.* 31, 310-316.
- Schatten, H., Schatten, G., Mazia, D., Balczon, R., and Simerly, C. (1986). Behavior of centrosomes during fertilization and cell-division in mouse oocytes and in sea-urchin eggs. *Proc. Natl. Aca. Sci. USA* 83, 105-109.
- Schulze, E. and Kirschner, M. (1986). Microtubule dynamics in interphase cells. *J. Cell Biol.* 102, 1020-1031.
- Schulze, E. and Kirschner, M. (1987). Dynamic and stable-populations of microtubules in cells. *J. Cell Biol.* 104, 277-288.
- Schulze, E. and Kirschner, M. (1988). New feature of microtubule behaviour observed *in vivo*. *Nature* 334, 356-359.
- Schulze, E., Asai, D. J., Bulinski, J. C., and Kirschner, M. (1987). Posttranslational modification and microtubule stability. *J. Cell Biol.* 105, 2167-2177.
- Schulze, E. and Kirschner, M. (1988). New features of microtubule behavior observed *in vivo*. *Nature* 334, 356-359.
- Scott, C. W., Spreen, R. C., Herman, J. L., Chow, F. P., and Davison, M. D. (1993). Phosphorylation of recombinant tau by cAMP-dependent protein-kinase: identification of phosphorylation sites and effect on microtubule assembly. *J. Biol. Chem.* 268, 1166-1173.

- Searle, B. M. and Bloom, S. E. (1979). Influence of the *bn* gene on mitosis of immature red blood cells in turkeys. *J. Heredity*. 70, 155-160.
- Sellitto, C. and Kuriyama, R. (1988). Distribution of pericentriolar material in multipolar spindles induced by colcemid treatment in Chinese-hamster ovary cells. *J. Cell Sci.* 89, 57-65.
- Sellitto, C., Kimble, M., and Kuriyama, R. (1992). Heterogeneity of microtubule organizing center components as revealed by monoclonal-antibodies to mammalian centrosomes and to nucleus-associated bodies from *Dictyostelium*. *Cell Motil.* 22, 7-24.
- Shimoda, C., Hirata, A., Kishida, M., Hashida, T., and Tanaka, K. (1985). Characterization of meiosis-deficient mutants by electron-microscopy and mapping of 4 essential genes in the fission yeast *Schizosaccharomyces-pombe*. *Mol. G. Genet.* 200, 252-257.
- Sluder, G., Miller, F. J., Cole, R., and Rieder, C. L. (1990). Protein-synthesis and the cell-cycle: centrosome reproduction in sea-urchin eggs is not under translational control. *J. Cell Biol.* 110, 2025-2032.
- Snyder, M. and Davis, R. W. (1988). *Spa1*, a gene important for chromosome segregation and other mitotic functions in *S. cerevisiae*. *Cell* 54, 743-754.
- Sobue, K., Fujita, M., Muramoto, Y., and Kakiuchi, S. (1981). The calmodulin-binding protein in microtubules is tau factor. *FEBS Lett.* 132, 137-140.
- Soltys, B. J. and Borisy, G. G. (1985). Polymerization of tubulin *in vivo*: direct evidence for assembly onto microtubule ends and from centrosomes. *J. Cell Biol.* 100, 682-1689.
- Spurling, N. W. (1981). Comparative physiology of blood clotting. *Comp. Biochem. Physiol.* 68, 541-548.

- Staiger, C. J. and Cande, W. Z. (1990). Microtubule distribution in *dv*, a maize meiotic mutant defective in the prophase to metaphase transition. *Dev. Biol.* 138, 231-242.
- Stearns, T., Evans, L., and Kirschner, M. (1991).  $\gamma$ -tubulin is a highly conserved component of the centrosome. *Cell* 65, 825-836.
- Stetzkowski-Marden, F., Deprette, C., and Cassoly, R. (1991). Identification of tubulin-binding proteins of the chicken erythrocyte plasma membrane skeleton which colocalize with the microtubular marginal band. *Eur. J. Cell Biol.* 54, 102-109.
- Sullivan, W., Minden, J. S., and Alberts, B. M. (1990). Daughterless-*abo*-like, a *Drosophila* maternal-effect mutation that exhibits abnormal centrosome separation during the late blastoderm divisions. *Develop.* 110, 311-323.
- Sullivan, K. F. (1988). Structure and utilization of tubulin isotypes. *Ann. Rev. Cell Biol.* 4, 687-716.
- Sunkel, C. E. and Glover, D. M. (1988). *Polo*, a mitotic mutant of *Drosophila* displaying abnormal spindle poles. *J. Cell Sci.* 89, 25-38.
- Swan, J. A. and Solomon, F. (1984). Reformation of the marginal band of avian erythrocytes *in vitro* using calf-brain tubulin: peripheral determinants of microtubule form. *J. Cell Biol.* 99, 2108-2113.
- Tablin, F., Reeber, M. J., and Nachmias, V. T. (1988). Platelets contain a 210k microtubule-associated protein related to a similar protein in HeLa-cells. *J. Cell Biol.* 90, 317-324.
- Tablin, F. and Castro, M. D. (1991). Bovine platelets contain a 280 kDa microtubule-associated protein antigenically related to brain MAP 2. *Eur. J. Cell Biol.* 56, 415-421.

- Tanaka, E. M. and Kirschner, M. W. (1991). Microtubule behavior in the growth cones of living neurons during axon elongation. *J. Cell Biol.* 115, 345-363.
- Tassin, A., Maro, B., and Bornens, M. (1985a). Fate of microtubule-organizing centers during myogenesis *in vitro*. *J. Cell Biol.* 100, 35-46.
- Tassin, A. M., Paintrand, M., Berger, Etassin, A. M., Paintrand, M., Berger, E. G., and Bornens, M. (1985b). The Golgi apparatus remains associated with microtubule organizing centers during myogenesis. *J. Cell Biol.* 101, 630-638.
- Thomas, J. H. and Botstein, D. (1986). A gene required for the separation of chromosomes on the spindle apparatus in yeast. *Cell* 44. 65-76.
- Toriyama, M., Ohta, K., Endo, S., and Sakai, H. (1988). 51-kD protein, a component of microtubule-organizing granules in the mitotic apparatus involved in aster formation *in vitro*. *Cell Motil.* 9, 117-128.
- Tousson, A., Zeng, C., Brinkley, B. R., and Valdivia, M. M. (1991). Centrophilin: a novel mitotic spindle protein involved in microtubule nucleation. *J. Cell Biol.* 112, 427-440.
- Trinczek, B., Marx, A., Mandelkow, E. M., Murphy, D. B., and Mandelkow, E. (1993). Dynamics of microtubules from erythrocyte marginal bands. *Mol. Biol. Cell* 4, 323-335.
- Tucker, J. B., Milner, M. J., Currie, D. A., Muir, J. W., and Forrest, D. A. (1986). Centrosomal microtubule-organizing centers and a switch in the control of protofilament number for cell surface-associated microtubules during *Drosophila* wing morphogenesis. *Eur. J. Cell* 41, 279-289.
- Tucker, R. P. (1990). The roles of microtubule-associated proteins in brain morphogenesis: a review. *Brain Res. R.* 15, 101-120.

- Tucker, J. B., Paton, C. C., Richardson, G. P., Mogensen, M. M., and Russell, I. J. (1992). A cell surface-associated centrosomal layer of microtubule-organizing material in the inner pillar cell of mouse cochlea. *J. Cell Sci.* 102, 215-226.
- Tucker, J. (1992). The microtubule-organizing centre. *Bioessays* 14, 861-867.
- Tucker, J. B., Paton, C. C., Henderson, C. G., and Mogensen, M. M. (1993). Microtubule rearrangement and bending during assembly of large curved microtubule bundles in mouse cochlear epithelial-cells. *Cell Motil.* 25, 49-58.
- Uzawa, S., Samejima, I., Hirano, T., Tanaka, K., and Yanagida, M. (1990). The fission yeast *cut1+* gene regulates spindle pole body duplication and has homology to the budding yeast *esp1* gene. *Cell* 62, 913-925.
- Vale, R. D. and Goldstein, L. S. B. (1990). One motor, many tails: an expanding repertoire of force-generating enzymes. *Cell* 60, 883-885.
- Vallen, E. A., Hiller, M. A., Scherson, T. Y., and Rose, M. D. (1992). Separate domains of *kar1* mediate distinct functions in mitosis and nuclear-fusion. *J. Cell Biol.* 117, 1277-1287.
- Vandré, D. D., Davis, F. M., Rao, P. N., and Borisy, G. G. (1986). Distribution of cytoskeletal proteins sharing a conserved phosphorylated epitope. *Eur. J. Cell Biol.* 41, 72-81.
- Verde, F., Labbe, J. C., Doree, M., and Karsenti, E. (1990). Regulation of microtubule dynamics by *cdc2* protein-kinase in cell-free-extracts of *Xenopus* eggs. *Nature* 343, 233-238.
- Vidair, C. A., Doxsey, S. J., and Dewey, W. C. (1993). Heat shock alters centrosome organization leading to mitotic dysfunction and cell death. *J. Cell. Physiol.* 154, 443-455.

- Wacker, I. U., Rickard, J. E., De Mey, J. R., and Kreis, T. E. (1992). Accumulation of a microtubule-binding protein, PP170, at desmosomal plaques. *J. Cell Biol.* 117, 813-824.
- Walker, R. A., O'Brien, E. T., Pryer, N. K., Soboeiro, M. F., Voter, W. A., Erickson, H. P., and Salmon, E. D. (1988). Dynamic instability of individual microtubules analyzed by video light microscopy: rate constants and transition frequencies. *J. Cell Biol.* 107, 1437-1448.
- Walker, R. A., Inoue, S., and Salmon, E. D. (1989). Asymmetric behavior of severed microtubule ends after ultraviolet microbeam irradiation of individual microtubules *in vitro*. *J. Cell Biol.* 108, 931-937.
- Webster, D. R., Wehland, J., Weber, K., and Borisy, G. G. (1990). Detyrosination of alpha-tubulin does not stabilize microtubules *in vivo*. *J. Cell Biol.* 111, 113-122.
- Wehland, J. and Weber, K. (1987). Tubulin tyrosine ligase has a binding-site on beta-tubulin: a 2-domain structure of the enzyme. *J. Cell Biol.* 104, 1059-1067.
- Weil, C. F., Oakley, C. E., and Oakley, B. R. (1986). Isolation of *mip* (microtubule-interacting protein) mutations of *Aspergillus nidulans*. *Mol. Cell. Biol.* 6, 2963-2968.
- Weisenberg, R. C. (1972). Microtubule formation *in vitro* in solutions containing low calcium concentrations. *Science* 177, 1104-1105.
- Welsh, M. J., Dedman, J. R., Brinkley, B. R., and Means, A. R. (1979). Tubulin and calcium-dependent regulator protein: effects of microtubule and microfilament inhibitors on localization in the mitotic apparatus. *J. Cell Biol.* 81, 624-634.

- Welsh, M. J., Dedman, J. R., Brinkley, B. R., and Means, A. R. (1978). Calcium-dependent regulator protein: localization in the mitotic spindle of eukaryotic cells. *Proc. Natl. Aca. Sci. USA* 75, 1867-1871.
- Wiedenmann, B., Rehm, H., and Franke, W. W. (1987). Synaptophysin, an integral membrane-protein of vesicles present in normal and neoplastic neuro-endocrine cells. *Ann. N. Y. Acad.* 493, 500-503.
- Winey, M., Goetsch, L., Baum, P., and Byers, B. (1991). *Mps1* and *mps2*, novel yeast genes defining distinct steps of spindle pole body duplication. *J. Cell Biol.* 114, 745-754.
- Wolfe, J. (1972). Basal body fine structure and chemistry. *Adv. Cell Mol. Biol.* 2, 151-192.
- Wolff, A., Denechaud, B., Chillet, D., Mazarguil, H., and Desbruyeres, E. (1992). Distribution of glutamylated alpha-tubulin and beta-tubulin in mouse-tissues using a specific monoclonal-antibody, GT335. *Eur. J. Cell* 59, 425-432.
- Woods, C. M. and Lazarides, E. (1988). The erythroid membrane skeleton: expression and assembly during erythropoiesis. *Ann. Rev. Med.* 39, 107-122.
- Yeh, E., Driscoll, R., Coltrera, M., Olins, A., and Bloom, K. (1991). A dynamin-like protein encoded by the yeast sporulation gene *spo15*. *Nature* 349, 713-715.
- Yeh, E., Carbon, J., and Bloom, K. (1986). Tightly centromere-linked gene (*spo15*) essential for meiosis in the yeast *Saccharomyces cerevisiae*. *Mol. Cell Biol.* 6, 158-167.
- Zhang, P. and Hawley, R. S. (1990). The genetic-analysis of distributive segregation in *Drosophila melanogaster*. 2. Further genetic-analysis of the *nod* locus. *Genetics* 125, 115-127.

Zheng, Y., Jung, K., and Oakley, B. R. (1991).  $\gamma$ -tubulin is present in *Drosophila melanogaster* and *Homo sapiens* and is associated with the centrosome. *Cell* 65, 817-823.